AN INVESTIGATION OF THE THEORETICAL AND DESIGN

ASPECTS OF UNSYMMETRICAL MULTI-CUTTING ACTION IN

DEEP-HOLE MACHINING

Vojislav Latinovic

A Thesis

in

The Faculty

of

Engineering

Presented in Partial Fulfillment of the Requirements
for the degree of Doctor of Engineering at
Concordia University
Montréal, Québec, Canada

March 1978

ABSTRACT

AN INVESTIGATION OF THE THEORETICAL AND DESIGN
ASPECTS OF UNSYMMETRICAL MULTI-CUTTING ACTION IN
DEEP-HOLE MACHINING

Vojislav Latinovic
Concordia University, 1978

A new design concept of multi-edge deep-hole machining
is presented. The work deals mainly with BTA metal cutting
systems.

The main feature of the design is that the cutting
head consists of multi-cutting edges unsymmetrically located
with respect to the rotational axis on the cutting head. This
provides a means of maximizing the metal removal rate per
revolution, and hence the productivity, without sacrificing the
essential advantages provided by single-edge deep-hole boring
tools. The role of a stabilizing cutting force resultant
necessary for self-guidance in machining holes of high length-
to-diameter ratio is explained for a single-edge cutting tool,
and extended to tools with unsymmetrical multi-cutting edges.

The design procedure for unsymmetrical multi-edge
cutting tools is investigated by formulating a mathematical
model which takes into account the following:

(a) Cutting edges are placed unsymmetrically on the
     cutting head in such a way that a predetermined
     cutting force resultant is transmitted onto the
     hole-wall by means of supporting pads;

(b) The cutting force resultant is chosen in such a
     way that, sufficient pressure is exerted onto the
     machined hole-wall to prevent separation of the
     wear pads from the wall and run-out of the tool.
     This pressure is limited to a value that permits
     a hydrodynamic lubricating action between the
     supporting pads and the hole-wall;

(c) The pressure variation between the supporting pads
     and the hole-wall caused by the hole size varia-
     tion is controlled in the same manner, as in
     single-edge cutting tools.

     The distribution of the cutting force on the cutt-
ing edges is formulated in terms of the fundamental cutting
parameters and mechanical properties of workpiece material,
utilizing a combined three-dimensional metal cutting theory
in conjunction with empirical test data.

     To achieve the design requirements stated above, a
multivariable, nonlinear, objective function is formulated,
and subsequently, modified to an unconstrained type with
bounded decision variables. A numerical direct search method,

iii

accelerated in distance, is selected to minimize the objective function. This procedure essentially minimizes the pressure difference among cutting-edges corresponding to a predetermined wear pad force required for tool self-guidance. The wear pad forces are estimated through an upper limit resulting from the hydrodynamic oil film lifting capacity of the wear pads and a lower limit established from a statistical analysis of the dynamic fluctuations of cutting forces.

To examine the validity of the developed optimization program, several case studies are undertaken for staggered tools known to be performing satisfactorily in industry. The theoretically computed design parameters compared very well with the design data of the tools examined. The optimization procedure developed is used to design two trepanning head prototypes. The unsymmetrical double and triple-edge BTA trepanning tools are then manufactured and tested on the production line. The test results showed good tool guidance and stability. Much higher material removal rates are possible compared to those achieved with single-edge tools without any loss of hole accuracy, straightness or surface finish.

An economical analysis conducted shows that the machining cost per unit length of a hole using multi-edge cutting tools is significantly decreased. Thus implementation of these tools in production should increase productivity at decreased cost.

Extension of this analysis to tools with a higher number of cutting edges requires a rigorous investigation of stresses and a study of the dynamic behaviour of the machine-tool-workpiece system.

ACKNOWLEDGEMENTS

TABLE OF CONTENTS

LIST OF FIGURES

(continued)

LIST OF TABLES

NOMENCLATURE

A	undeformed chip cross-sectional area
A_c	chipmouth area
b	width of cut, width of wear pad
$b_{L,R}$	lower and upper bound for width of cut
c	cutter pocket-size factor, constant in Merchant's shear angle relationship
c_k	cutting force for $b = 1$ mm and $s = 1$ mm
$c_{kp,kq}$	cutting force for $b = 1$ mm and $s = 1$ mm in the directions p and q
c_L	cost per unit length of hole
c_M	machine cost per unit time
c_1, c_2	constants in Oxley's shear angle relationship
C	material constant
C_T	direct tool cost
d	diameter of cutting head
d_t	diameter of chipthroat hole
D	diameter of cutting head
e	eccentricity of unbalanced mass
f	tool feed
F	cutting force component perpendicular to the tool axis
$F_{p,q,r}$	cutting force components in the directions p,q and r
$F_{F,R,T}$	cutting force components in the feed, radial and tangential directions

$(h_{i+1} - h_i)$	height difference between two adjacent cutting edges
H_B	Brinell hardness
i	subscript
j	subscript, imaginary unit
k	subscript, stage subscript
k_w	positive weighting factor
K	slope in an S_s vs σ_n diagram, material constant
K_p	unit cutting force
ℓ	subscript, chipthroat length
L	length of wear pad hole length
m	subscript, number of cutting zones
n	number of cutting edges, number of variables, number of revolutions per minute
n_c	number of cutting edges
n_v	number of variables
N	cutting speed in rps
p	width of cutting zone
P	unbalanced force
r	radius of cutting head
$\vec{r}$	position vector of cutting force application point with respect to tool axis
r_i	radius of chipmouth
r_c	radial distance of chipmouth center
r_t	chip ratio
R	cutting force resultant
R_s	supporting force resultant, limiting hydrodynamic force

$R_{x,y}$	cutting force resultant in the direction x and y
s	effective depth of cut in direction of F_q
s_0	shear strength of material with no normal stress
S_s	shear strength of material in cutting
t	undeformed chip thickness, nondimensional tool life
t_c	deformed chip thickness
T	cutting torque, tool feed, tool life between grinds
T_{CH}	tool replacement time
u	exponent to the width of cut
v	cutting speed
v_c	chip velocity
w	exponent to the depth of cut
x	decision variables
$x_{1,2}$	exponents to the width of cut
X	current base point
X_x	base point resulting from current move
X_{xx}	previous base point
$Y_{1,2}$	exponent to the depth of cut
Y	functional value at base point
Y_y	functional value resulting from current set of exploratory moves or pattern move
Y_{yy}	functional value resulting from current move
$Y_{1,2,3}$	objective functions

α normal rake angle, acceleration factor

β chipthroat angle with respect to tool axis

δ "minimum" step size

$\delta_{k\ell}$ Kroncker delta

$\delta_{1,2}$ operators

Δ deviation from the mean, current step size

Δs difference in depths of cut

$\Delta\psi$ cutter pocket angle

ζ chipmouth area factor

$\zeta_{p,q}$ correction factor for cutting force in the directions p and q

η error factor

θ angle between cutting force F and cutting edge

κ approach angle

λ angle defining location of supporting pad with respect to x-axis

μ absolute viscosity of coolant

ξ correction factor

ρ mass density, reduction factor for step size

σ_n normal stress

ϕ angular location of cutting edge with respect to x-axis, normal shear angle, cost rate factor

ϕ_C cost break-even factor

ϕ_{CM} cost rate factor for constant machine cost and cost per unit length of hole

ϕ_M cost rate factor for constant machine cost

$\phi_{L,R}$ lower and upper bounds of the variable ϕ

ψ chipmouth angle

CONVERSION TABLE OF UNITS

Length   :   1 in = 25.4 mm

             1 ft = 304.8 mm

Area   :   1 in^2= 6.4516 cm^2

Volume   :   1 gallon = 4.546 litres

             1 U.S. gallon = 3.7854 litres

Mass   :   1 slug = 14.594 kg

Mass
Density   :   1 slug/ft^3 = 226.222 kg/dm^3

Force   :   1 lb = 4.448 N

             1 kp = 9.8066 N

Pressure :   1 psi = 6.894757 kPa

             1 kp/cm^2 = 980.665 Pa

Viscosity: 1 reyn = 6.894757 x 10^4 P

Power   :   1 HP = 745.7 W

CHAPTER I

INTRODUCTION

CHAPTER I

INTRODUCTION

Hole machining operations are employed extensively
in industry and constitute an important phase of manufactur-
ing. As in other areas of metal cutting, the search for
improved hole machining methods which remove material at
higher rates without loss of accuracy and machined surface
quality, continues. This work presents a new development
in this field which exploits the advantages of multi-edge
cutting action.

Results of this research work show that such an
approach is feasible technically, as well as economically.

1.1 HISTORICAL BACKGROUND

Historically, men first used hand drills during the
New Stone Age (about 4,000 B.C.). The device was a bow-
drill consisting of a wooden shaft tipped by a sharp piece
of hard stone. The shaft was rotated in a wooden frame and
loaded by a heavy piece of stone to provide the thrust. The
rotation was produced in alternate directions by a bow-handle
with a cord fixed to the ends and wrapped around the shaft
in the middle [1]. Egyptian stone carvings reveal that
hole-making was not an unknown operation to the ancients of
Egypt as early as 2,700 B.C. Basically, the latter device
produced holes via the grinding effect of a hand-rotated

stone [2].

The problem of producing holes of a depth exceeding the hole diameter by many times, known as deep-hole machining, has existed for many centuries. It was first faced in the Middle Ages when holes had to be drilled in the center of logs which were used as water mains until replaced by cast iron pipes late in the 17th[th] Century. Such drilling was performed by long hand drills in logs erected vertically. A deck built around the upper end of the log was employed to facilitate access during the operation [2].

The machine shown in Fig. 1.1 was designed about 1495 by master artist Leonardo da Vinci. The design has been saved in a collection entitled "Codex Atlanticus (393r-b)" owned by the Ambrosiana Library in Milan. This machine remarkably resembled a modern deep-hole machine and may be considered as its earliest prototype. The machine often mistaken for a lathe was designed to drill holes in the center of logs. The drilling mechanism is in the foreground but the novel aspect is the set of automatically adjustable chucks which clamp the log in the four radial positions. The chucks ensure that the axis of the log always remains in the center of the machine regardless of the log diameter. It is not known, however, whether the machine had ever been actually constructed or whether it was simply an example of Leonardo's own inventive genius [2,3].

3
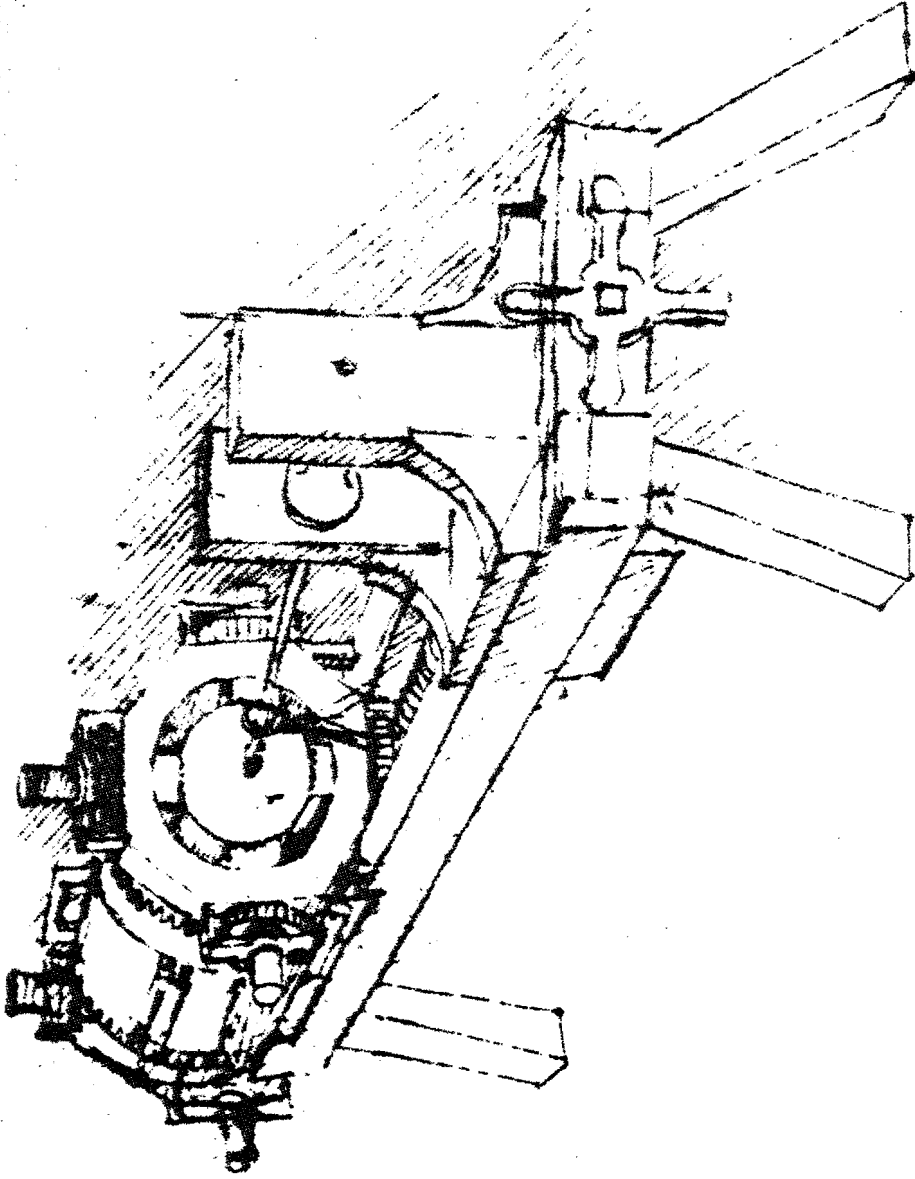
FIG. 1.1   LEONARDO DA VINCI'S DRILLING MACHINE, REPRODUCED FROM
"CODEX ATLANTICUS - 393r-b", 1495

Deep-hole drilling in metal was first attempted in the production of gun barrels. During the period between 1500 and 1750, the town of Suhl in Thüringen, Germany was known as the center of deep-hole drilling. At that time a water mill was employed as the machine tool with spade bits as the cutting tools. Two barrels could be drilled simultaneously by two parallel boring splindles. The feed and the thrust were produced by the operator. An appropriately designed lever developed a certain force amplification and an infinitely variable feed. The drilling was performed at 80 rpm and it required 8 to 10 tool bits to complete a barrel. With current technology 15 to 18 such barrels can be manufactured without regrinding the tool [1,2].

It seems that the machine tools we find in modern shop practice have been developed in the relatively short span of about 400 years, beginning in the 16th century and that the lathe was one of the earliest machine tools [4]. Little information is available about the gun-boring machines used before 1700, except for those mentioned. The earliest reliable information on methods and machines relates to the first half of the 18th century. In 1713, a vertical gun-boring machine is said to have been invented by a Swiss named Maritz who later worked in Holland, which seems to have been ahead of other countries in regard to gun-boring machines during the early years of the century. One of the illustrations given by Diderot in his encyclopedia is believed to re-

present Maritz's machine. A cutter head mounted on the end of a boring bar was rotated by animal power and a downward feed motion was given to the gun barrel. The frame of the machine was made almost entirely of wood and formed part of the structure housing it. The use of the structure of a building to form part of a machine tool continued well into the second half of the 19th century [5].

The first boring machine in which the gun was rotated and the feed motion was given to the boring tool appears to have been produced about 1758 by Verbruggen, in collaboration with Ziegler. This machine, in which the axis of rotation of the gun is horizontal, was of massive construction and is regarded as the first example of a machine tool for engineering applications, as distinct from ornamental and artistic use [5].

The cutters used in these gun-boring machines consisted essentially of a spade drill with two boring cutters suitable for drilling a hole in the solid. The other cutters employed were suitable for enlarging and cleaning up existing holes. It is of interest to note that the actual cutting portions are separate replaceable bits [5].

Although it seems probable that some other form of a drilling machine in addition to the bow-drill type had been produced before 1700, no conclusive evidence has been unearthed. The first example of a drilling machine seems to be a small unit made prior to 1782 by Vaucanson, a French engineer,

who achieved fame in several fields of engineering and made
notable advances in machine-tool design and construction.
This machine, as well as his lathe, mark the transition from
the older wooden-bed machine to the all-metal 'engineering'
type of machine tools [5].

The invention of the twist drill in the United
States in 1860 provided important steps in the field of
drilling. Available evidence confirms that Morse in 1862,
commenced in a very limited way, to make twist drills in
Bridgewater, but did not secure the aid of capital until the
summer of 1864, when the Morse Twist Drill and Machine
Company was formed and its works moved to New Bedford [6,35].

1.2   REVIEW OF PREVIOUS WORK

The earliest known study of the mechanics of cutt-
ing processes is that made by a French investigator,
Cocquilhat, in 1851. He investigated the work required to
remove a given volume of material in drilling iron, brass,
stone and other materials. Other pioneers in the area of
cutting mechanics and chip formation were Joessel, Tresca
and Reuleaux in France, Time, Zvorykin and Briks in Russia,
Mallock in England and Taylor in the United States - in the
area of tool wear and tool life [24].

The first significant scientific gathering in
America on drilling occurred at the XII Annual Meeting of

the ASME in Boston, November 1885. A paper on "Twist Drills" was presented by W.H. Thorn, and dealt with the early problems of drilling - the introduction of standard drill diameters, shank taper and establishment of optimal helix, cutting and clearance angles. This event set the stage for subsequent research work on drilling and boring which, in turn, contributed to a tremendous progress in this area of metal working.

Though the initial history of drilling is obscure, it appears that intensive research work on drilling dates back to the 1900's. The earliest attempt to conduct torque and thrust measurements while drilling in different materials is attributed to Bird and Fairfield [6]. By that time, many researchers tried to determine the power absorbed in drilling experimentally. Among these the names of Boston, Oxford, Gilbert, D.Smith, Kronenberg and Poliakoff are most prominent [8,9,10].

In 1944 and 1945, Merchang [11,12] formulated the first analytic model of the cutting process. This analysis applies in general terms to quite a large range of cutting conditions and it has stimulated later researchers to rethink the assumptions on which the model is based.

In 1952, Shaw, Cook and P.A.Smith [13] demonstrated the similarity between drilling and conventional turning operations. Oxford, Jr. [14] employed a quick stop device to

"freeze" the chip formation process, in 1955. He found that while the action along the cutting lip is similar to other cutting processes, the action of the chisel edge produces extrusion by high compressive loads. Shaw and Oxford,Jr. [15] in 1957, applied dimensional analysis and arrived at relations which are in good agreement with the experimental results in terms of the torque and thrust, in drilling.

All these researchers have assumed that the cutting operation is a steady-state process and the resulting cutting forces are assumed to represent the steady-state means, the flucturations being disregarded. However, knowledge of the nature and magnitude of the cutting force fluctuations is essential for an accurate dynamic analysis and stability of machine tools. Also, some very important parameters such as machinability, surface texture of a machined workpiece, tool life and power consumption depend upon the magnitude and frequency of these fluctuations.

Albrecht [17] in 1964, proved that the major cutting parameters are dynamic and time-dependent, the mean values of which are identical to the steady-state solutions of Merchant. Williams [19] in 1969, introduced the dynamic geometry of a twist drill and investigated the effect of the feed velocity on the cutting geometry of the drill cutting edges.

Recent research work revealed that cutting forces in metal are stochastic in nature possessing a high degree of randomness. Bickel, Kwiatowski, Al Samarai, Opitz and Weck are among the first who have recognized this phenomenon. Osman and Sankar [28] treated the random force variations as stationary and Gaussian signals in their proposed short-time acceptance test for machine tools.

Maragos [29] has proven experimentally that the cutting forces in turning are stochastic and Gaussian distributed only in the finishing operation. Subsequent work by Rakhit, Sankar and Osman [30] verified that the cutting forces in turning are random and Gaussian distributed and furthermore, that the surface texture is highly correlated with the cutting force fluctuations. Chahil [31] in a recent experimental investigation of the torque and thrust in drilling, has confirmed that these variables are random, stationary and Gaussian distributed with most of the power concentrated at certain dominant frequencies.

The Beisner process for deep-hole machining, init-ially developed in Germany during the early 1940's represents

the most economical method of hole-machining with high length-to-diameter ratio [1,2,32-55]. It produces holes of high accuracy of size, parallelism, straightness and surface finish and represents one of the most significant technological advances in the last 30 years. The method consists of a single-edge cutting head with carbide wear pads. This tooling, when integrated with a high pressure coolant system which removes the chips back through the interior of the boring bar, works exceptionally well. Boring tool experts have concluded that this system is optimum for all hole-making and a series of boring heads have been designed having the distinguished feature of the single-edge cutting tool with carbide pads. This bore-machining method has become known as the BORING & TREPANNING ASSOCIATION or BTA method. Figure 1.2 illustrates the principle of this method.

1.3 STABILITY AND SELF-GUIDANCE IN HOLE-MACHINING METHODS

1.3.1 Twist Drilling

Due to the symmetrical location of the cutting lips, a twist drill is subject to a completely balanced force system. The drilling process becomes unstable, due to any disturbance that might arise from uneven grinding or wear of the drill cutting edges. Such an imbalance of forces can only be controlled by the encastré effect of the drill, which might not be sufficient in the case of long drills to prevent

PRESSURE HEAD

STEADY REST

TOOL HEAD

BORING BAR

GEAR PUMPS

MAGNETIC FILTER

MAGNETIC SEPARATOR DRUM

CHIP TRAPS
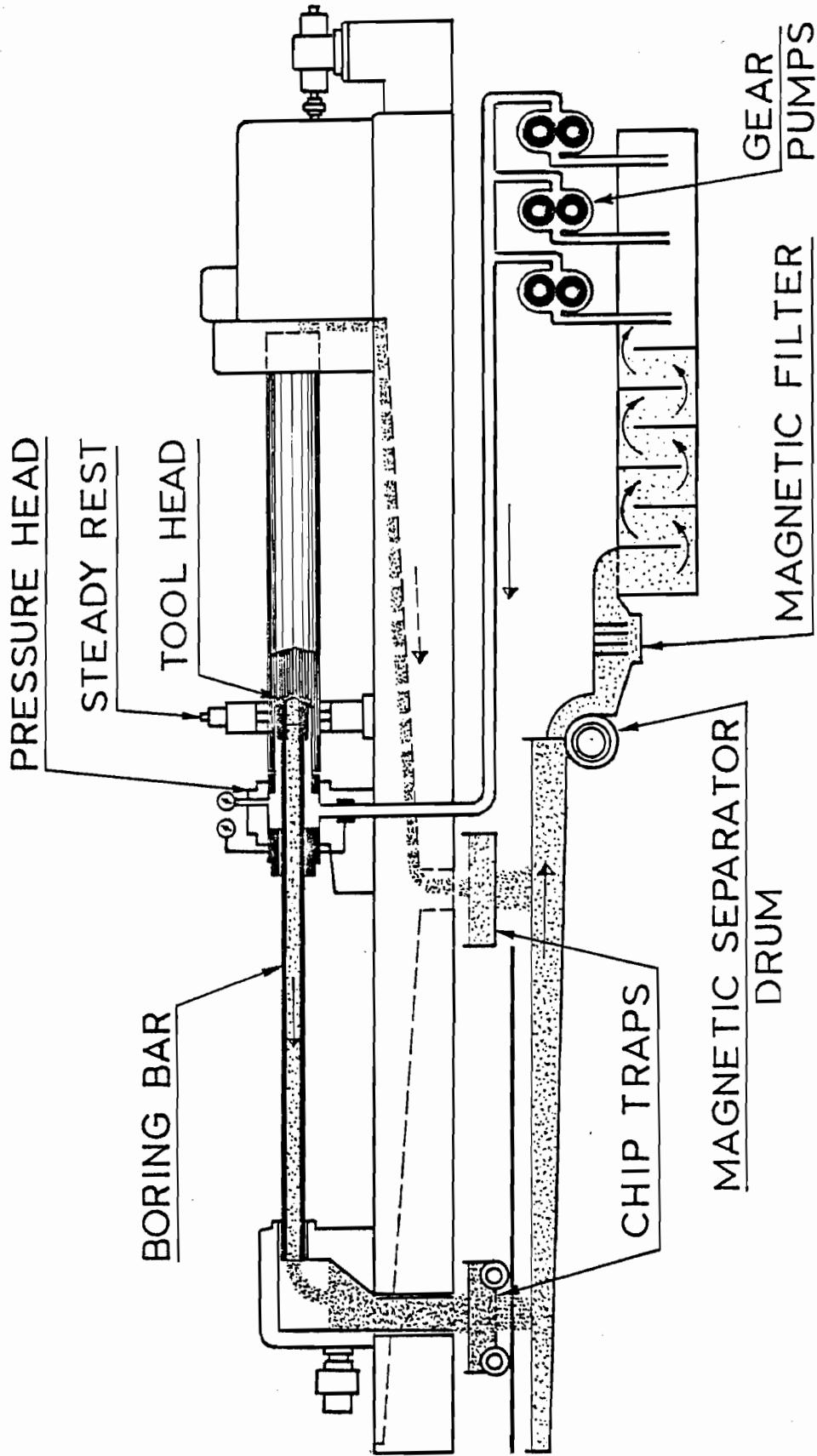
FIG. 1.2 THE PRINCIPLE OF BTA DEEP–HOLE MACHINING

waviness and considerable run-out of the drilled hole. This
instability is the major reason why twist drills are unsuitable
for drilling holes with high length-to-diameter ratio.

1.3.2 Boring

Boring is a machining process in which internal dia-
meters are generated in relation to the center-line of the
spindle by means of single-point cutting tools, and is mostly
used for enlarging and finishing drilled holes or other circu-
lar contours. Although most boring operations are done on
simple, straight-through holes, ranging upward in diameter
from 1/4 in (6 mm), the process is also applied to a variety
of other configurations. Tooling can be designed for boring
of blind holes, holes with "bottle" configurations, circular-
ly contoured cavities and bores with numerous steps, under-
cuts and counter-bores. The process is not limited by length-
to-diameter ratio of holes. With the workpiece properly sup-
ported holes having lengths that exceed the diameter (or vice-
versa) by a factor of 50 or more have been successfully bored.

1.3.3 Gundrilling

Gundrills are single-edge cutting tools. The length of
a hole theoretically has no limit, but in practice, the
limiting factor is the torsional rigidity of the shank. The
single edge construction with its supporting arrangement
forces the cutting edge to cut in a true circular pattern. By

this principle of guidance, the tip follows the direction of its own axis. It follows that it would take mechanical force to divert the tip from its straight direction and true circular cutting action.

Due to the single-edge cutting action, gundrills require aid during the initial cut into a workpiece. In fact, until the bearing area of the tip has started to enter the machined hole, the tool cannot support itself. Therefore, either an accurate pre-bored start must be machined into the workpiece, or a starting bushing provided in the pressure head.

1.3.4 BTA Boring

This method basically utilizes single-edge cutting tools with internal chip removal and differs from the conventional gundrills in tip construction, fluid induction and chip removal. However, the guidance principle is identical to that of gundrilling because of the single cutting edge and supporting bearing arrangements. The tool cuts in a true circular pattern and the cutting head follows the direction of its own axis.

Figure 1.3 shows three typical examples of BTA tools which are produced as standard items by various tool manufacturers. These tools have one cutting edge and two guide (wear) pads in common.
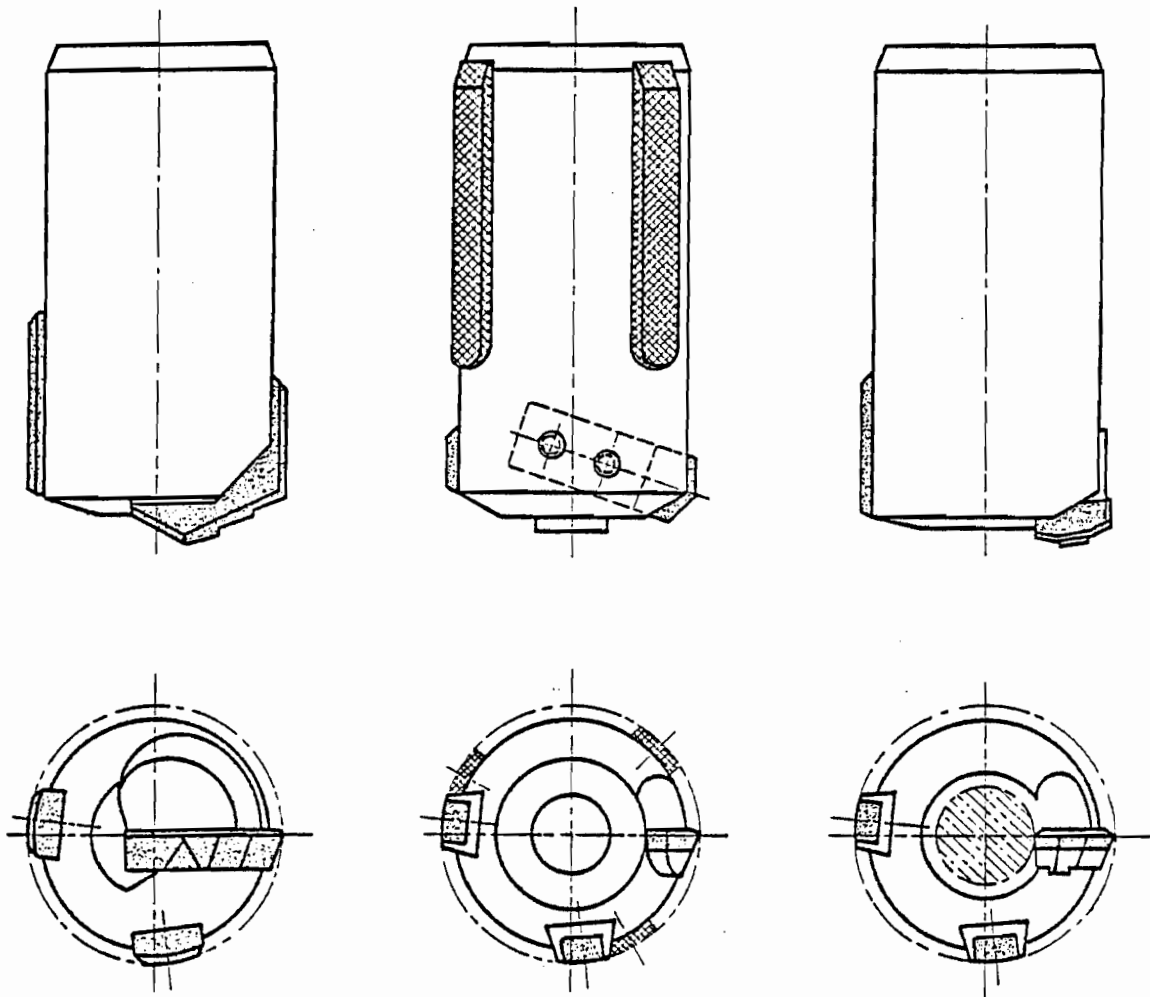
a) SOLID BORING   b) COUNTER-BORING   c) TREPANNING

FIG. 1.3   TYPICAL EXAMPLES OF   BTA   TOOLS

The solid boring head, shown in Fig. 1.3(a) is a single-edge end cutting tool which cuts into solid metal. The chips exit through the hollow interior of the head and the boring bar. The counterboring head shown in Fig. 1.3(b) is a single-edge end cutting tool which does not cut to center, but may remove more material than a conventional reamer. The chips exit through the hollow interior of the head and boring bar. The trepanning head shown in Fig. 1.3(c) is a single-edge end cutting tool which cuts into the solid by removing an annular groove leaving a turned core in the center. The chips may be exhausted either around the perimeter of the tool, or through the inside of the head and boring bar between the inner wall of the bar and the core.

Special deep-hole machining tools such as the ejector tool for solid boring and the skiving tool for counter boring are also in use. The skiving tool represents a finishing tool designed for small cutting depths; the floating cutter is self-adjustable to cut equal depths on both ends. The ejector tool is designed for a double-walled boring bar. The coolant is introduced between the outer tube and the inner tube, and carried back away with the chips through the inner tube. The most important feature of the tool is that it represents a three-edge arrangement, two edges located on one side, and a third one 180° from the other two edges. One cutting edge starts at the periphery of the head and cuts through approximately 0.4 of the radius. The second cutting edge cuts through

the center approximately 0.4 of the radius. The third one located at 180 deg., cuts the remainder of the area, partially overlapping the area cut by the other two edges. This arrangement gives the tool partially balanced cutting forces, and takes some of the load off of the supporting pads. Another advantage of the tool is that it allows a combination of the carbide grades to best meet requirements for the toughness and hardness (wear resistance) of each cutting edge. However, the tool does not take full advantage of the multi-edge cutting principle, since the length of the three cutting edges covers only one tool radius and, therefore, is equivalent to single-edge tools, in terms of metal removal rate.
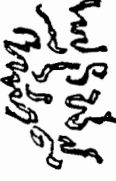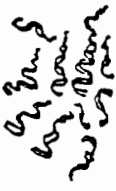
1.3.5 Significance of Deep-Hole Machining

Despite the existing controversy about the limit of length-to-diameter ratio which separates the so-called deep-holes from shallow ones, it is widely accepted that economical machining of holes in which length-to-diameter ratios exceed a value of about ten, can only be done by one of the deep-hole machining methods. Moreover, due to its capability of machining holes of high accuracy without follow-up operations, the single edge BTA boring method becomes competitive even for holes of length-to-diameter ratio less than one.

Though the gundrills and BTA boring tools have in common the single-edge cutting and supporting bearing arrangement, hence an identical guidance principle which forces the tool to cut in a true circular pattern and follow the direction of its own axis, they differ in tip construction, fluid induction and chip removal. Besides the difference that gundrills work with the so-called external chip removal system, where chips are in contact with the machined bore wall and the BTA boring tools work with the internal chip removal system where chips-bore wall contact does not occur, the essential difference between these two methods is in the chip formation. While in gundrilling the chips must be continuous for successful removal, in BTA boring the chips must be narrow and short enough to exit freely through the very restrictive chip mouth and throat. For that purpose, the cutting edge of a BTA tool is divided into 2 or 3 steps (chip separators) and has chip-breakers to produce short chips of C-shape. This difference in chip formation makes BTA boring more efficient than gundrilling, where an excessive increase in feed rate might produce a heavy backbone in the chip and a blockage of the chip pass.

Table 1.1, summarizes the deep-hole operations and shows the optimal geometry of chip-breaker and chip forms for each operation. Not less important in the chip-formation process are cutting speeds and feeds. In general, the higher the speeds, the thinner the chips that are produced and the higher

TABLE 1.1 GEOMETRY OF CHIP BREAKER AND CHIP FORMS FOR DEEP-HOLE MACHINING

No.	TOOL			CHIP TYPE	SYMBOL	CHIP FORM
1		SOLID-GUN DRILL	—	CONTINUOUS		
2		TREPANNING GUN-DRILL	—	CONTINUOUS		
3		SOLID-BTA	$b = 1,4$ $t = 0,4$ $r = 0,5$	SHORT		
4		TREPANNING-BTA	$b = 1,6$ $t = 0,4$ $r = 0,5$	SHORT		
5		COUNTER BORING -BTA	$b = 1,8$ $t = 0,8$ $r = 0,8$	SHORT		
6		SKIVING	—	CURLY		
7		EJECTOR	$b = 1,4$ $t = 0,4$ $r = 0,5$	SHORT		

the feed rates, the thicker the chips that are produced.

Coolants also play an important role in chip-formation and control. A high-quality coolant will let the chips slide freely on the cutting edge, thus thinning the chip and allowing increased feeds. The main functions of the coolant under pressure in deep-hole machining are summarized as follows:

(a) it forces the chips back out of the hole being cut;

(b) it provides lubricating and cooling effects to the bearing areas of the tool pads and tool-chip interface;

(c) it applies an axial force to dampen the thrust vibrations of the tool and end-play in the spindle bearings of the machine;

(d) the coolant antiweld characteristics prevent the formation of built-up edges (BUE).

1.4 SCOPE OF THE RESEARCH WORK

From the previous review of the methods available for hole machining, it is clear that the single cutting-edge BTA boring method at this stage of development represents the most economical method of machining accurate holes with good straightness, and surface finish. However, the upper limit

of feed rates for these tools is controlled by the condition
of chip formation and the upper limit of cutting speeds
depending on the permissible tool wear and tool life required.
Therefore, any further increase in the removal rates can only
be achieved by the introduction of tools with cutting edges
that cover more than one tool radius. Such tools however, have
shown inconsistent tool performance [36] when the cutting
edges are symmetrically located on the boring head. In this
case, the cutting forces are symmetrically distributed on the
boring head and hence, the resultant becomes indeterminate.
This usually leads to waviness and considerable run-out. After
evaluating a large number of test results using this type of
tool [36], the following conclusions may be reached:

(1) the feed rate per revolution can be greatly in-
      creased by increasing the number of cutters with-
      out sacrificing tool life;

(2) the straightness of the machined hole is not affect-
      ed by an increase in metal removal.

Because of the inconsistency experienced with this
type of tool in terms of bore straightness, the following
design concept is proposed as the basis of this research
work:

(1) Cutting edges should be placed unsymmetrically on the boring head in such a way that a predetermined cutting force resultant is transmitted to the hole-wall by the supporting wear pads;

(2) the cutting force resultant should be selected in such a way that, on one hand, enough pressure is exerted onto the machined hole-wall to prevent run-out of the tools; on the other hand, this pressure should be limited to a value that permits a hydro-dynamic lubrication action between the supporting pads and the hole-wall;

(3) the pressure variation between the supporting pads and the hole-wall caused by the hole size variation controlled similarly to that of single-edge cutting tools. This requires that one of the cutting edges controlling the hole size be located opposite the wear pads.

In summary, this work presents an analytical investigation supported by an experimental verification of this design concept.

In Chapter II, the model of cutting forces in deep-hole machining with single-edge tools is described. Based on the cutting edge geometry, both the cutting mechanics approach

and the empirical approach are discussed and mathematical expressions for the three cutting force components - tangential, radial and feed, are derived. The expressions are cross-checked by numerical examples for typical shear-angle relations and trends illustrated by diagrams. The results are compared with available experimental data and finally, the equations for computing the force components are established.

Chapter III deals with the design concept of a staggered unsymmetric multi-edge tool. The mathematical model developed for a single-edge cutting tool is applied to this tool to compute the magnitude of each cutting force component. The resultant force is determined on the basis of the cutters' location on the head, and the wear pads located in such a way that tool guidance is secured. Two such tools were designed and built by a tool manufacturing company, one solid boring and the other, a trepanning head. Tests carried out by the company proved successful.

Staggered unsymmetrical multi-edge tools proved the possibility of tool optimization for a predetermined cutting force resultant, in terms of the angular location of cutters, relative to each other, but did not allow any significant increase in the feed rate compared to single-edge tools. However, analysis of the test results indicated the possibility of optimizing an unsymmetrical multi-edge tool design, such as that carried out in Chapter IV. In this chapter, an objective

function for tool optimization is derived in terms of the
supporting reaction and the difference in the cutting force
per unit width of cut. A direct search method is adapted to
carry out the tool optimization, in terms of parameters of
the tool, such as the cutting edge angular locations and the
widths of cut. Flow charts of the computer program are
given in a general, subscripted form. Several different tools
are optimized, using the program and are designed according
to the optimal parameters. Two trepanning heads and a solid
boring head are selected for manufacturing and testing.

Chapter V describes the experimental set-up. The
testing of the tools is carried out on a deep-hole boring
machine with workpieces taken from the production line.
The tools selected were trepanning heads of 4.145 inches
(105.282 mm) nominal size, one with three and the other one
with two standard inserts located at optimal positions for
achieving the predetermined supporting reactions. The effect
of the cutting force fluctuations on the tool stability and
guidance was investigated by the use of the two heads, opti-
mized for different cutting force reactions.

Chapter VI gives the results of tests and discusses
the tool performance in terms of tool guidance and stability,
chip formation, hole size accuracy and hole straightness. It
discusses the effect of the cutting edge geometry with regard
to the front profile, the chip-breakers, and the circle land
clearance.

Chapter VII, summarizes the results and gives the conclusions and recommendations for possible future investigation.

The Appendices contain relevant analyses, a derivation of the equations, computer programs and layouts of the tools designed and tested.

CHAPTER II

MATHEMATICAL MODELLING OF CUTTING FORCES IN
DEEP HOLE MACHINING

CHAPTER II

MATHEMATICAL MODELLING OF CUTTING FORCES IN
DEEP HOLE MACHINING

The principal concept of the method developed in
this work is based on the prediction of the cutting forces
in deep-hole machining with a single-edge cutting tool. The
analysis, therefore produces equations for the cutting
force in terms of the fundamental cutting parameters such as
the shear strength of workpieces, the undeformed chip cross-
sectional area, the friction angle, the shear angle, the
tool geometry and cutting conditions. This is accomplished
through the cutting mechanics in free metal cutting with a
single cutting edge, as well as mechanics of metal cutting
in turning and drilling with a small feed and large width
of cut. The results of empirical testing of the cutting
forces in turning and drilling are also used to modify as
necessary the formulation of the cutting forces in deep-
hole machining.

In deep-hole machining, the resultant cutting force
R is commonly resolved into three components, the tangential
or power contributing component $\vec{F}_T(\vec{F}_p)$ parallel to the cutt-
ing velocity vector, the radial component $\vec{F}_R$ and the feed
component $\vec{F}_F$, see Figure 2.1. As it can be seen,the tangential
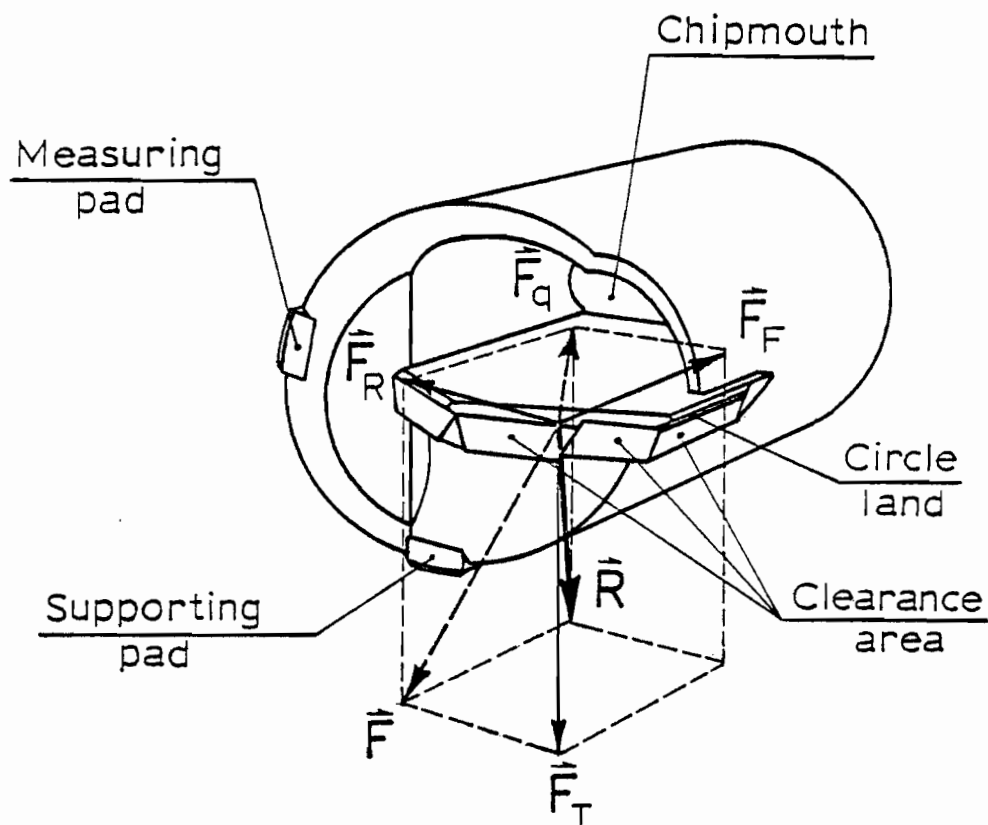
FIG. 2.1 CUTTING FORCES ACTING ON BTA SOLID
BORING CUTTER

and radial components act in the plane perpendicular to the tool axis and can be represented by force vector $\vec{F}$. Also, the feed and radial components can be considered as the force vector $\vec{F}_q$ which acts in the radial plane containing the tool axis. This force may also, under certain assumptions, be considered normal to the machined surface.

2.1   PREDICTION OF CUTTING FORCES FROM METAL CUTTING ANALYSIS

In oblique metal-cutting, it is convenient to consider three force components - one parallel to the cutting velocity vector, i.e., the power contributing force, one perpendicular to the machined workpiece surface and the third perpendicular to the other two. These are denoted by F_p, F_q and F_r, respectively. In orthogonal cutting the component F_r vanishes and components F_p and F_q reduce to relatively simple equations in terms of the fundamental cutting parameters.

Deep-hole machining may be treated as ortho-gonal cutting. In this operation, the cutting edge cuts through the center, on one side of the hole, leaving no area of material to be extruded as with the chisel edge of a twist drill. The cutting edge coincides with the radial direction and hence, is always perpendicular to the cutting velocity vector, except for a limited region at the center, where an effect of the feed velocity on the cutting geometry of the cutter should be expected, due to a small radial misalignment
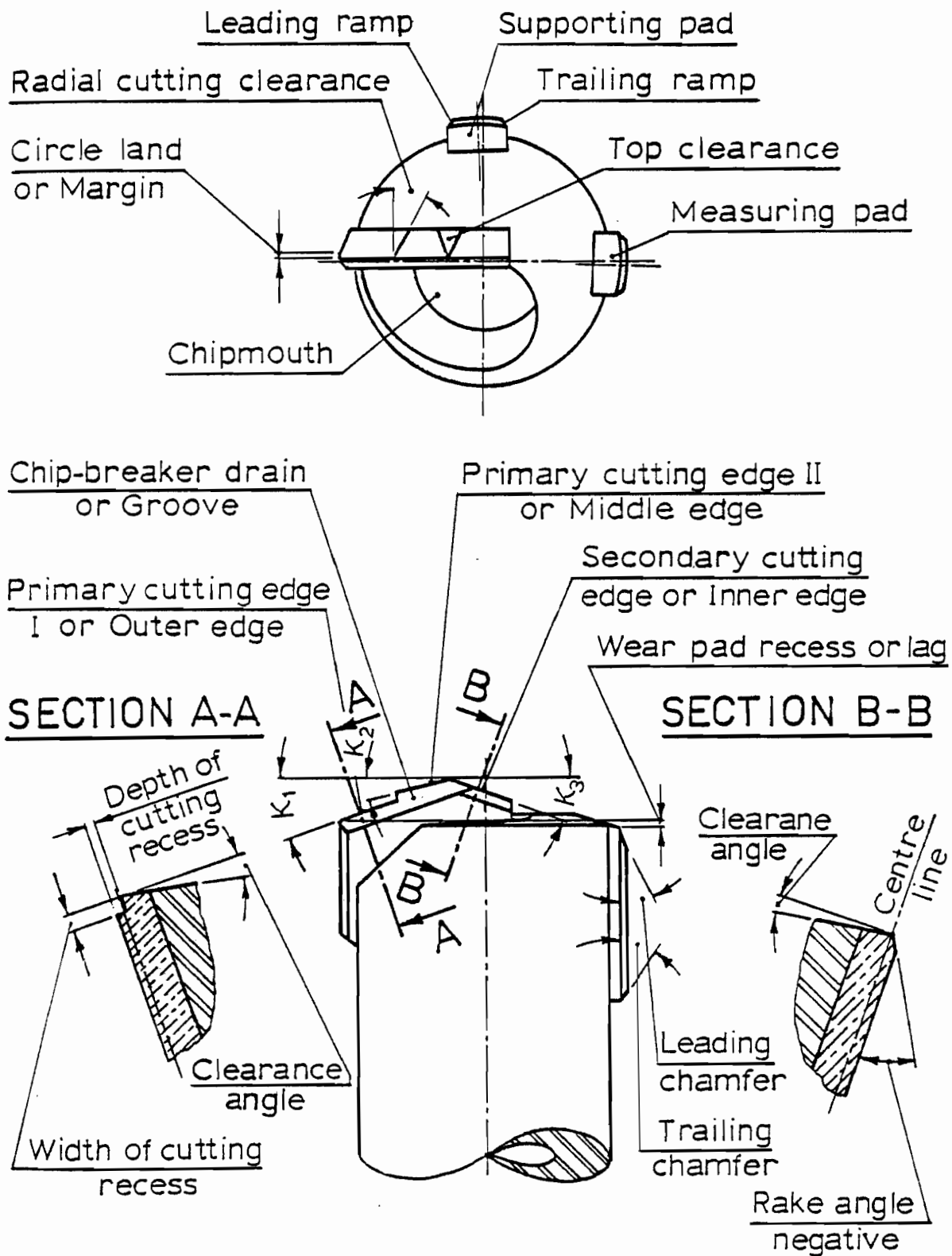
FIG. 2.2   TOOL GEOMETRY OF A TYPICAL   BTA   SOLID
BORING HEAD

Recent research work revealed that cutting forces in metal are stochastic in nature possessing a high degree of randomness. Bickel, Kwiatowski, Al Samarai, Opitz and Weck are among the first who have recognized this phenomenon. Osman and Sankar [28] treated the random force variations as stationary and Gaussian signals in their proposed short-time acceptance test for machine tools.

Maragos [29] has proven experimentally that the cutting forces in turning are stochastic and Gaussian distributed only in the finishing operation. Subsequent work by Rakhit, Sankar and Osman [30] verified that the cutting forces in turning are random and Gaussian distributed and furthermore, that the surface texture is highly correlated with the cutting force fluctuations. Chahil [31] in a recent experimental investigation of the torque and thrust in drilling, has confirmed that these variables are random, stationary and Gaussian distributed with most of the power concentrated at certain dominant frequencies.

The Beisner process for deep-hole machining, initially developed in Germany during the early 1940's represents

of the cutting edge. Figure 2.2 shows the tool geometry of
a typical BTA solid boring head. If the cutting velocity is,
evaluated in terms of the radius and compared to the
feed velocity, it is apparent that this effect would become
insignificant at a radius of a few tenths of a millimeter.
Also, the obliquity caused by radial misalignment of the
middle cutting edge in trepanning tools is insignificant due
to the large radius at which this zone is located. Therefore,
it is apparent that the cutting process in deep-hole machining
represents almost pure orthogonal cutting and Merchant's
analysis [11], based on the thin-shear-plane model, applies
with insignificant error. This analysis assumes the follow-
ing to hold:

  (1) The tool tip is sharp and no rubbing or ploughing
       occurs between the tool and the workpiece;

  (2) the deformation is two-dimensional, i.e., no side
       spread;

  (3) the stresses on the shear plane are uniformly dis-
       tributed;

  (4) the resultant force R on the chip applied at the
       shear plane is equal, opposite and co-linear to
       the force R', as applied to the chip at the tool-
       chip interface.

Under these conditions a combined force diagram shown in Fig. 2.3 could be constructed. The resultant force R may be related to the other force components as the friction force F and the shear force F_s as well as the corresponding normal force components N and F_n. From the diagram, if by expressing the shear force in terms of shear strength S_s and shearing area in the shear plane and then substituting in R, the power and thrust components can be determined from

$$F_p = \frac{S_s A}{\sin\phi} \frac{\cos(\tau-\alpha)}{\cos(\phi+\tau-\alpha)} \qquad (2.1)$$

$$F_q = \frac{S_s A}{\sin\phi} \frac{\sin(\tau-\alpha)}{\cos(\phi+\tau-\alpha)} \qquad (2.2)$$

where

A = bs - undeformed chip cross-sectional area

s = effective depth of cut in the direction of F_q

b = width of cut

ϕ = normal shear angle

τ = normal friction angle

α = normal rake angle

From the geometrical considerations of the tool and chip it follows

$$\tan\phi = \frac{r_t \cos\alpha}{1-r_t \sin\alpha} \qquad (2.3)$$

where

$$r_t = \frac{t}{t_c} \quad \text{is the ratio of undeformed to deformed}$$

chip thickness

Equation (2.3) allows ϕ to be calculated provided the chip ratio is known from an experimental investigation.

From Stabler's [24] original chip-flow rule it follows

$$\tan(\phi+\tau) = \frac{\cos\alpha}{1 - \sin\alpha} \tag{2.4}$$

for which Stabler's shear-angle relationship is a solution

$$\phi = 45 - (\tau-\frac{\alpha}{2}) \tag{2.5}$$

Since more than a dozen of shear-angle relations have been proposed by different researchers, it would be interesting to compare the results obtained with the different forms. Such a comparison was undertaken and the outcome is discussed in Appendix 2.

For the shear strength on the shear plane S_s, Merchant [12] derived the following equation

$$S_s = \frac{S_0}{1 - K \tan(\phi+\tau-\alpha)} \tag{2.6}$$

which resulted from $S_s = S_0 + K \sigma_n$; σ_n being the compressive normal stress in the shearing plane and S_0 the shear strength under no compressive stress.

The slope K in an S_s vs σ_n - diagram can be experimentally determined for each particular material. Merchant found for SAE 4340 steel $K = 0.175$ and $S_o = 69,000$ psi, and for N.E. 9445 steel $K = 0.23$ and $S_o = 58,000$ psi.

In order to apply equations (2.1) and (2.2) all fundamental parameters have to be determined for a given chip cross-sectional area. In addition to the assumptions already made, some further implications have to be stated:

(1)   All parameters are at average values over the length of a cutting edge. This is important, not only because of the dynamic character of the cutting parameters but also because of the fact that the velocity linearly increases with the radius and this change in cutting speed affects the chip ratio and all other parameters. From numerous experiments [21,22,23] it is evident that the cutting forces increase with a decrease in the cutting speed. In spite of this fact, it seems reasonable to assume that the chip ratio and hence, the specific cutting force along the cutting edge, are relatively constant and equal to an average value. The evidence available from tests in deep-hole machining [62] supports such an assumption and shows that the associated error is not significant.

(2)   Side shear forces are neglected, although it is
        obvious that in deep-hole machining, several side
        shear areas exist, one for each chip separator.
        Because of a large chip slenderness ratio, the error
        due to these forces may be considered insignificant.

(3)   The assumption of no side spread implies that the
        chip ratio is independent of the width of cut. The
        experimental evidence [22] confirms such an
        assumption, although a slight effect has been register-
        ed.

(4)   Friction forces which occur at the flank surface
        of the cutters as a result of contact between the work-
        piece surface and the cutting flank are neglected,
        although the experience with twist drills confirms
        the existence of such forces. If they are to be
        accounted for, they may be taken constant along the
        cutting edge, acting in the direction of F_p [26].

        Since the cutting geometry is known in advance, such
parameters as the rake angles α_k and approach (front) angles
κ_k are known for each chip zone p_k. So the three cutting
force components can be calculated over m chip zones, similar
to those for a turning tool, particularly the modified
Kolesov's tool for turning [25] - see Fig. 2.4:
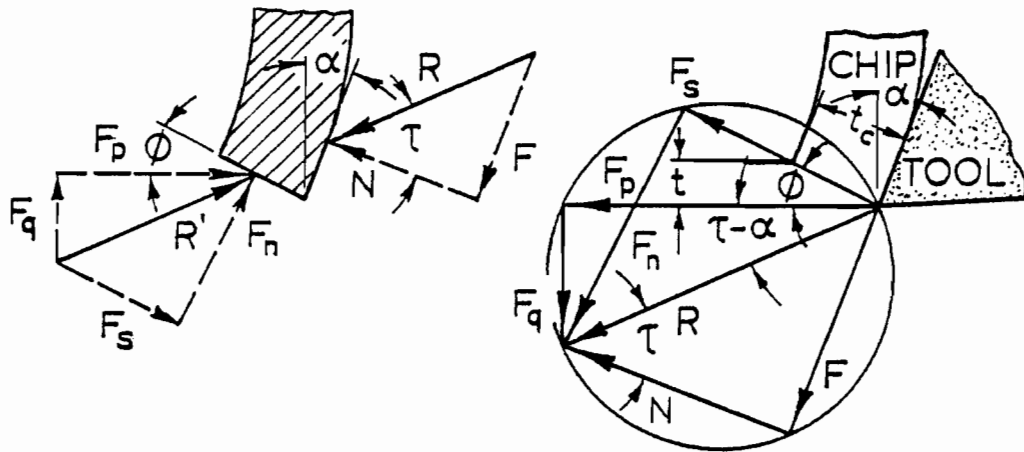
FIG. 2.3   COMBINED FORCE DIAGRAM IN ORTHOGONAL
          CUTTING
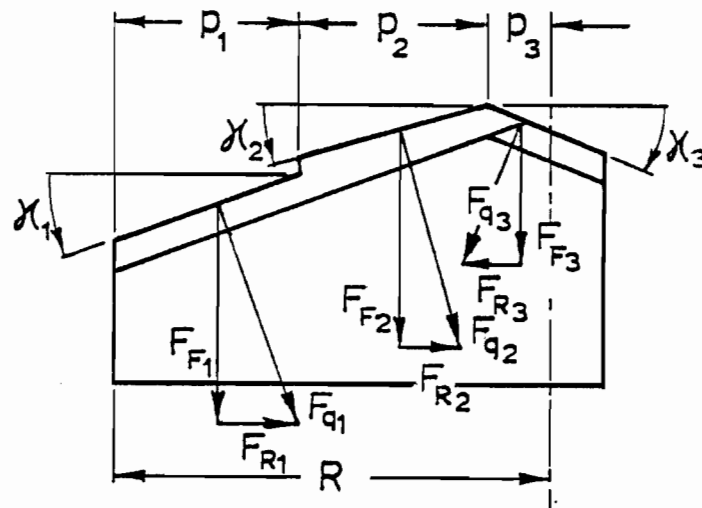
FIG. 2.4   RADIAL AND FEED COMPONENTS OF THRUST
          FORCES

$$F_T = \sum_{k=1}^{m} F_{pk} \; ; \qquad k = 1,2,\ldots,m \quad (2.7)$$

$$F_R = \sum_{k=1}^{m} F_{qk} \sin \kappa_k ; \; k = 1,2,\ldots,m \quad (2.8)$$

$$F_F = \sum_{k=1}^{m} F_{qk} \cos \kappa_k ; \; k = 1,2,\ldots,m \quad (2.9)$$

where

$$F_{pk} = \frac{S_s \, b_k \, s_k}{\sin\phi_k} \; \frac{\cos(\tau_k - \alpha_k)}{\cos(\phi_k + \tau_k - \alpha_k)} \quad (2.10)$$

$$F_{qk} = \frac{S_s \, b_k \, s_k}{\sin\phi_k} \; \frac{\sin(\tau_k - \alpha_k)}{\cos(\phi_k + \tau_k - \alpha_k)} \quad (2.11)$$

where b_k is the width of cut, and s_k the depth of cut for each chip zone p_k. The approach angles κ_k are taken with corresponding positive or negative signs. For example, the cutter shown in Fig. 2.4 has κ_3 of negative sign, since the negative radial force should point outwards.

In this way, the cutting forces in deep-hole machining may be predicted for a single cutting edge by the use of equations (2.7) to (2.11) derived from the thin-shear-plane model. Appendix 2 gives 2 numerical examples tabulated in Tables A2.1 and A2.2 and illustrated in Fig. A2.1 and Fig. A2.2. Further implications of this approach will be discussed in the conclusion to the chapter.

2.2 PREDICTION OF CUTTING FORCES FROM EMPIRICAL TESTING

The empirical method of determining the cutting forces supplies information for specific cutting operations and usually considers the influence of practical rather than fundamental variables. Deep-hole machining has not yet been empirically tested and no data are yet available for that process. However, it is possible to apply the data from turning and twist drilling, the two operations having been extensively tested in the past. These operations are, by the nature of the cutting process, similar to deep-hole machining operations and the data available from their testing may help in an effort to predict the cutting forces in deep-hole maching by an empirical approach.

2.2.1 Turning Operation

The turning operation is an operation that has been tested the most. Many researchers have done extensive work in the area of cutting force prediction through empirical testing[21, 22,23]. According to Kronenberg [23] the main cutting force F_T can be evaluated from either the so-called elementary cutting force law

$$F_T = A \ K_p \qquad (2.12)$$

where

A = bs - an undeformed chip cross-sectional area

b = depth of cut

s = feed per revolution

K_p = unit cutting force given by

$$K_p = c_k \ \xi(A) = c_k \ b^{-v} \ s^{-w} \qquad (2.13)$$

or the Extended cutting force law

$$F_T = c_k \ b^x \ s^y \qquad (2.14)$$

where x and y are exponents depending on the workpiece material and c_k is the cutting force for b = 1 mm and s = 1 mm. This specific cutting force represents a very important material constant in cutting mechanics. Since the chip cross-sectional area of 1 mm^2 represents a unit well within practically encountered chip cross-sectional areas it is widely accepted in the practice of metal cutting.

From a comparison of (2.12) and (2.14), it is evident that the unit cutting force K_p is not constant but a function of b and s. It has been proven, however, that K_p is not affected by the depth of cut b, and that s non-linearly affects K_p. In other words, for the same chip cross-sectional area, K_p will be larger when the so-called slenderness ratio is

larger, i.e., when the ratio of the depth of cut to the feed per revolution is larger.

While a deep cut and small feed (i.e., a large slenderness ratio) permits an increase in the cutting speed according to the so-called extended cutting speed law, this combination of the depth of cut and feed also increases the unit cutting force K_p. An increase in the cutting force, however, is a disadvantage because no increase in the metal removal results. However, larger forces do arise and hence, larger deformations of the machine and workpiece occur. The combined increase of cutting speed and cutting force caused by a large slenderness ratio requires also an increase in machine power. This means that a deep cut favors tool life; a shallow cut favors the metal removal rate and accuracy of turning. In other words, power requirements and cutting forces decrease as the chip cross-section approaches the shape of the square; this, however, occurs at the expense of tool life which is adversely affected thereby.

From equations (2.12),(2.13) and (2.14), it follows that

$$F_T = c_k \, b^{1-u} \, s^{1-w} = c_k b^x \, s^y \qquad (2.15)$$

and since b does not affect K_p, $u = 0$ and $x = 1$. The exponents y and w can be determined from experimental data. Due to lack of such information in deep-hole machining, it was decided to use data established for the turning operation.

Such data were found in the VDF machine tool catalogue [68].
It has been successfully used for the torque and power predic-
tion in turning for a long period of time in Germany, and
elsewhere. The data were plotted in the log-log grid for three
characteristic groups of materials as shown in Fig. 2.5.

As can be seen from the diagram, there are three groups
of materials whose plots could be satisfactorily fitted by
straight lines for the range of the variable s between
0.1 and 0.5 mm. Linear extrapolation can be used for
s less 0.1 mm. Also the values of K_p for s = 1 mm, denoted
by c_k are determined by linear extrapolation to ensure the
correct values of K_p between 0.05 and 0.5 mm. This procedure
is commonly used in the empirical approach. The slope of the
sets of straight lines represents the exponent w of the variable
s. This follows from equation (2.13) if its logarithm is
taken, keeping in mind that u = 0

$$\log K_p = \log c_k - w \log s \qquad (2.16)$$

Obviously, from this equation $K_p = c_k$ when s = 1 mm.

Table 2.1 gives relevant parameters evaluated from the
diagram in Fig. 2.5. These values are valid only for the
range of s stated that happens to be encountered mainly in
the practice of deep-hole machining.
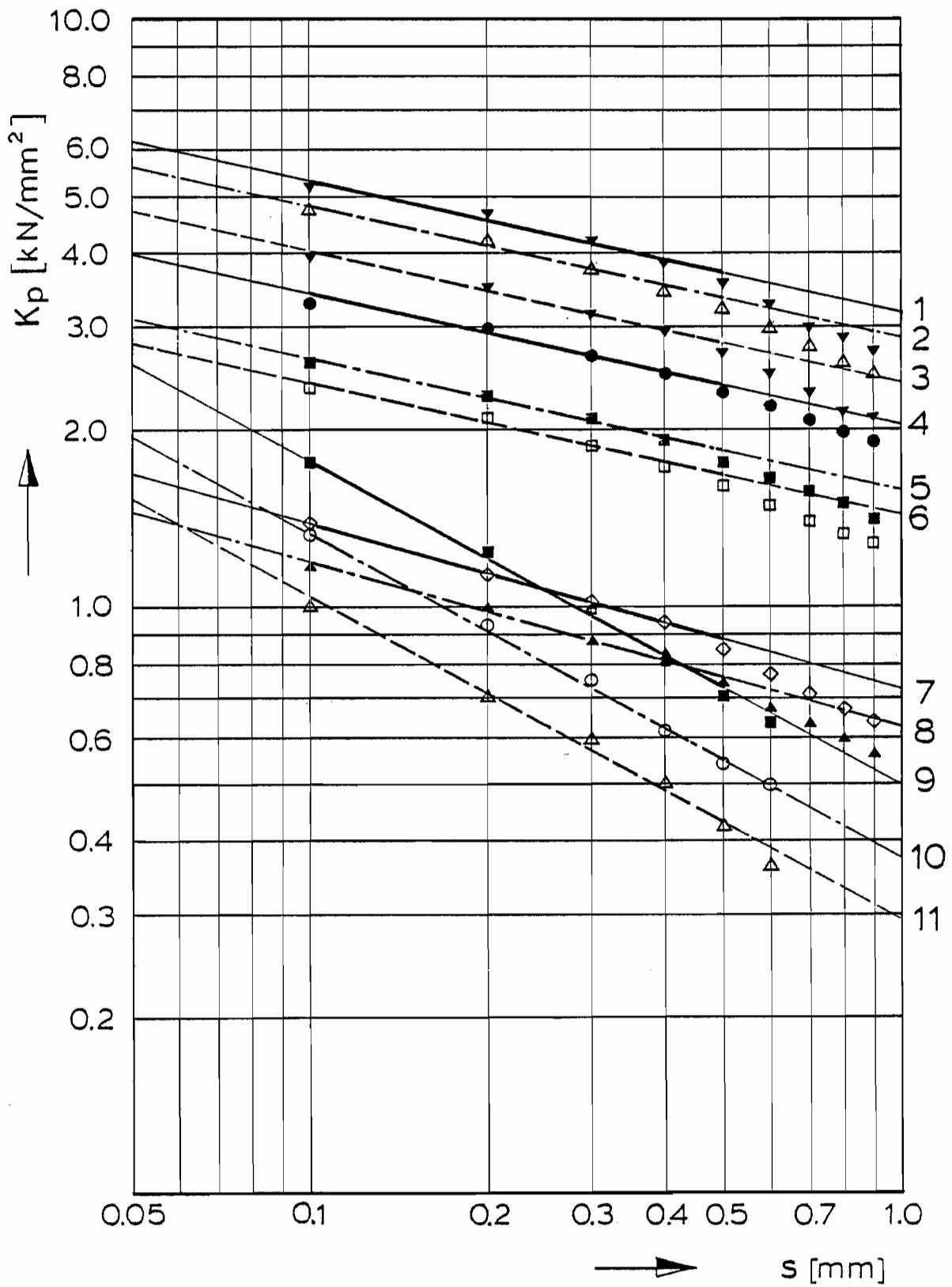
FIG. 2.5 UNIT CUTTING FORCE vs FEED IN TURNING

Data from [21] which represent a collection of the results of several German, American and Russian researchers, is condensed in Table 2.2 . In addition to the parameters relevant to the main cutting forces F_T, the Table contains parameters for determining the radial F_R and the feed F_F components, as proposed by several Russian authors [21]

$$F_R = c_k \ b^X \ s^Y \qquad (2.17)$$

$$F_F = c_k \ b^X \ s^Y \qquad (2.18)$$

If the values from Table 2.1 are compared to those given in Table 2.2, it results in the exponent for steel being identical, while for cast iron, brass and in particular, with regard to aluminum, large differences exist. In addition, from looking at Table 2.2, it can be observed that the radial and feed components are affected nonlinearly by the depth of cut, the exponents being 0.9 for the radial and 1.1 for the feed component.

Zorev [22] gives diagrams on log-log grids for steel and cast iron for the evaluation of different types of cutting operations. This parameter is in work units per volume and hence is identical to the unit cutting force K_p. If the exponent y is evaluated from these diagrams, its value varies

TABLE 2.1 VALUES RELATED TO DIAGRAM IN FIG. 2.1

No.*	MATERIAL	EXPONENT				Unit Cutting Force N/mm^2
		u	w	x	y	
1	Austenitic manganese steel					3150
2	Alloy steel 1400 - 1600 N/mm^2					2900
3	Alloy steel 950 - 1000 N/mm^2	0.	0.22	1.0	0.78	2400
4	Alloy cast iron 400 H$_B$					2050
5	Cast iron 180 - 260 N/mm^2					1580
6	Cast bronze; Cast steel					1450
7	Alloy for inject molding	0.	0.28	1.0	0.72	730
8	Brass; Duralumin					630
9	Al-alloy 80 H$_B$					500
10	Piston alloy	0.	0.54	1.0	0.46	385
11	Pure aluminium					295

* Numbers designate the plots given in the diagram.

TABLE 2.2 VALUES OF c_k, x AND y RELATED TO EQUATIONS (2.15), (2.17) AND (2.18)

		Cast Iron			Structural Steel			Cr-Ni-Steel		Cr-Steel		Bronze		Brass		Aluminium	
		H_B [kN/mm²]			s_u [kN/mm²]							H_B [kN/mm²]					
		1.4	1.8	2.0	0.45	0.6	0.7	0.5	0.7	0.45	0.7	0.2–0.3	0.3–0.38	0.22–0.36	0.36–0.48	0.6–0.8	0.8–1.0
F_T	c_k	0.96	1.1	1.11	1.57	1.71	1.84	1.78	2.03	1.72	2.03	0.8	1.0	0.7	0.85	0.4	0.6
	x	1.0			1.0			1.0		1.0		1.0		1.0		1.0	
	y	0.73			0.78			0.78		0.78		0.73		0.78		0.80	
F_R	c_k	1.02	1.08	1.11	0.72	0.91	1.03	0.86	1.13	0.79	1.13	–		–		–	
	x	0.9			0.9			0.9		0.9		–		–		–	
	y	0.75			0.75			0.75		0.75		–		–		–	
F_F	c_k	0.44	0.55	0.6	0.44	0.55	0.63	0.53	0.69	0.48	0.69	–		–		–	
	x	1.10			1.10			1.10		1.10		–		–		–	
	y	0.65			0.55			0.55		0.55		–		–		–	

between 0.8 and 0.9 with the mean at 0.86 for steel and be-
tween 0.78 and 0.84 with the mean at 0.8 for cast iron. These
values are slightly higher than those in Table 2.1 and
Table 2.2.

Kronenberg [23] indicates that the unit cutting
force can be evaluated by the use of an exponent for the feed of
w = 0.2 from the A.S.M.E. Manual. This value was originally
accepted for SAE 1020 steel, but further analysis showed that
this relation between the feed and the unit cutting force for
other steels can be averaged, resulting in parallel lines.
This value of the exponent is 0.8.

2.2.2 Twist Drilling Operation

The forces of interest in twist drilling are the tangent-
ial or power contributing component usually expressed by the
torque T and the thrust component in the direction of feed
along the drill axis F_F. The radial components cancel out due
to drill symmetry. The torque and thrust are generally
evaluated from empirical testing, though there were attempts
for the evaluation of torque from basic cutting mechanics by
an analytical approach [26] . In the latter case, the chisel
edge effect had to be eliminated by drilling a pilot hole.

The torque and thrust force derived from an analysis of
empirical testing follow relations of the form

$$T = C\ D^{X_1} f^{Y_1} \qquad\qquad (2.19)$$

$$F_F \quad K\ D^{X_2} f^{Y_2} \qquad\qquad (2.20)$$

where

   f = feed

   D = drill diameter

   C and K are material constants dependent on the drill geometry and cutting fluid and x_1, x_2 y_1 and y_2 are exponents experimentally determined for various materials.

   Boston and Oxford [8] have found $x_1 = 2.0$, $x_2 = 1.0$ $y_1 = 0.6$ and $y_2 = 0.6$ for cast iron and $x_1 = 1.8$, $x_2 = 1.0$, $y_1 = 0.78$ and $y_2 = 0.6$ for steel.

   Other investigators [9] these constants have been determined for various materials using different cutting fluids. They concluded that the exponents x_1, x_2, y_1 and y_2 remained unchanged within certain groups of materials such as those in the turning operation. However, the material constants C and K for different steels varied with the strength of material and the cutting fluid used. While a change in these constants was somewhat proportional to the ultimate strength of the metal, the effect of the cutting fluids was recorded through a decrease in these constants, ranging up to 33 per cent, compared to drilling dry.

These constants, seem to be different in small commercial drills because of the smaller effect of the chisel edge, as was found by Boston and Gilbert [10]. If the drill diameter is between 1/8 and 1/2 inch then $y_2 = 0.87$ for steel. For the SAE 1020 steel, they found that $Y_2 = 0.78$, an exponent which is identical to Y_1.

Meanwhile, Kronenberg proposed using $x_1 = 1.803$ and $Y_1 = 0.803$ [15].

Shaw and Boston, Jr. [15] treated the problem in a semi-analytical fashion computing the torque and thrust using dimensional analysis. They derived general equations for drill torque and thrust considering the influence of web thickness. When a standard drill is assumed with the web to diameter ratio, a constant equal to about 0.18, approximated in the normal range of feeds, their relations simplify to

$$T = 0.087 \ H_B \ D^{1.8} f^{1.8} \qquad (2.21)$$

$$F_F = K' H_B D \ f^{0.63} \qquad (2.22)$$

Equation (2.21) is identical to Kronenberg's relation and equation (2.22) is very close to the original relation of Boston and Oxford. An interesting feature of these relations is the proportionality of the cutting forces to the Brinell hardness.

2.3   COMPUTATION OF CUTTING FORCE
COMPONENTS

From the evidence of the cutting force prediction through both cutting mechanics and empirical testing, it seems that equations (2.7) to (2.11) can be used for calculating of the forces provided a reliable experimental relation between the chip ratio and the effective depth of cut is available. From the computations given in Appendix 2, based on a hypothetical relation derived from tests in turning, it appears that the best agreement with the experimentally measured force components was achieved from an approximation of Oxley's shear angle relationship[24]. Hence, this is in agreement with a recommendation for the general use of this relationship in cutting force evaluation from the cutting mechanics, provided that the constants c_1 and c_2 are determined in each particular case of application to suit the range of cutting conditions under consideration [24]:

$$\phi = c_1 - c_2(\tau-\alpha) \qquad (2.23)$$

In addition, an investigation into the chip ratio-depth of cut relation should be carried out to find a relationship similar to those given by (A2.8) and (A2.13) in Appendix 2. The investigation should be conducted in deep-hole machining operations and most probably can provide such results of a much narrower range of the variable s than it was possible to do in the turning operation, but still sufficiently wide

for this purpose.

Since such an investigation is not the major concern
of this work, a combination of the theoretical approach,
based on cutting mechanics and the empirical approach, based
on tests in turning and drilling is used. Namely, the thrust
force component will be evaluated empirically and then re-
solved into the radial and feed components, depending on the
tool geometry defined by angles κ. In addition, the
unit cutting forces will be evaluated from experimental data
in deep-hole machining for a particular material and multi-
pliers, based on the tensile strength and Brinell hardness,
established for other materials. Such correlations of
theoretical and empirical cutting force laws have already been
used in turning [23,25].

Accordingly, the thrust force formulation must contain
the radial and feed component raised to the same power. In
turning steel, this exponent can be an average of 0.55 and
0.75, as given in Table 2.2, for the radial and feed components.
This value of 0.65 seems to be close to the values of 0.6-0.63
found by many researchers for the thrust force in drilling.
In addition, the trend of the unit cutting force found with
this value of the exponent seems to be in good agreement with
trends resulting from some shear-angle relations, see the
diagram in Fig. A2.2 - Appendix II.

The exponent y in the main cutting force seems
to be less difficult to select. Namely, in turning this ex-
ponent varies from 0.78 to 0.9 for steel. In drilling steel
it was established at an average value of 0.8. So, an appropriate
value for this exponent, from the experimental results, is
0.8, although trends of the unit cutting force from the
diagram in Fig. A2.2 - Appendix 2, favours a slightly higher
value.

The exponent for the depth of cut in turning x is
one for the main cutting force. For the radial and feed force
components, however, it was found to be 0.9 and 1.1, respective-
ly. If it is to be a common exponent for the thrust force, an
average value of 1.0 should be selected. This value is in
agreement with the value of the exponent for the diameter in the
thrust force in drilling. This is also in agreement with the
assumption that no side spread occurs in chip, formation which
means that the chip ratio and hence, the unit cutting force, are
not affected by the width of cut b.

Therefore, the relationship between the cutting force
components and the chip cross-sectional area can be expressed
by the extended cutting force law

$$F_{pk} = C_{kp} \; b_k^{x_1} \; s_k^{y_1} \qquad (2.24)$$

$$F_{qk} = C_{kq} \; b_k^{x_2} \; s_k^{y_2} \qquad (2.25)$$

where $x_1 = 1.0$, $y_1 = 0.8$, $x_2 = 1.0$, $y_2 = 0.65$ and C_{kp} and C_{kq} are unit cutting forces for $s = 1$ mm. They are computed from the experimental values of the tangential and radial cutting force components. As stated, these unit cutting forces are taken as constant along the cutting edge of a tool except for the inner zone where higher values were found, both analytically and experimentally, and taken into account through the multipliers ζ_p and ζ_q; the multipliers giving an average increase over the zone.

Equations (2.24) and (2.25) are used instead of equations (2.10) and (2.11), but equations (2.7) to (2.9) are unchanged and they constitute the governing equations for the prediction of the cutting forces in deep-hole machining with a single-edge cutting tool. They are to be used for both solid-boring and trepanning tools.

As an example of the tool for which experimental data are available from recent research work [62, 70] the tool can be taken with the following parameters: $D = 50$ mm, $p_1 = 6.5$ mm, $p_2 = 14$ mm, $p_3 = 4.5$ mm, $\kappa_1 = 18$ deg, $\kappa_2 = 12$ deg, $\kappa_3 = 20$ deg, the workpiece material is DIN-C60 steel similar to SAE 9255, cutting speed 90 m/min and feed 0.14 mm/rev. The cutting force components experimentally measured $F_T = 9250$ N, $F_R = 1040$ N and $F_F = 7000$ N.

By the use of equations (2.7) to (2.9), taking into account equation (2.24) and (2.25), we can compute c_{kp} and c_{kq}

since the multipliers can be evaluated from the experimental results at $\zeta_p = 1.16$ and $\zeta_q = 1.28$

$$F_T = \sum_{k=1}^{3} c_{kp} \, b_k^{X_1} \, s_k^{Y_1} \qquad (2.26)$$

since c_{kp} and s are common to all zones,

$$F_T = c_{kp} s^{Y_1} (p_1^{X_1} + p_2^{X_1} + \zeta_p p_3^{X_1}) \qquad (2.27)$$

from which c_{kp} as the only unknown, can be determined. Using the given data, it was found that $c_{kp} = 1733.68$ N/mm^2.

Similarly,

$$F_R = \sum_{k=1}^{3} c_{kq} \, b_k^{X_2} \, s_k^{Y_2} \, \sin \kappa_k \qquad (2.28)$$

or in an expanded form

$$F_R = c_{kq} \, s^{Y_1} (p_1^{X_2} \sin\kappa_1 + p_2^{X_2} \sin\kappa_2 + \zeta_q p_3^{X_2} \sin\kappa_3) \qquad (2.29)$$

from which c_{kq} can be determined. If the given data is used then $c_{kq} = 1265.68$ N/mm^2.

But if the value of c_{kq} can also be computed from the feed component

$$F_F = \sum_{k=1}^{3} c_{kq} \, b_k^{X_2} \, s_k^{Y_2} \, \cos \kappa_k \qquad (2.30)$$

which in expanded form becomes

$$F_F = c_{kq} \ s^{Y_2}(p_1^{X_2} \ \cos\kappa_1 + p_2^{X_2} \ \cos\kappa_2 + \zeta_q p_3^{X_2}\cos\kappa_3) \qquad (2.31)$$

from which c_{kq} = 993.55 N/mm^2. Ideally, the values computed from the radial and feed components should coincide. Because of the simplified model of the cutting forces used and possible errors occurring in the experimental measurements, these two values differ. The value used in subsequent calculations is the average of these two, hence c_{kq} = 1129.61 N/mm^2.

The cutting force components computed from these parameters are included in Table A2.1, from which it can be seen that they agree very well with the values computed from an approximation of Oxley's shear angle relationship. A comparison of the experimental results is not meaningful.

Another example of the tool for which experimental data are available from [1] is:

D = 35 mm, p_1 = 8.25 mm, p_2 = 5.65 mm, p_3 = 3.6 mm, κ_1 = 18 deg, κ_2 = 12 deg, κ_3 = − 20 deg, workpiece material the steel DIN C.60 − similar to the steel SAE 9255, cutting speed 107.75 m/min and feed 0.16 mm/rev. The cutting force components measured experimentally are F_T = 5000N, F_R = 2800 N and F_F = 5300 N. The cutting force components evaluated from these parameters are tabulated in Table A2.2. The forces in row 7 are based on the empirical relation using the unit

cutting forces computed in the first example. They agree best with the results obtained from Oxley's shear angle relationship, but differ significantly from the measured components. The difference is remarkable in the radial component which is the major reason why the data could not be used as a base for the empirical cutting force computation.

This difference in the cutting force components, particularly in the tangential and radial forces which constitute the cutting force F in the plane normal to the tool axis, affects the angle θ between F_R and F, often called the phase angle. This angle plays an important role in tool guidance since it defines the wear pad locations. It is defined by:

$$\theta = \tan^{-1}\left(\frac{F_T}{F_R}\right) = \cos^{-1}\left(\frac{F_R}{F}\right) \qquad (2.32)$$

From Tables A2.1 and A2.2, in Appendix 2, the differences in θ between the last three rows (6,7 and 8) of the first tool and rows 6 and 7 of the second tool are about one degree, which is certainly tolerable, from the viewpoint of the wear pads' location. But, the difference between these θ-s and the value obtained experimentally for the second tool is about 24 degrees and hence, it is unreliable in the prediction of the cutting force direction.

The experimental evidence concerning the cutting force components in deep hole machining reported in [35] shows a

ratio of (F_T/F_R) = 4.25 for workpiece material EN8, giving an angle θ of approximately 77 deg. Unfortunately, nothing was reported on the tool geometry used, except that its diameter was 22 mm, so any further comparison with the two examples is not possible. Nevertheless, the example proves that the cutting force components reported in [62,69] are more likely to occur in deep hole maching than those reported in [1]. This is why the data obtained from the first example are more reliable for further use in the prediction of the cutting forces in deep-hole machining.

Another aspect, which is important from the viewpoint of tool guidance, is the variation of θ due to fluctuations in F_R and F_T caused by feed variations. These feed variations are necessary in order to control the chip formation. This can be illustrated by an example likely to occur in practice. Suppose an optimal effective cutting depth is 0.15 mm and for purposes of chip formation control, it is varied ± 50 per cent. If the exponent y_1 and y_2 were identical, θ would not vary at all. For values of y_1 and y_2 equal 0.8 and 0.65 respectively, selected for further use, it appears that the given variation in s would cause θ to range between −0.63 and + 0.33 deg, which may be considered well below the significant variation in a cutting force direction. The same cutting depth variation would, however, cause cutting force variation in a magnitude of between − 42.5 and + 38.2 per cent. These cutting force variations, both in magnitude and direction during a period of

initial feed variation to achieve stable cutting with optimal chip form, should be within certain permissible limits, in order to make this feed variation possible. The example illustrates that during that period, the cutting force will vary in magnitude while retaining an almost constant direction. This agrees with the experimental results reported in [35] which show that although the cutting force magnitudes vary for different feed-speed combinations, their relationship appears to remain constant.

The greatest number of reports on experimental cutting force measurements in turning show that the radial components are more affected by the variation in the depth of cut than the tangential component [59], although there are reports which reveal a linear relationship between the force components and the effective depth of cut [58]. From this analysis, the latter is unlikely to be true, except for large positive rake angles, when the chip ratio seems to be independent of the depth of cut [22].

CHAPTER III

DESIGN CONCEPT AND EXPERIMENTAL RESULTS USING
STAGGERED UNSYMMETRICAL MULTI-EDGE TOOLS

CHAPTER III

DESIGN CONCEPT AND EXPERIMENTAL RESULTS USING
STAGGERED UNSYMMETRICAL MULTI-EDGE TOOLS

3.1 BASIC CONCEPT

The concept of staggered multi-edge tools with cutters
unsymmetrically located on the cutting head represents a step
forward, compared to the conventional single-edge tools. In
this tool, each cutter cuts over its circular zone, partly
overlapping with each other, as shown in Figure 3.1(a). The
name comes from their staggered or zigzag arrangement with
possible overlapping of the cutters.

This tool has an advantage over the conventional single-
edge tool in partially balanced cutting forces. Similarly as
that of the ejector tools, this arrangement takes some of the
load off   the supporting pads. In Fig. 3.1, a single
pad has a symbolic meaning to designate the direction in which
the tool should be supported. In actual tools, each pad is
replaced with at least two wear pads, conveniently
located relative to this position, depending on what amount of
friction is anticipated at the wear pads.

Another advantage is that the cutters can be combined
at will, as far as their approach angles κ are concerned, in-
cluding the use of standard carbide or trepanning inserts.
In addition, carbide grades can be combined, taking for the

outer and middle cutters higher grades to meet higher hardness requirements and for the inner cutter, lower grades to meet higher toughness requirements.

The concept also allows better design flexibility in order to achieve maximum tool strength by proper location of chipmouths and chipthroats. This, by itself, contributes to the better balance of the mass in rotated tools.

Flexibility of the concept in achieving an optimal resultant force transmitted to the bore-wall is illustrated in Fig. 3.1. An initial arrangement with the three cutters located as shown in (a) would give the resultant force $\vec{R}$ (b) with the support reaction $\vec{R}_s$. This arrangement, obviously, would not be good for two reasons, first, the outer cutter which controls the hole size is not located opposite nor nearly opposite to the supporting pad to ensure an efficient hole-size controlling effect, and secondly, the tool would not be capable of supporting itself during its initial cut into a workpiece because $\vec{F}_1$, the cutting force of the middle cutter which cuts first, is not pointing against the supporting pad. The latter could be achieved by interchanging the location of the middle and outer cutters, but the hole size controlling effect would be completely lost. Moreover, a small initial oversize or undersize would tend to increase rapidly. But, if the inner cutter is angularly displaced by $\Delta\phi_3$ counter-clockwise, the cutting force of this cutter, although constant in magnitude, will change to the vector $\vec{F}_3'$ with a new cutting force
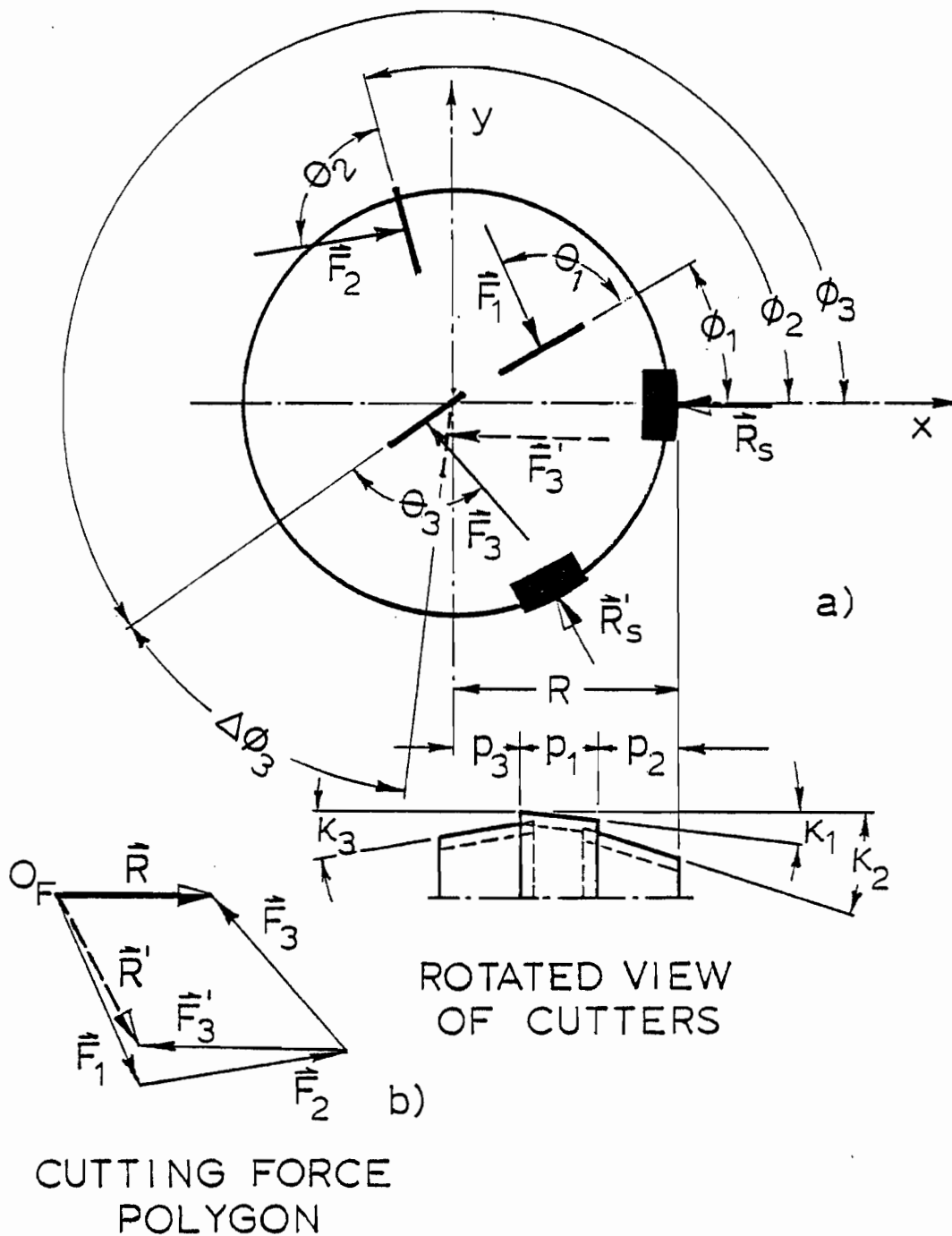
FIG. 3.1   SOLID BORING HEAD WITH STAGGERED
              CUTTERS

resultant $\vec{R}'$, as shown in (b). The new arrangement has the

support reaction $\vec{R}'_s$ which eliminates the shortcoming of the

previous set-up. Namely,the outer cutter,which controls the

hole size is located nearly opposite to the supporting pad and

the tool will be supported during its initial cut, since the

force $\vec{F}_1$ points against the supporting pad.

The example illustrates the possibility of achieving

an optimal tool arrangement by simple trial and error approach.

Though the cutting forces remain constant in magnitude, the

concept leaves a lot of possibilities in the attainment of a

predetermined cutting force resultant and hole size controll-

ing conditions by angularly displacing the cutters and/or inter-

changing their locations.

The staggered unsymmetrical tool, although a multi-edge

tool,does not take full advantage of the multi-edge cutting

principle since the length of all cutting edges covers only

one tool radius. Therefore, this is equivalent to a single-edge

tool in terms of metal removal rate. However, because of

the possibility of combining carbide grades, it may allow a

slightly higher feed rate or an extended tool life, compared

to a single-edge tool.

The cutting force system, acting upon a staggered un-

symmetrical multi-edge tool, as presented in Fig. 3.1, implies

that all elastic effects are negligible. Namely, the boring

bar with the cutting head is considered as a beam fixed at one

end and loaded by the cutting force resultant at the other end.
This resultant will be fully transmitted to the supporting
pad if the so-called encastré effect is neglected. This effect
is greatly affected by the amount of clearance and film thick-
ness between the supporting pad and the machined bore. In the
case of thin-film lubrication, this clearance is infinitely
small and therefore, elastic effects can be neglected.

The problem of cutting force balance can be described
analytically in the Cartesian coordinate system x-y for a tool
of n cutting edges. $\vec{F}_1, \vec{F}_2, \ldots, \vec{F}_n$ are the cutting forces;
$\theta_1, \theta_2, \ldots, \theta_n$ are the angles between the cutting forces and
corresponding cutting edges, often called the phase angles,
$\vec{T}$ is the drive torque and $\vec{R}_s$ is the supporting pad reaction.
From the equilibrium conditions

$$\vec{T} + \sum_{i=1}^{n} (\vec{r}_i \times \vec{F}_i) = 0; \quad i = 1, 2, \ldots, n \qquad (3.1)$$

and

$$\vec{R}_s = -\sum_{i=1}^{n} (\vec{F}_i) \qquad (3.2)$$

Expressing equation (3.2) in complex form,

$$\vec{R}_s = |\vec{R}_s| \, e^{j\lambda} = -\sum_{i=1}^{n} |\vec{F}_i| \, e^{j(\phi_i + \theta_i)} \qquad (3.3)$$

where λ is the angle of $\vec{R}_s$ vector with respect to the x-axis.
Equation (3.3), written in trigonometric form becomes

$$|\vec{R}_s| = \{[\sum_{i=1}^{n} |\vec{F}_i| \cos(\phi_i + \theta_i)]^2$$

$$+ [\sum_{i=1}^{n} |\vec{F}_i| \sin(\phi_i + \theta_i)]^2\}^{\frac{1}{2}} \qquad (3.4)$$

The line of action of $\vec{R}_s$ is given by the angle λ as

$$\lambda = \tan^{-1}[\sum_{i=1}^{n} |\vec{F}_i| \sin(\phi_i + \theta_i) / \sum_{i=1}^{n} |\vec{F}_i| \cos(\phi_i + \theta_i)] \qquad (3.5)$$

Equation (3.5) determines the location of the supporting pad in terms of the cutting edge locations, phase angles and the number of cutters. By controlling $\vec{F}_i, \phi_i, \theta_i$ and n, the conditions necessary for tool guidance and stability can be determined. The cutting force magnitudes can be found from equations (2.26) and (2.28) as:

$$|\vec{F}_i| = (F_{Ri}^2 + F_{Ti}^2)^{\frac{1}{2}} \qquad (3.6)$$

and the phase angles θ_i from equation (2.32). The number of cutters can be conveniently selected for each particular tool.

By expanding equation (3.4) and taking into account

$$F_{Ri} = |\vec{F}_i| \cos \theta_i \qquad (3.7)$$

$$F_{Ti} = |\vec{F}_i| \sin \theta_i \qquad (3.8)$$

we get

$$|\vec{R}_s| = \{[\sum_{i=1}^{n} (F_{Ri} \cos \phi_i - F_{Ti} \sin \phi_i)]^2$$

$$+ [\sum_{i=1}^{n} (F_{Ri} \sin \phi_i + F_{Ti} \cos \phi_i)]^2\}^{\frac{1}{2}} \qquad (3.9)$$

and also

$$\lambda = \tan^{-1} \left\{ \frac{\sum_{i=1}^{n} (F_{Ri} \sin\phi_i + F_{Ti} \cos\phi_i)}{\sum_{i=1}^{n} (F_{Ri} \cos\phi_i - F_{Ti} \sin\phi_i)} \right\} \qquad (3.10)$$

Equations (3.9) and (3.10) together with equations (2.26) and (2.28) can be used for direct computation of the supporting pad reaction and its angular location on the cutting head for a given tool diameter, number of cutting edges, their geometry and the feed selected for each particular workpiece material.

3.2 OPTIMIZATION OF THE TOOLS

The supporting pad reaction R_s and its angular location λ are parameters which, in addition to the widths of cut and angular locations, determine the cutting head shape. Hence, a designer must know them in advance before making any layout of the head. R_s should be large enough to eliminate the possibility of an indeterminate supporting force R_s. At present, R_s can be taken approximately equal to the magnitude of the cutting

force in a single-edge tool, but more precise criterion will be developed in the next chapter.

Since the widths of cut are determined by the tool diameter and can be approximated from R/n, where n is the number of cutters, and since the tool is designed for a particular workpiece material, the cutting force magnitude is constant and can be calculated. The locations of the cutter, ϕ_i, however, as well as the supporting pad location λ are parameters which may be varied in order to attain a predetermined R_s. This 'trial and error' procedure could be done best graphically, but better accuracy would be achieved analytically, by using equations (3.9) and (3.10). The trial and error procedure is lengthy and an optimization procedure would do the job faster.

Our objective is obviously achievement of a predetermined R_s, so the objective function can be constructed from equations (3.9) and (3.10) as follows:

$$Y(\phi_i, \lambda) = \left| \left\{ \left[\sum_{i=1}^{n} F_{Ri} \cos(\phi_i - \lambda) - F_{Ti} \sin(\phi_i - \lambda) \right]^2 \right. \right.$$

$$\left. \left. + \left[\sum_{i=1}^{n} F_{Ri} \sin(\phi_i - \lambda) + F_{Ti} \cos(\phi_i - \lambda) \right]^2 \right\}^{\frac{1}{2}} \right| - |\vec{R}_s|$$

$$(3.11)$$

with the constraint given by equation (3.10).

The objective function can be greatly simplified by rotating the coordinate system at λ counter-clockwise

$$Y(\phi_i) = \left| \sum_{i=1}^{n} (F_{Ri}\cos \phi_i - F_{Ti}\sin \phi_i) \right| - |\vec{R}_s| \qquad (3.12)$$

with the constraint

$$\sum_{i=1}^{n} (F_{Ri}\sin \phi_i + F_{Ti}\cos \phi_i) = 0 \qquad (3.13)$$

In addition to the constraint (3.13) the system is subject to additional restrictions in terms of the variable ϕ_i. Namely, the outer cutter must be located in an angular zone opposite the   supporting pad and the cutting force vector of the cutter making the initial cut must point against the supporting pad.These restrictions can be taken into account by prescribing the lower and upper bounds for the corresponding parameters ϕ_i.

It is obvious that the system (3.12) is subject to the equality constraint (3.13), so that a modified objective function can be constructed to give an unrestricted form as follows:

$$Y(\phi_i) = \left| \sum_{i=1}^{n} (F_{Ri}\cos \phi_i - F_{Ti}\sin \phi_i) \right| - |\vec{R}_s|$$

$$+ k_w \left| \sum_{i=1}^{n} (F_{Ri}\sin \phi_i + F_{Ti}\cos \phi_i) \right| \qquad (3.14)$$

where k_w is the positive weighting factor.

As we see from (3.14) the modified objective function represents a multivariable, unconstrained, nonlinear function which should be a minimum; preferably zero.

The method used to minimize (3.14) is basically a numerical, direct search method accelerated in distance proposed by Hooke and Jeeves [63]. The procedure requires no derivatives and assumes a unimodal function; therefore, if more than one minimum exists or the shape of the surface is unknown, several sets of starting values are recommended [64,65].

The algorithm minimizes the function

$$F(x_1, x_2, \ldots, x_n) \tag{3.15}$$

in the following procedure:

(1) A base point is picked and the objective function evaluated.

(2) A local exploration is made in each direction by stepping x_i, a distance Δ, to each side and evaluating the objective function to see if a lower function is obtained.

(3) If there is no function decrease, the step size is reduced and exploration is repeated from the previous best point.

(4) If the value of the objective function has decreased a new temporary base point $x_{i,0}^{(k+1)}$ is located using the two previous base points $x_i^{(k+1)}$ and $x_i^{(k)}$:

$$x_{i,0}^{(k+1)} = x_i^{(k+1)} + \alpha \left[x_i^{(k+1)} - x_i^{(k)} \right] \qquad (3.16)$$

where

i = the variable subscript $1,2,\ldots,n$

0 = the temporary base point

k = the stage subscript (a stage is the end of n searches)

α = an acceleration factor $\alpha \geq 1$

(5) If the temporary base point results in a lower function value a new local exploration is performed about this point, a new base point is located and the value of F checked. This expansion continues as long as F decreases.

(6) If the temporary base point does not result in a lower function value, a search is made from the previous best point.

(7) The procedure terminates when the convergence criterion is satisfied.

A descriptive flow chart for the pattern search is given in Fig. 3.2, while a descriptive flow chart for the exploratory moves is given in Fig.3.3. The detailed flow chart given in Fig. 3.4 contains three stages of the variables X and Y during their transformation, the interpretation is as follows:

X = current base point

X_x = base point resulting from current move

X_{xx} = previous base point

Y = functional value at base point

Y_y = functional value resulting from current set of exploratory moves or pattern move

Y_{yy} = functional value resulting from current move

Δ = current step size

δ = "minimum" step size

ρ = reduction factor for step size, $\rho < 1$

$X \rightarrow X_x$ = the value of variable X is to become the new values of the variable X_x

$E:Y_y, X_x$ = a set of exploratory moves are to be carried out which will affect the values of the variables Y_y and X_x

A FORTRAN computer routine has been adapted for this particular task and is used to optimize the tool designs presented in the next section.
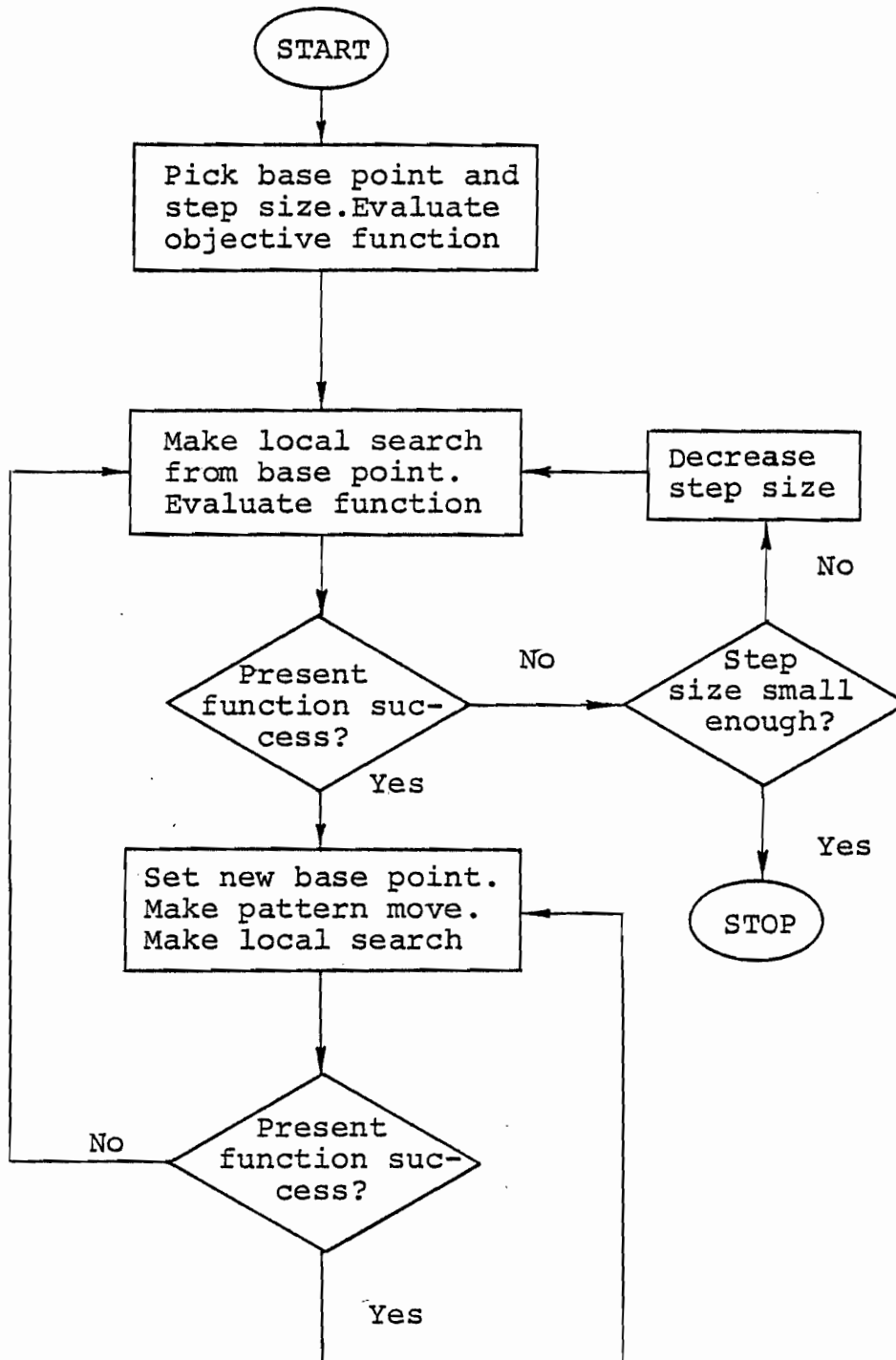
FIG. 3.2   DESCRIPTIVE FLOW CHART OF PATTERN
          SEARCH
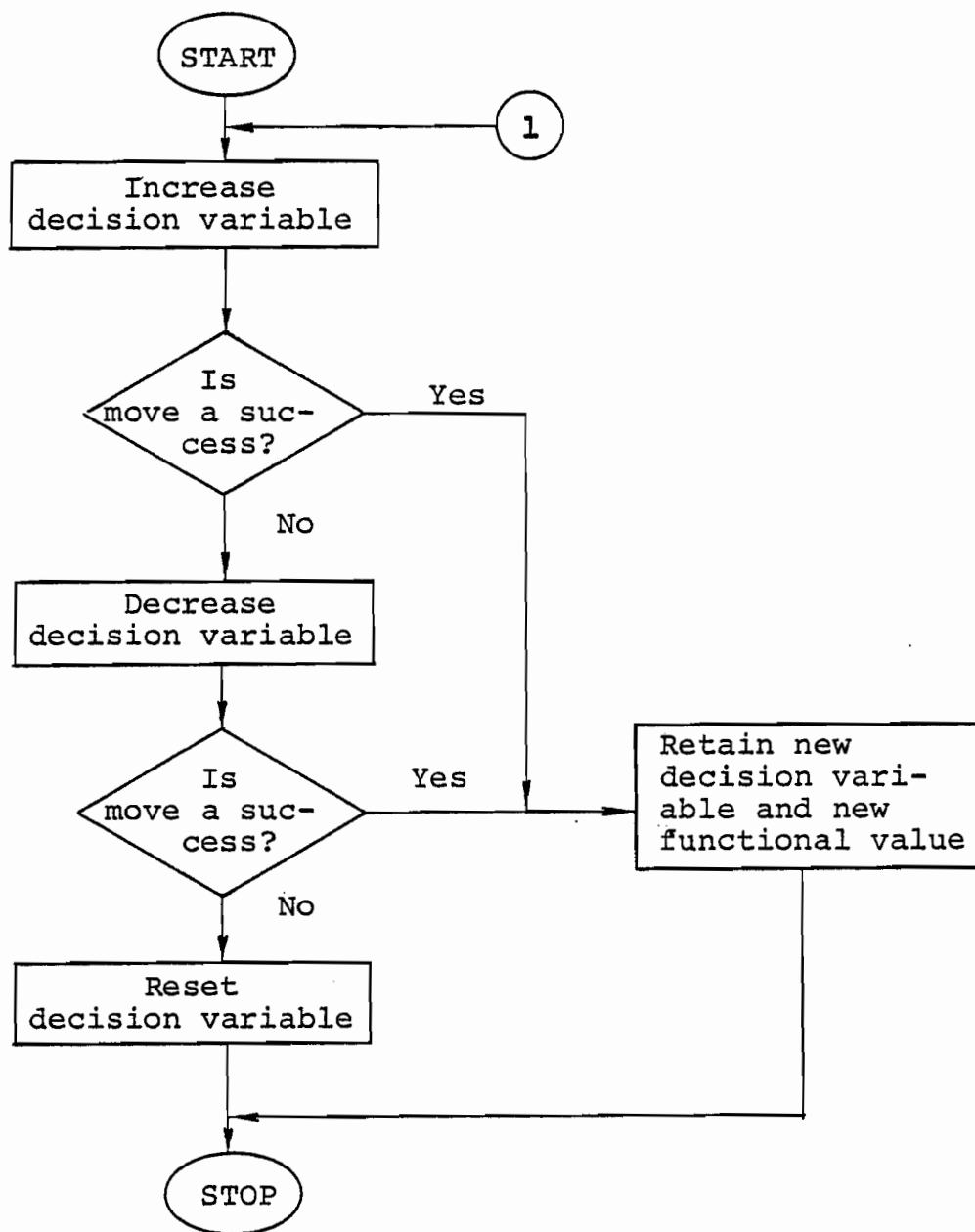
FIG. 3.3   DESCRIPTIVE FLOW CHART OF EXPLORATORY
MOVES

START

Read: X, Δ, δ
Calculate Y

$\dot{Y} \rightarrow Y_y \qquad X \rightarrow X_x$

E: Y_y, X_x

$\rho\Delta \rightarrow \Delta$

$Y_y < Y$?

No

$\Delta < \delta$?

No

Yes

Yes

STOP

$X \rightarrow X_{xx}, X_x \rightarrow X, Y_y \rightarrow Y$

$2X_x - X_{xx} \rightarrow X_x$ calculate

$Y_{yy} \cdot Y_{yy} \rightarrow Y_y$; E:$Y_y$;$X_x$

No

$Y_y < Y$?

Yes
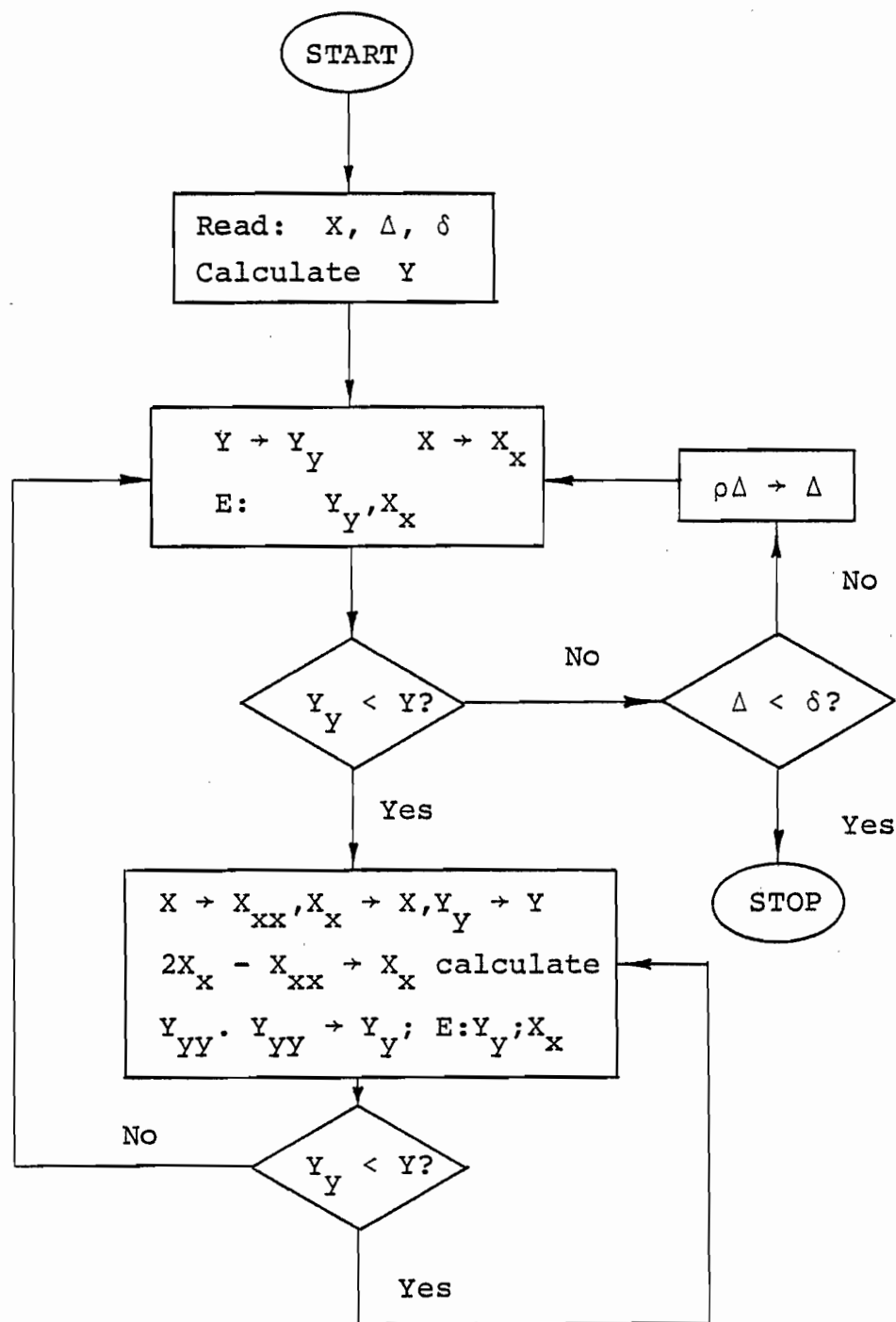
FIG. 3.4   DETAIL FLOW CHART OF PATTERN
          SEARCH

The program has originally been written as a maximization technique but was translated into the minimization algorithm by changing the sign of the objective function

$$\text{Maximize}\{-F(X_1,X_2,\ldots,X_n)\} = \text{Minimize } \{F(X_1,X_2,\ldots,X_n\}$$

The selection of the direct search method was prompted by its general suitability to small nonlinear problems. Since the chip-forming conditions and space problems in locating large numbers of cutters on a cutting head, together with the machine power and torsional rigidity of the boring bar do not allow too large a number of cutters to be used, it was decided to develop a technique capable of handling optimization of tools with a maximum of five cutters. For staggered tools the angular positions of the cutters constitute decision parameters. As it will be shown in the next chapter, the number of decision parameters in solid boring tools is at most, double. Thus, a problem where such small numbers of decision variables constitute a nonlinear objective function is best optimized with a direct search method. In addition, experience during the testing of the program showed that the parameters tend to change in one direction, while causing the objective function to converge to a minimum. This justified the application of the method accelerated in distance. The acceleration was in some cases, such that hundreds of times larger step sizes than the initial one were realized

between some of the base function evaluations. This also made normalization of decision variables unnecessary, because the algorithm, itself, accelerates a change of the variables with the larger effect on the objective function to converge to a minimum at each stage of the optimization process.

Sometimes it happens that the optimum achieved is a local, rather than a global one. This can be easily determined from the computer printouts. In this event, a change in either of the weighting factors, or in the vector of initial estimates for the decision variables, helps to achieve the global minimum which is zero by definition of the objective function.

The computer routine consisting of a main program and five subroutines appeared to be convenient and fast. The program listing and typical outputs are given in Appendix IV. The main program supplies the input data, calls for the sub-routines and prints the output. The first two subroutines carry out the pattern search and exploratory moves, as shown in the descriptive flow charts in Figs. 3.2 and 3.3, respectively. The third subroutine supplies lower and upper bounds for the decision variables. The fourth subroutine computes the radial and tangential cutting force components and evaluates the objective function. The last, fifth subroutine computes the resultant cutting torque and the resultant feed force, and evaluates the deviations in magnitude and direction for the resultant cutting force. A detailed analysis of

variations of the cutting forces is given in the next chapter.

The computer program is written in FORTRAN
and the calculations are performed on a CDC-6400 computer.
Some typical outputs show that the total number of functional
evaluations varies between 290 and 350, the number of the
base evaluations between 35 and 65, and the central processor
time, between 5.6 and 5.9 seconds.

3.3 DESIGN OF THE TOOLS

Two staggered tools, a solid boring head and a tre-
panning head, were optimized by trial and error, for the
purpose of testing, before the optimization technique was
developed. The same tools were optimized by the use of the
optimization procedure on the computer, based on the same
resultant force transmitted to the bore-wall.

The layouts of both the tested tools and the tools
resulting from the optimization by computer are shown side-by-
side, in Fig.3.5 and Fig. 3.6. Fig. 3.5 shows the solid
boring head of the two staggered, standard trepanning inserts,
unsymmetrically located, and Fig. 3.5 shows the trepanning
head with two staggered, standard trepanning inserts un-
symmetrically located. The standard trepanning inserts proved
convenient for use in testing the tools, because of their
fast and easy replacement in case of failure. A comparison
of the tools optimized by trial and error, and the tools
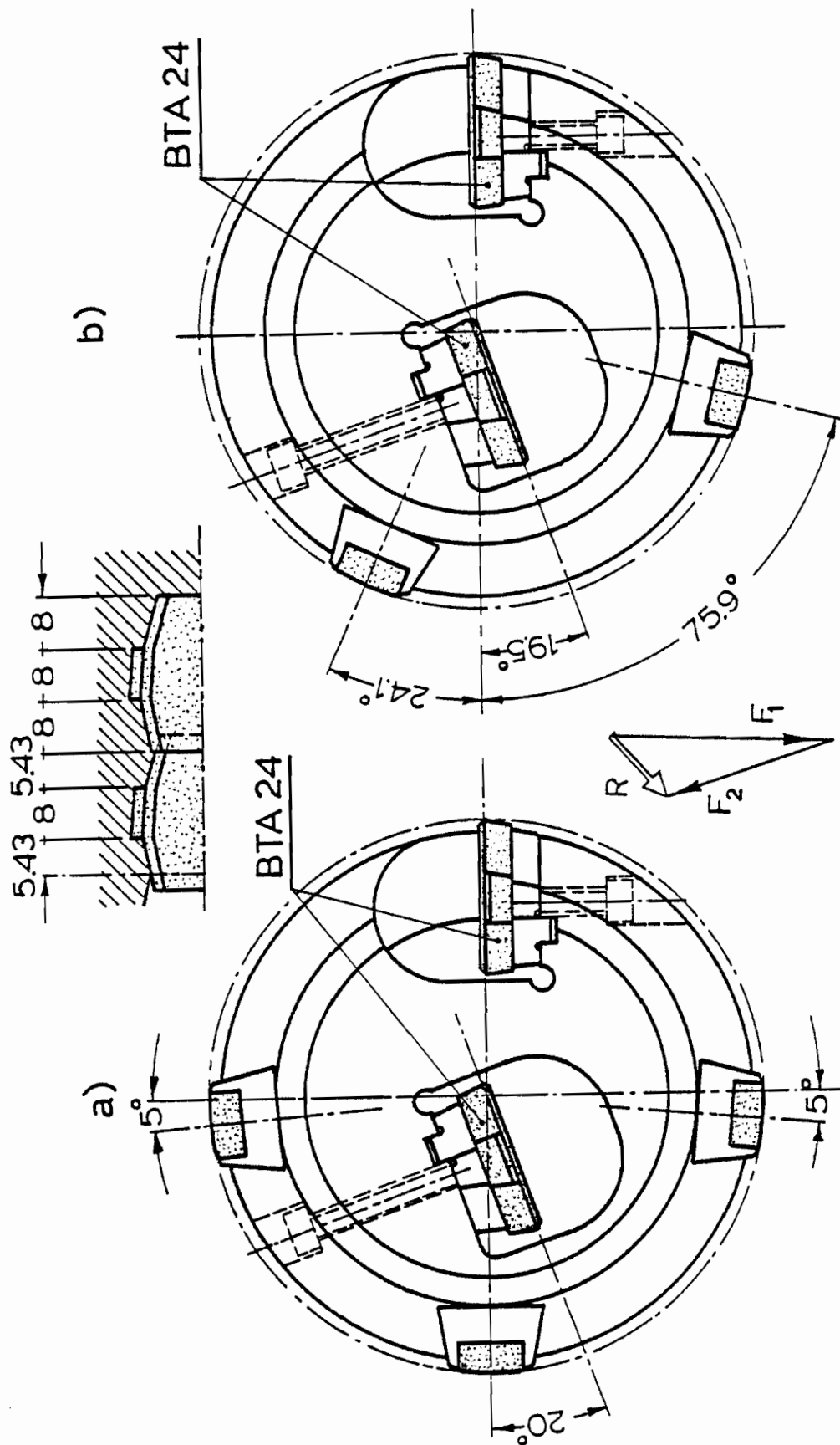
FIG. 3.5   3.375" DIA SOLID BORING HEAD WITH TWO STAGGERED CUTTERS

(a)   OPTIMIZED BY TRIAL AND ERROR AND TESTED
(b)   OPTIMIZED ON THE COMPUTER
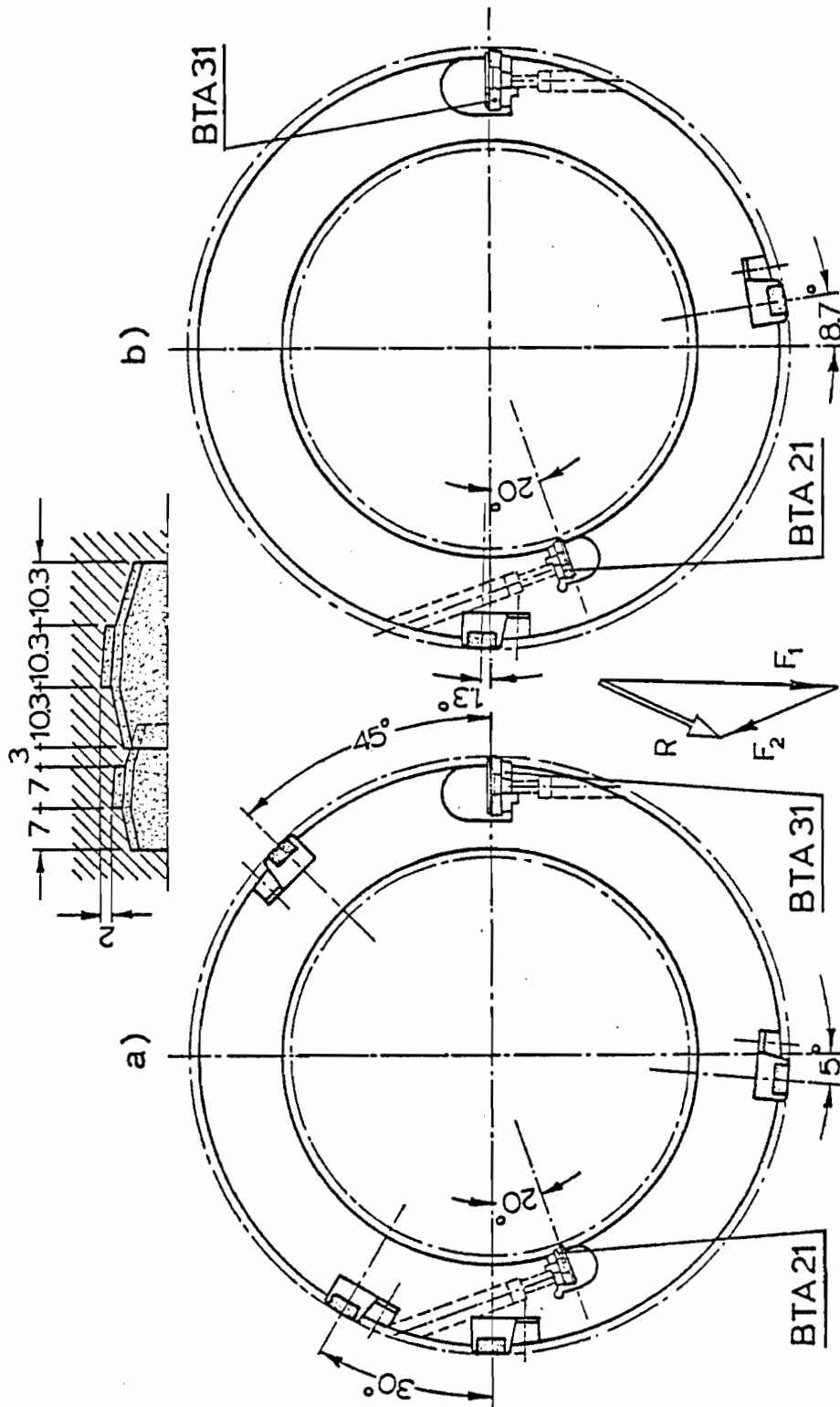
FIG. 3.6   11.760" DIA TREPANNING HEAD WITH TWO STAGGERED CUTTERS

(a)   OPTIMIZED BY TRIAL AND ERROR AND TESTED
(b)   OPTIMIZED ON THE COMPUTER

optimized by computer reveals that the differences are significant, including the difference in the concept of the tool supports, although they were optimized for the same supporting reaction. While in the optimization by trial and error, the supporting reaction is guessed in percentage of the cutting force exerted by a single cutter, in the optimization by computer this reaction is numerically evaluated at a predetermined value,provided the workpiece material and the feed are known. Moreover, its variations in magnitude and direction are predictable, provided information on the fluctuations of the cutting forces is available. If the deviations in magnitude and direction of the supporting reaction indicate that the tool stability is not ensured, an increase in this reaction would lead to an improvement in stability conditions. How the mechanism of a conditioned stability behaves, will be discussed in detail in the next chapter. For the present, however, it can be stated that the stability conditions for the solid boring head have been found satisfactory. Table 3.1, indicating the main parameters of the two tools, reveals that deviations of the supporting reaction of this tool are quite significant, particularly the deviation in direction. The purpose of these two examples is not to revise the optimum of the tools achieved by trial and error, but to check how the new technique handles problems already solved by the other method. It appeared that the two techniques did not yield the same optima, although the differences are tolerable, from a practical point of view. The

computer technique developed here, is, no doubt, more reliable and much faster. If combined with the statistical analysis of the cutting forces, it will yield the optimum of a tool with any number and geometry of cutting edges feasible in the practice of deep-hole machining.

3.4   TESTING OF THE TOOLS

A tool manufacturing company manufactured the two tools, shown in Fig. 3.5 and Fig. 3.6. The solid boring head was tested under the following conditions:

Application:	Rotating workpiece
Workpiece Material:	AISI 4140, 28/30 Rc.
Spindle Speed:	450 rpm
Surface Cutting Speed:	121 m/min (398 fpm)
Feed per Revolution:	0.339 mm/rev (0.0133 ipr)
Feed Rate:	152 mm/min (6 ipm)
Coolant Flow Rate:	(105 gpm, U.S.)
Coolant Pressure:	0.86 MPa (125 psi)

The trepanning head was tested with two workpiece materials, under the following cutting conditions:

Test No. 1

Application:	Rotating tool
Workpiece Material:	Heppenstall Grade H550-Die Steel 1.125
Boring Bar Speed:	100 rpm
Surface Cutting Speed:	94 m/min (308 fpm)
Feed per Revolution:	0.178 mm/rev (0.007 ipr)
Feed Rate:	17.8 mm/min (0.7 ipm)
Coolant Flow Rate:	(350 gpm,U.S.)
Coolant Pressure:	0.48-0.69 MPa (70-100 psi)
Tool Headstock Power:	43.5-49.5 KW (58.3-66.3 HP)
Feed Force:	14.7-27.1 kN (3,300-6,100 lbs)

Test No. 2

Application:	Rotating tool
Workpiece Material:	INCONEL 600
Boring Bar Speed:	60 rpm
Surface Cutting Speed:	56.3 m/min (185 fpm)
Feed per Revolution:	0.147-0.168 mm/rev (0.0058-0.0066 ipr)
Feed Rate:	8.8-10.1 mm/min (0.35-0.41 ipm)
Coolant Flow Rate:	(280 gpm, U.S.)
Coolant Pressure:	0.96-1.1 MPa (140-160 psi)
Tool Headstock Power:	22.8-25.2 (30.5-33.8)
Feed Force:	9.78-17.78 kN (2,200-4,000 lbs)

The tests revealed that the staggered tools, if optimized, work well and can deliver slightly higher feed rates than single-edge tools. The cutting operation is stable with no runouts. Also, no significant difference in hole accuracy and surface finish was found as compared to a single-edge cutting.

In addition, the tests with the trepanning head, during which the total power consumption and feed force were recorded, revealed that the cutting torque and feed force computered from the mathematical model developed in Chapter II, are in good agreement with the recorded values. Table 3.2 contains these values, as predicted and as recorded during the tests.

The torque and feed force as calculated by the computer and shown in Table 3.2, were corrected for differences in the effective cutting depth and shear strength of the workpiece material. The values of the feed force are in good agreement, the recorded values being higher because they include the effect of friction. The cutting torque and power are in agreement with a reported value of 65.2 per cent of the total power found in a single-edge cutting [60] but only for the first workpiece material. The difference recorded for the second workpiece indicates that the exponent $Y_1 = 0.8$ established for steel does not hold well for a non-ferrous alloy such as INCONEL 600. As expected, a reliable force prediction is possible only if an accurate value of the exponent Y is available for the workpiece material.

TABLE 3.1   MAIN PARAMETERS OF THE TOOLS SHOWN IN
FIGS. 3.5 AND 3.6

TOOL	SOLID BORING	TREPANN-ING
Number of cutters	2	2
Location of 1st cutter [deg]	0.0	0.0
Location of 2nd cutter [deg]	119.5	120.0
Workpiece material	SAE 9255	SAE 9255
Feed rate [mm/rev]	0.33	0.17
Supporting reaction R_s [kN]	6.5	7.0
Direction of R_s [deg]	41.9	64.7
Resultant cutting torque [kNcm]	65.61	252.80
Resultant feed force [kN]	23.08	16.80
Deviation of R_s in magnitude[kN] (based on reference [69])	1.143 1.45*	1.048 1.315*
Deviation of R_s in direction [deg] (based on reference [69])	14.63 18.81*	5.83 7.52*

* Deviations based on the assumption that the variations
  of cutting force components are ± 10 per cent for both
  radial and tangential component.

TABLE 3.2   FEED FORCE AND POWER AS PREDICTED
AND RECORDED

Test No.	Average Feed Force		Average Torque		Average Power		Efficiency
	Calc.	Record	Calc.	Record	Calc.	Record	Per Cent
	kN	kN	kNcm	kNcm	kW	kW	
1	19.47	20.9	295.06	444.02	30.9	46.5	66.4
2	13.58	13.78	202.59	381.97	12.73	24.0	53.0

CHAPTER IV

OPTIMIZATION AND DESIGN PROCEDURE OF
UNSYMMETRICAL MULTI-EDGE CUTTING TOOLS

CHAPTER IV

OPTIMIZATION AND DESIGN PROCEDURE OF
UNSYMMETRICAL MULTI-EDGE CUTTING TOOLS

The basic concept of unsymmetrical multi-edge tools has already been formulated in Chapter I. The essential difference between the staggered tools and the multi-edge tools is that the total width of the cutting edges of the latter, covers more than the tool radius. All cutting edges are identically ground in the front profile and each cutter cuts a chip of the cross-section proportional to the angular spacing from the preceding cutter. The larger this spacing, the thicker the chip, and the larger cutting force components are exerted onto the cutting edge. Moreover, when cutting edges of different widths are used the effective cutting depths per cutting edge will be uneven and a function of the widths of the preceding cutters. Therefore, it becomes obvious that for such a tool of varying cutting widths, a relation between the cutting widths and the angular location of the cutters at one end and the cutting force components on the other end is required. Because of its complexity, this relationship deserves careful consideration.

4.1 CUTTING FORCE COMPONENTS IN MULTI-EDGE TOOLS

Figure 4.1 shows a force diagram of a tool with n cutting edges. $\vec{F}_1, \vec{F}_2, \ldots, \vec{F}_n$ are the cutting forces, $\theta_1, \theta_2, \ldots, \theta_n$
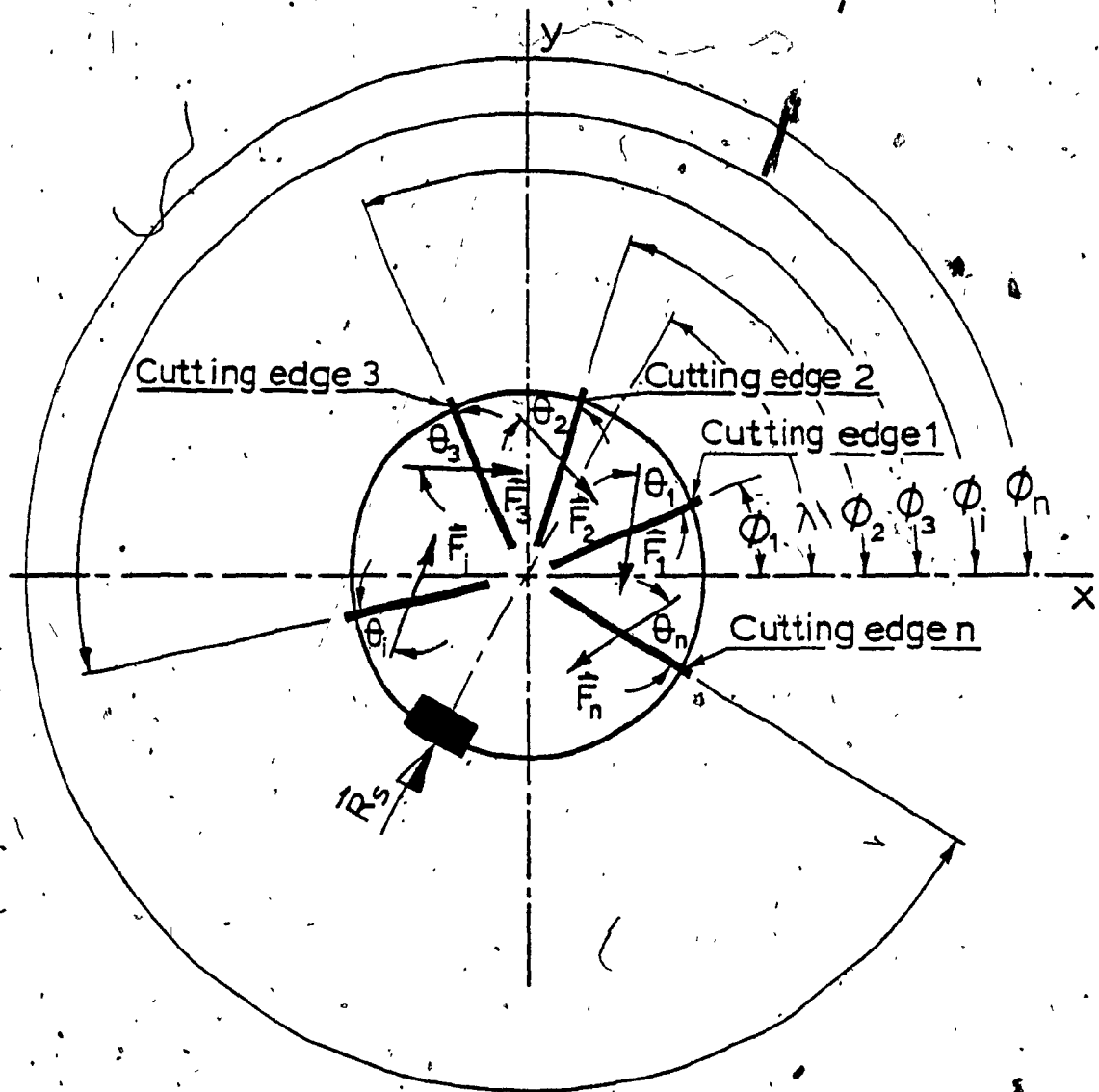
FIG. 4.1 FORCES IN UNSYMMETRICAL MULTI-EDGE
          BORING HEAD

are the corresponding phase angles of cutting edges $1, 2, \ldots, n$.
$\vec{T}$ is the drive torque and $\vec{R}_s$ is the supporting pad reaction.
Summing all forces and moments to zero will result in equations identical to (3.1) to (3.10) developed for staggered tools.
However, there will be a difference in the cutting force components
F_{Ri} and F_{Ti}. While these components in the staggered tools
are constant in magnitude and can change only in their
direction, in multi-edge tools, they vary with both
the cutting width and the angular location. In addition,
the phase angles θ are a function of the cutting width. So,
equations (3.9) and (3.10) are still the governing equations
defining the amount of force transmitted to the bore wall $\vec{R}_s$
and the direction of this force, λ. These equations become:

$$|\vec{R}_s| = \{ [\sum_{i=1}^{n} (F_{Ri} \cos \phi_i - F_{Ti} \sin \phi_i)]^2$$

$$+ [\sum_{i=1}^{n} (F_{Ri} \sin \phi_i + F_{Ti} \cos \phi_i)] \}^{\frac{1}{2}} \qquad (4.1)$$

$$\lambda = \tan^{-1} \left\{ \frac{\sum_{i=1}^{n} (F_{Ri} \sin \phi_i + F_{Ti} \cos \phi_i)}{\sum_{i=1}^{n} (F_{Ri} \cos \phi_i - F_{Ti} \sin \phi_i)} \right\} \qquad (4.2)$$

Since it is not feasible to locate more than one cutter
in the zone of inner cutting edges, the question arises whether
it is profitable to use the multi-edge solid boring tool,

because it is going to act, anyway, as a single-edge tool in that particular zone. The answer is affirmative because the outer and middle zones are exposed to much higher temperatures during the cutting operation than the inner zone. Since tool life is inversely proportional to temperature, adding cutters in these zones would result in extended tool life and/or increased feed rate. Recent experiments conducted with single-edge cutting tools revealed that temperatures measured 1.25 mm behind the cutting edge and 40 deg. from the rake face at the centre of rotation at the tool point, and at the circle land, are in the proportion of 1:2.5: 4.5 [60,69]. The explanation for this is a linear increase in the cutting speed, from the center of rotation towards the hole surface. The inner zone has a much lower cutting speed and hence, temperature. Pressure welds occur at the places of contact, between the workpiece material and tool material, but mechanical wear is relatively limited, due to low temperature. A steady built-up edge, formed on the rake face of the cutting edge, is of such hardness that it functions as a cutting edge and prevents wear of the rake face. At the middle zone the cutting speeds are higher, the temperatures are higher with increased mechanical wear due to pressure, and heat welds occur as a result. The thermal and mechanical stresses on the built-up edge reach a level sufficient enough

to break it. These loosened, very hard particles are forced at high pressure between the chip and rake face, as well as between the workpiece and the tool flank causing heavy mechanical wear. At higher cutting speeds, the temperature is higher and the strength of the pressure welds is lower. This prevents the formation of an excessive built-up edge at the outer zone. [46]. The described wear mechanism indicates that the middle zone of a deep-hole cutting edge is equally critical as the outer zone with regard to tool life. This suggests a multi-edge solid boring tool which has multi-edges extended over the outer and middle zone and single-edges in the inner zone.

The fact that the solid boring multi-edge tool will be acting as a single-edge tool in the middle zone is a serious limitation. A great change for partially overcoming this limitation is sought in the possibility of using a much less negative rake angle at this zone than the (-30 deg presently used, and also in the application of tougher grades of carbide for this portion of the cutter.

Evidently, for this type of multi-edge tool, a mathe-matical model is needed to analyze the cutting force compon-ents as functions of width of cut measured from the outer tool point. In addition, an evaluation of the cutting force components over any width of cut located between the outer tool point and the center of rotation should be
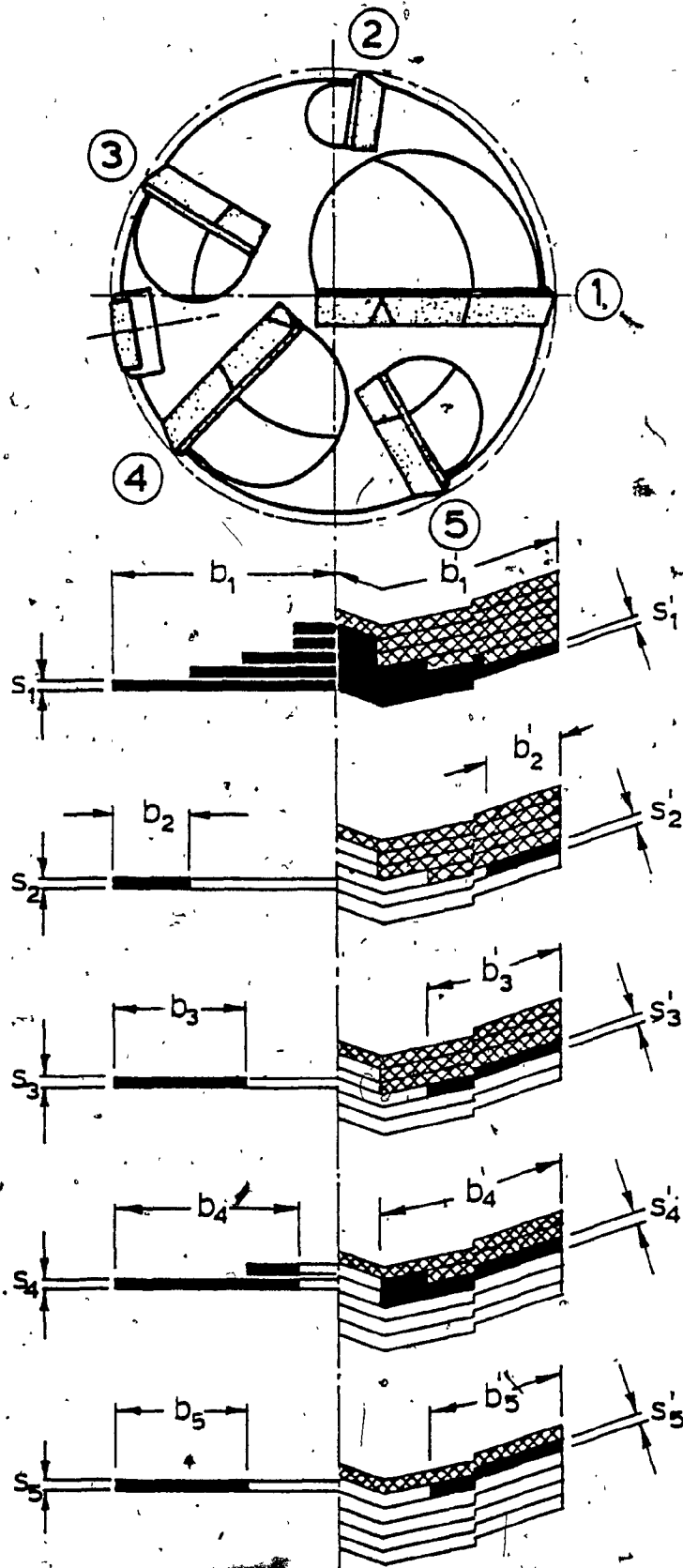
FIG. 4.2 ARBITRARY TOOL DESIGN WITH EDGE PENETRATIONS.

possible.

Such a model should be applicable to any arbitrary tool with n cutting edges for any possible sequence of cutting widths which might occur during the optimization procedure. An arbitrary tool design with sequential edge penetrations is illustrated in Fig. 4.2. It shows on the right side, the actual chip cross-sections, and on the left side, a simplified representation of these. The simplification does not affect the chip cross-sectional area since $sb = s'b'$, but it contains an error in the force computation, due to differences in the chip slenderness. The error can be assessed from the factor by which the computed forces are less than the actual ones:

$$\eta = \left.\right)(\cos\kappa_i)^{x-y} \tag{4.3}$$

The least values of the factor are $\eta = (\cos 18^\circ)^{0.35} =$ 0.983 for the radial components and $\eta = (\cos 20^\circ)^{0.2} = 0.988$ for the tangential components. As it can be seen, the radial forces are affected by 1.7 per cent and the tangential forces by 1.2 per cent. Since the tangential components constitute most of the resultant force, it can be safely claimed that the resultant force is affected by less than 1.5 per cent. The effect of this error on the tool optimum is, insigni- ficant because it is more or less equal for all cutters. For that reason, and for the sake of simplicity, it is ignored.

If the effective depth of cut s_o is taken as a unit depth, then equations (2.27), and (2.29) and (2.31) can be converted into continuous functions of width of cuts b_i measured from the outer tool point, as the origin:

$$F'_{Ti} = c_{T_1} b_i + c_{T_2}(b_i - p_1)\delta_1 + c_{T_3}[b_i - (p_1 + p_2)]\delta_2 \quad (4.4)$$

$$F'_{Ri} = c_{R_1} b_i - c_{R_2}(b_i - p_1)\delta_1 - c_{R_3}[b_i - (p_1 + p_2)]\delta_2 \quad (4.5)$$

$$F'_{Fi} = c_{F_1} b_i + c_{F_2}(b_i - p_1)\delta_1 - c_{F_3}[b_i - (p_1 + p_2)]\delta_2 \quad (4.6)$$

where $i = 1, 2, \ldots, n$. Because the cutters form a continuous and closed cycle the subscripts are replaced as follows:

If $i = 0$ then $i = n$

If $i = n + 1$ then $i =$

δ_1 and δ_2 are operators defined as follows:

$$\delta_1 = \begin{cases} 1 & \text{if} & b_i - p_1 > 0 \\ 0 & \text{if} & b_i - p_1 \leq 0 \end{cases} \quad (4.7)$$

$$\delta_2 = \begin{cases} 1 & \text{if} & b_i - (p_1 + p_2) > 0 \\ 0 & \text{if} & b_i - (p_1 + p_2) \leq 0 \end{cases} \quad (4.8)$$

A graphical presentation of equations (4.4), (4.5) and (4.6) is given in Fig. 4.3. The coefficients representing the slopes
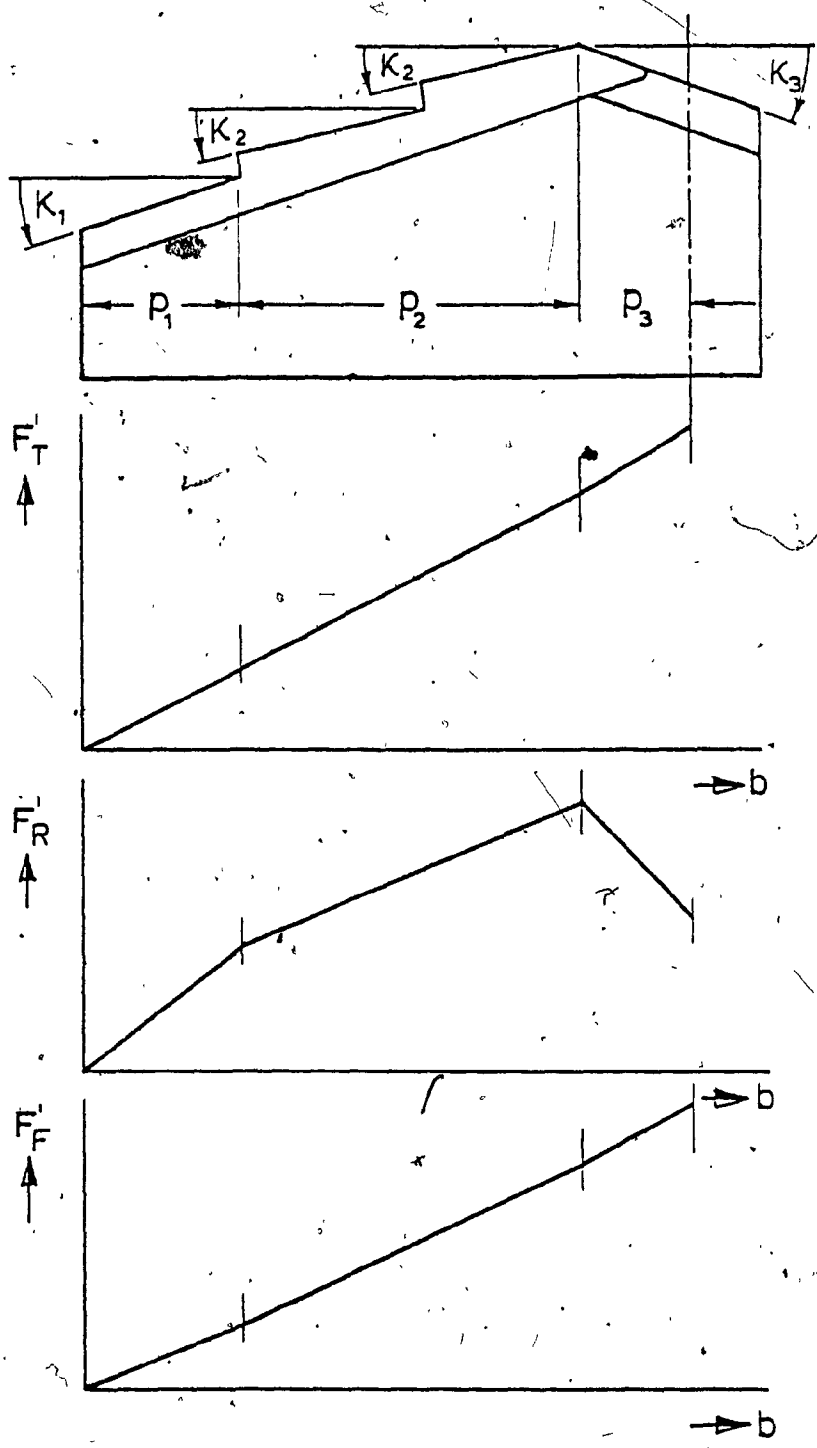
FIG. 4.3 CUTTING FORCE COMPONENTS vs WIDTH OF CUT

in the diagram are obtained by comparison of these equations and equations (2.27),(2.29) and (2.31), respectively. They are as follows:

$$c_{T_1} = c_{Kp}, \quad c_{T_2} = 0, \quad c_{T_3} = (\zeta_p - 1)c_{Kp} \qquad (4.9)$$

$$c_{R_1} = c_{Kq} \sin \kappa_1; \quad c_{R_2} = c_{Kq}(\sin\kappa_1 - \sin\kappa_2)$$
$$c_{R_3} = c_{Kq}(\sin\kappa_2 - \zeta_q \sin\kappa_3) \qquad (4.10)$$

$$c_{F_1} = c_{Kq}\cos\kappa_1; \quad c_{F_2} = c_{Kq}(\cos\kappa_2 - \cos\kappa_1)$$
$$c_{F_3} = c_{Kq}(\cos\kappa_2 - \zeta_q \cos\kappa_3), \qquad (4.11)$$

The relations as presented in Fig. 4.3, resulted from a combination of the theoretical approach, based on the cutting mechanics and the empirical approach, based on tests in the turning and drilling operations. No experimental work had been done to judge how good they are until recently, when this work was already in an advanced stage. Recent reports [62,69] reveal that the cutting force components recorded during deep-hole machining tests using a single-edge solid boring head, are in good agreement with the results obtained from equations (4.4) to (4.18). If the diagrams plotted for the cutting force components versus the cutting width measured from the center of rotation are converted into diagrams of the type shown in Fig. 4.3, and compared qualitatively, they appear to
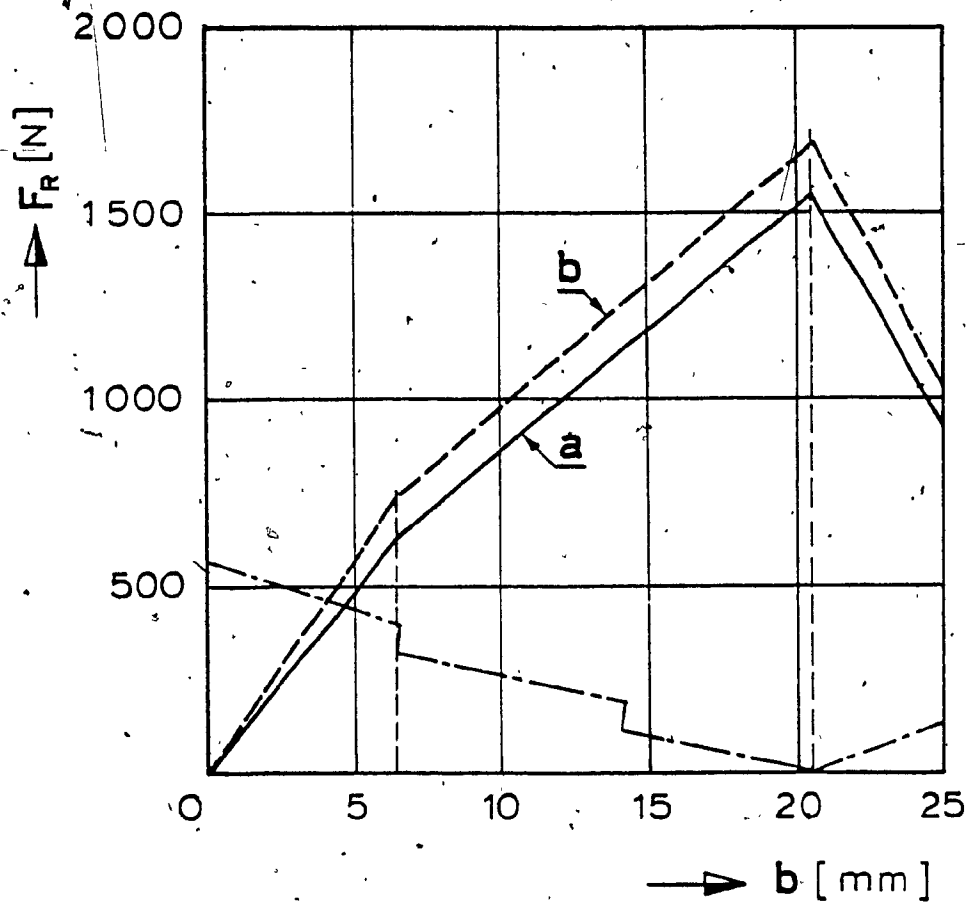
FIG. 4.4   RADIAL FORCE   vs WIDTH OF CUT

(a)   CALCULATED FROM EQUATION (4.5)
(b)   REPORTED IN [62, 70]

be very close. Such a diagram for the radial force component
is shown in Fig. 4.4. The other two force components - the
tangential and the feed component appear to agree even better.

The total cutting force components, as well as the
cutting torque can be determined if the increments of the
cutting forces per unit depth are multiplied by the correspond-
ing effective depths to the exponent y for every zone and
summed for each cutting edge. Such calculation is possible
because the exponent of the cutting width is unity. Although
it seems impossible to express exactly these operations
analytically, the general equations are written under the
conditions that the subscript m and the increments of the
cutting forces per unit depth $\Delta F_T'$, $\Delta F_R'$ and $\Delta F_F'$ are deter-
mined for each cutting edge:

$$F_{Ti} = \sum_{j=i}^{m} \Delta F_{Tj}' (s_k \delta_{k\ell})^{Y_1} \tag{4.12}$$

$$F_{Ri} = \sum_{j=i}^{m} \Delta F_{Rj}' (s_k \delta_{k\ell})^{Y_2} \tag{4.13}$$

$$F_{Fi} = \sum_{j=i}^{m} F_{Fj}' (s_k \delta_{k\ell})^{Y_2} \tag{4.14}$$

where

$$k = i, i+1, \ldots, m; \quad \ell = 1, 2, \ldots, j$$

$$i = 1, 2, \ldots, n; \quad \text{with subscripts replacements}$$

if $\quad i = 0 \quad$ then $\quad i = n$

if $\quad i = n+1 \quad$ then $\quad i = 1$

$\delta_{k\ell}$ is the Kroneker delta defined:

$$\delta_{kl} = \begin{cases} 1 & k = \ell \\ 0 & k \neq \ell \end{cases}$$

For the purpose of calculating the cutting force components and the cutting torque, an appropriate computer program has been used. In order to handle all possible sequences of the cutting edges, the program is written in general, subscripted form. A detailed flow-chart is given in Fig. 4.5. The logic is intended primarily for solid boring tools, but it is equally applicable to trepanning tools.

The model shown in Fig. 4.5, has been tested with numerous tools having various numbers of cutters located in increasing, decreasing or mixed sequences. It has proven applicable to any number of cutters. For example, for the tool shown in Fig. 4.2, the cutting force components and the torque of cutter No. 1, can readily be written down by inspection:

```
                    START
                      │
                      ▼
            ┌─────────────────┐    Yes     ┌──────────────────────┐
            │  0.0<B(I)≤P₁     │──────────▶ │   δ₁=0 , δ₂=0         │
            │      ?          │            │   Evaluate           │
            └─────────────────┘            │ F'_T(I),F'_R(I),F'_F(I)│
                      │ No                 └──────────────────────┘
                      ▼
┌──────────────────────┐  Yes  ┌─────────────────┐
│   δ₁=1 , δ₂=0        │◀──────│  P₁<B(I)≤P₁+P₂   │
│   Evaluate           │       │      ?          │
│ F'_T(I),F'_R(I),F'_F(I)│      └─────────────────┘
└──────────────────────┘               │ No
                                        ▼
                            ┌──────────────────────┐
                            │   δ₁=1 , δ₂=1        │
                            │   Evaluate           │
                            │ F'_T(I),F'_R(I),F'_F(I)│
                            └──────────────────────┘
```

$$0.0 < B(I) \leq P_1 \ ?$$

$$\delta_1 = 0, \ \delta_2 = 0 \quad \text{Evaluate} \quad F'_T(I), F'_R(I), F'_F(I)$$

$$P_1 < B(I) \leq P_1 + P_2 \ ?$$

$$\delta_1 = 1, \ \delta_2 = 0 \quad \text{Evaluate} \quad F'_T(I), F'_R(I), F'_F(I)$$

$$\delta_1 = 1, \ \delta_2 = 1 \quad \text{Evaluate} \quad F'_T(I), F'_R(I), F'_F(I)$$

$$I = 0$$

①

$$I + 1 \rightarrow I$$

$$J_2 = I, \ B_2 = B(I)$$
$$F(I) = 0.0, \ T(I) = 0.0$$

②

③
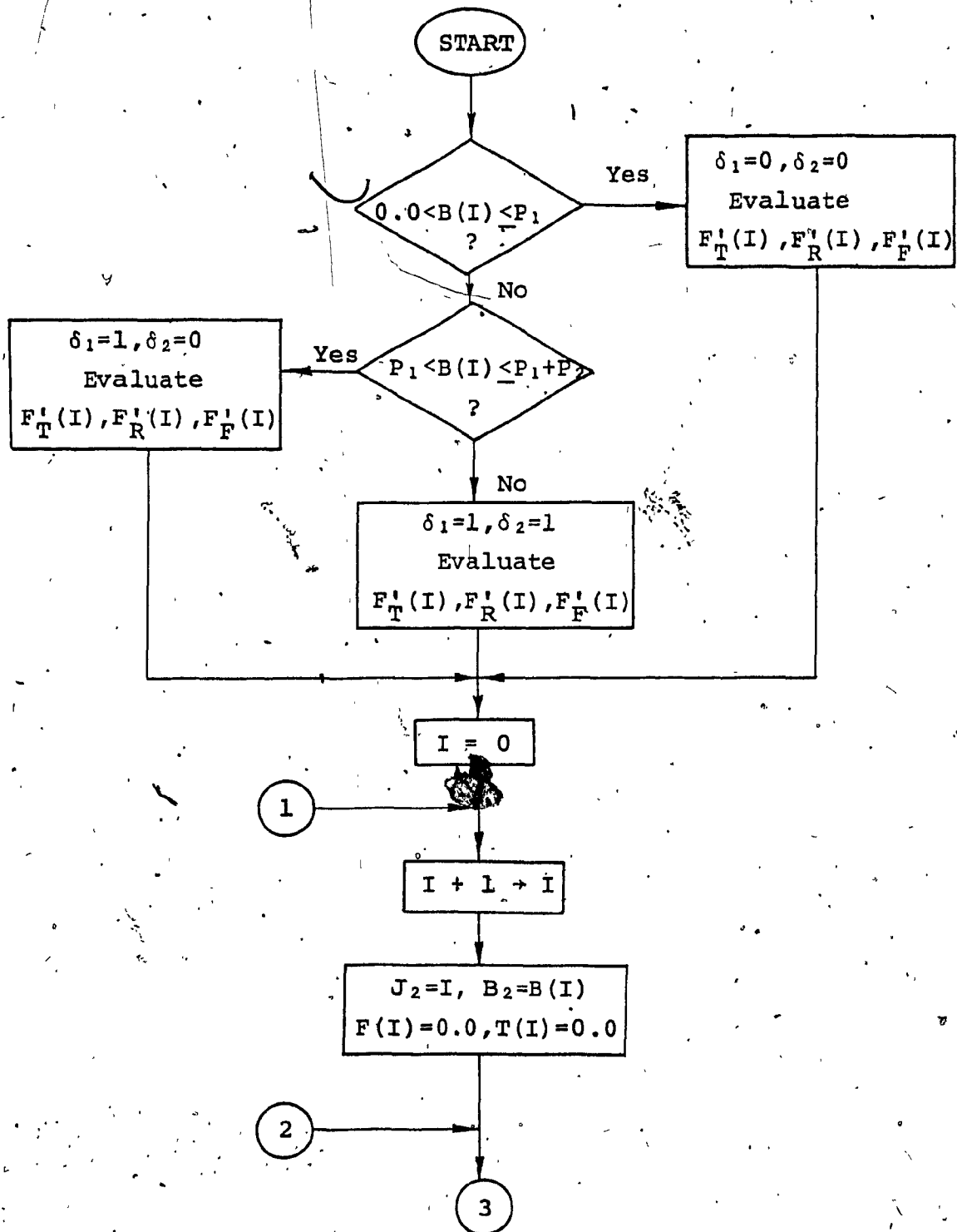
FIG: 4.5   DETAIL FLOW CHART OF EVALUATION OF
           CUTTING FORCES AND TORQUE IN MULTI-
           EDGE TOOL

FIG. 4.5   DETAIL FLOW CHART OF EVALUATION OF
CUTTING FORCES AND TORQUE IN MULTI-
EDGE TOOL   (continued)

$$F_T(I) \leftarrow F_T(I) + [F_T'(J_2) - F_T'(J_1)X_N][S(I) + S_s]^Y$$
$$F_R(I) \leftarrow F_R(I) + [F_R'(J_2) - F_R'(J_1)X_N][S(I) + S_s]^Y$$
$$F_F(I) \leftarrow F_F(I) + [F_F'(J_2) - F_F'(J_1)X_N][S(I) + S_s]^Y$$
$$T(I) \leftarrow T(I) + \{[F_T'(J_2) - F_T'(J_1)X_N][S(I) + S_s]^Y\}$$
$$* \{[B(J_2) - B(J_1)X_N]/2 + [D/2 - B(J_2)]\}$$
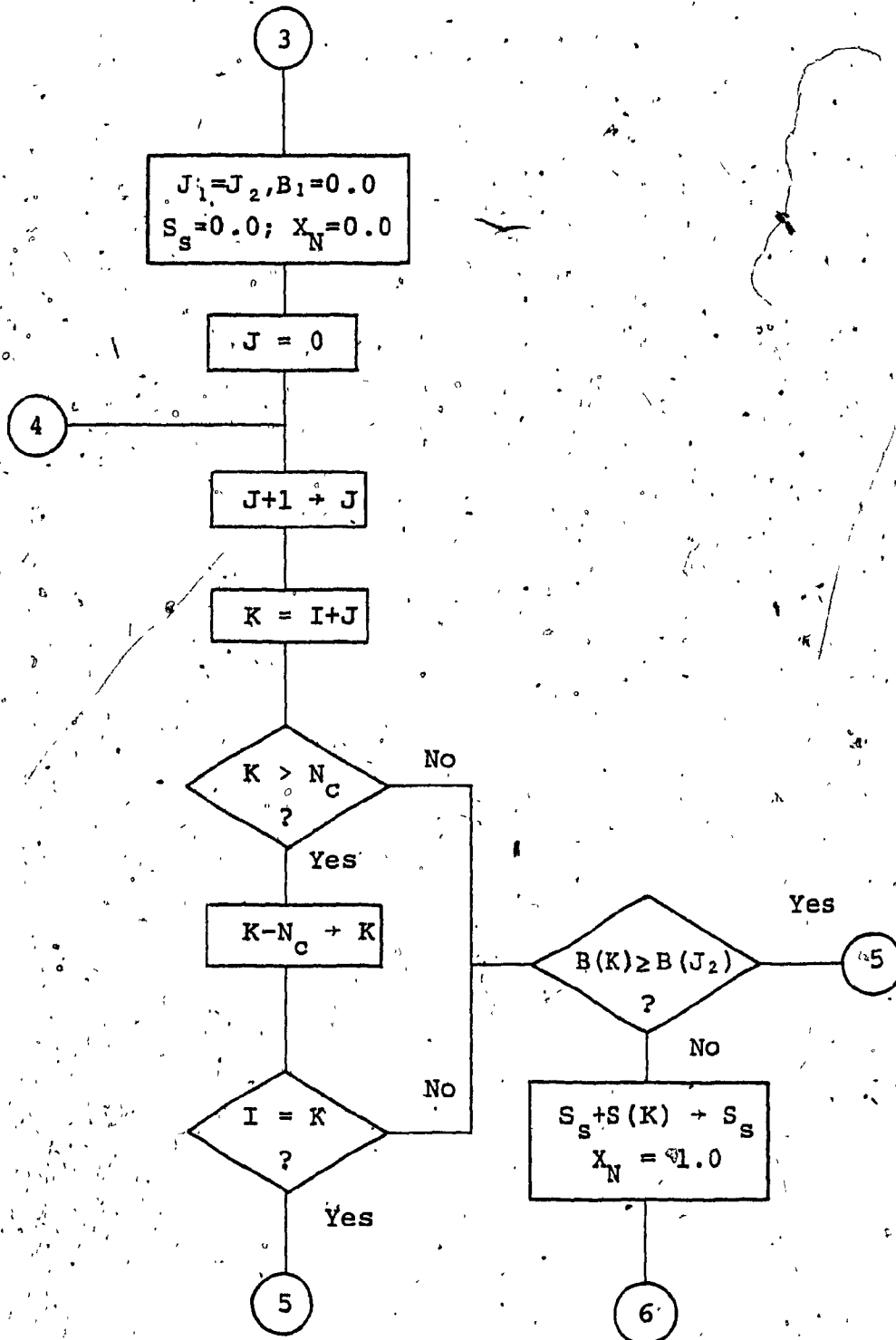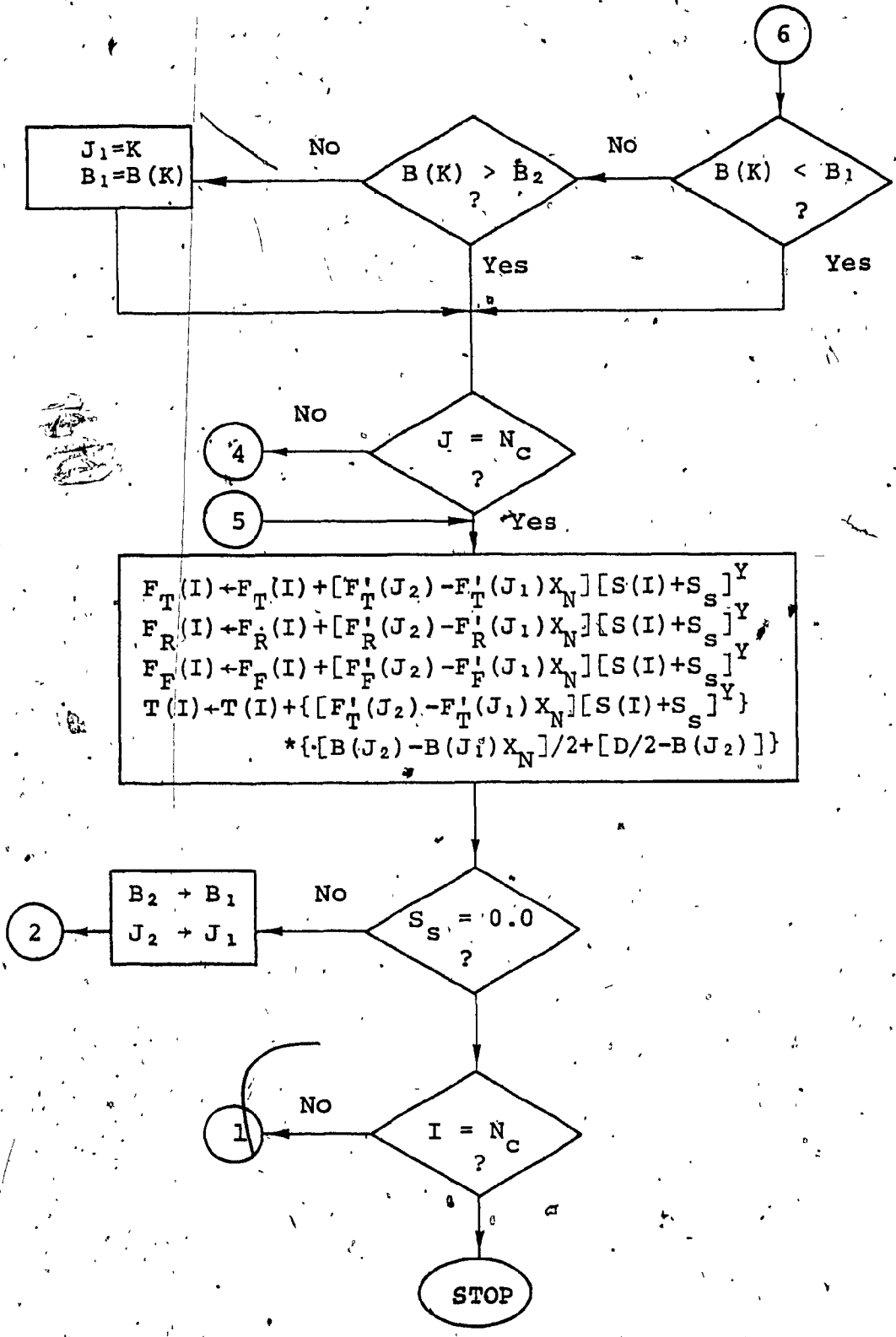
FIG. 4.5   DETAIL FLOW CHART OF EVALUATION OF
CUTTING FORCES AND TORQUE IN MULTI-
EDGE TOOL   (continued)

$$F'_{T_1} = (F'_{T_1} - F'_{T_4})(s_1+s_2+s_3+s_4+s_5)^{Y_1} + (F'_{T_4} - F'_{T_3})$$

$$* (s_1+s_2+s_3)^{Y_1} + (F'_{T_3} - F'_{T_2})(s_1+s_2)^{Y_1} + F'_{T_2} s_1^{Y_1} \quad (4.15)$$

$$F_{R_1} = (F'_{R_1} - F'_{R_4})(s_1+s_2+s_3+s_4+s_5)^{Y_2} + (F'_{R_4} - F'_{R_3})$$

$$* (s_1+s_2+s_3)^{Y_2} + (F'_{R_3} - F'_{R_2})(s_1+s_2)^{Y_2} + F'_{R_2} s_1^{Y_2} \quad (4.16)$$

$$F_{F_1} = (F'_{F_1} - F'_{F_4})(s_1+s_2+s_3+s_4+s_5)^{Y_2} + (F'_{F_4} - F'_{F_3})$$

$$* (s_1+s_2+s_3)^{Y_2} + (F'_{F_3} - F'_{F_2})(s_1+s_2)^{Y_2} + F'_{F_2} s_1^{Y_2} \quad (4.17)$$

$$T_1 = (F'_{T_1} - F'_{T_4})(s_1+s_2+s_3+s_4+s_5)^{Y_1}[\tfrac{1}{2}(b_1-b_4) + (\tfrac{D}{2} - b_1)]$$

$$+ (F'_{T_4} - F'_{T_3})(s_1+s_2+s_3)^{Y_1}[\tfrac{1}{2}(b_4-b_3) + (\tfrac{D}{2} - b_4)]$$

$$+ (F'_{T_3} - F'_{T_2})(s_1+s_2)^{Y_1}[\tfrac{1}{2}(b_3-b_2) + (\tfrac{D}{2} - b_3)]$$

$$+ F'_{T_2} s_1^{Y_1} \tfrac{1}{2}(D-b_2) \quad (4.18)$$

Equations (4.15) to (4.18) are given for one cutting
edge only and are intended to illustrate the expansion
of the general equations. They show how lengthy these
equations would be if written in an expanded explicit form.
Yet, these equations are for only one tool configuration and
hence, insufficient for tool optimization with varying cutt-
ing widths. Although quite complex, the model is also suit-
able for a very simple tool, as for example, a trepanning
tool, since most of the logic would be bypassed.
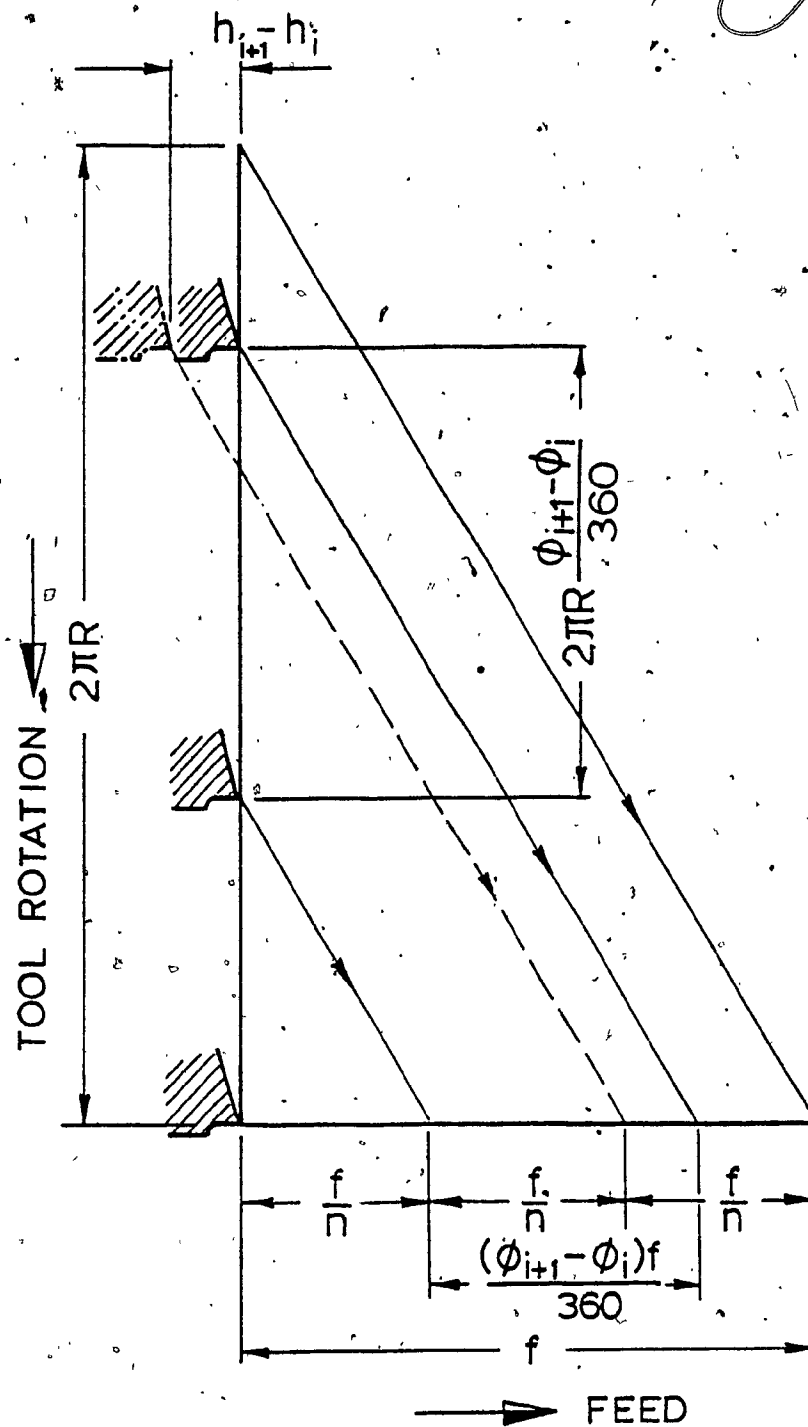
FIG. 4.6. CUTTING DEPTH IN RELATION TO ANGULAR
SPACING

The effective depth of cut for the ith cutting edge will be approximately equal to the edge penetration which is proportional to the angular spacing from the preceding cutting edge, as illustrated in Fig. 4.6:

$$s_i = \frac{\phi_{i+1} - \phi_i}{360} f; \quad i = 1,2,\ldots,n \qquad (4.19)$$

Fig. 4.6 also reveals the possibility of grounding (or setting) the cutting edges at different levels, in order to achieve even cutting edge penetrations. This is feasible for small numbers of cutters only, for example, in trepanning tools where standard identical inserts can be levelled in such a way that the height difference between any two adjacent cutting edges can be calculated from.

$$(h_{i+1} - h_i) = (\frac{1}{n} - \frac{\phi_{i+1} - \phi_i}{360}) f; \quad i = 1,2,\ldots,n \qquad (4.20)$$

In equations (4.19) and (4.20) f denotes the feed per revolution, and the interchangeability of subscripts differing by n integers is valid.

4.2 UNBALANCED FORCES

The analysis based on the cutting force resultant applies only in the case when the tool is stationary and the workpiece rotates. In practice, however, cases where the tool rotates and the workpiece is either stationary or rotates

in the counter-direction are encountered more frequently. There-
fore, the effect of the tool imbalance must be investigated.
Because of the geometrical configuration of the boring head,
it is obvious that the center of gravity of the tool does
not coincide with the axis of rotation. In single-edge tools,
the inertia force due to tool imbalance affects the final
force resultant transmitted to the bore-wall in both the
magnitude and the direction. The direction of the inertia
force is thought to fall between the two wear pads, because
the center of gravity is located on that side of the head. The
magnitude of this force, however, is thought to be insignifi-
cant compared to the cutting force. Since these tools perform
well and exhibit good stability, no attention has been paid to
this effect in single-edge deep-hole machining.

Since a complete analysis of the tool imbalance has not
been conducted yet, a brief analysis is undertaken
here, with the intention of mathematical modelling of the un-
balanced forces, similar to that of the cutting forces. In
addition, the analytic description of geometric parameters of
a boring head is intended for the optimization of multi-edge
tool design as will be shown in this chapter.

An optimum fit to a variety of shapes of the chipmouth
used by tool manufacturers was found to be that shown by lined
regions in Fig. 4.7. It is simple to manufacture and can be
described by the simple equation

$$r_i^2 + (r+r_i-\xi b_i)^2 = (r-r_i)^2 \ ; \qquad i = 1,2,\ldots,n \qquad (4.21)$$

Equation (4.21) is derived from the condition that the chipmouth circle touches the cutting edge (point M), normal to the cutting edge at ξb; (point N) and the contour circle of the head (point P), Fig. 4.7.

The solution to (4.21) is

$$r_i = \xi b_i - d + \sqrt{d^2 - \xi d b_i} \ ; \qquad i = 1,2,\ldots,n \qquad (4.22)$$

where d is the diameter of the head.

The factor ξ defines the location of the chipmouth circle with respect to the cutting edge. For the best fit of the chipmouth shape, its value should be between 1.1 and 1.2.

The location of the center of the chipmouth circle is given by

$$r_{ci} = r - r_i \ ; \quad \psi_i = \sin^{-1}\left(\frac{r_i}{r_{ci}}\right) ; \ i = 1,2,\ldots, n \qquad (4.23)$$

The chipthroat diameter follows from Fig. 4.7.

$$d_{ti} = 2r_i \cos\beta \ ; \qquad i = 1,2,\ldots,n \qquad (4.24)$$

The imbalance eccentricity is

$$e_i = r_{ci} - \frac{\ell}{2}\sin\beta \ ; \qquad i = 1,2,\ldots,n \qquad (4.25)$$
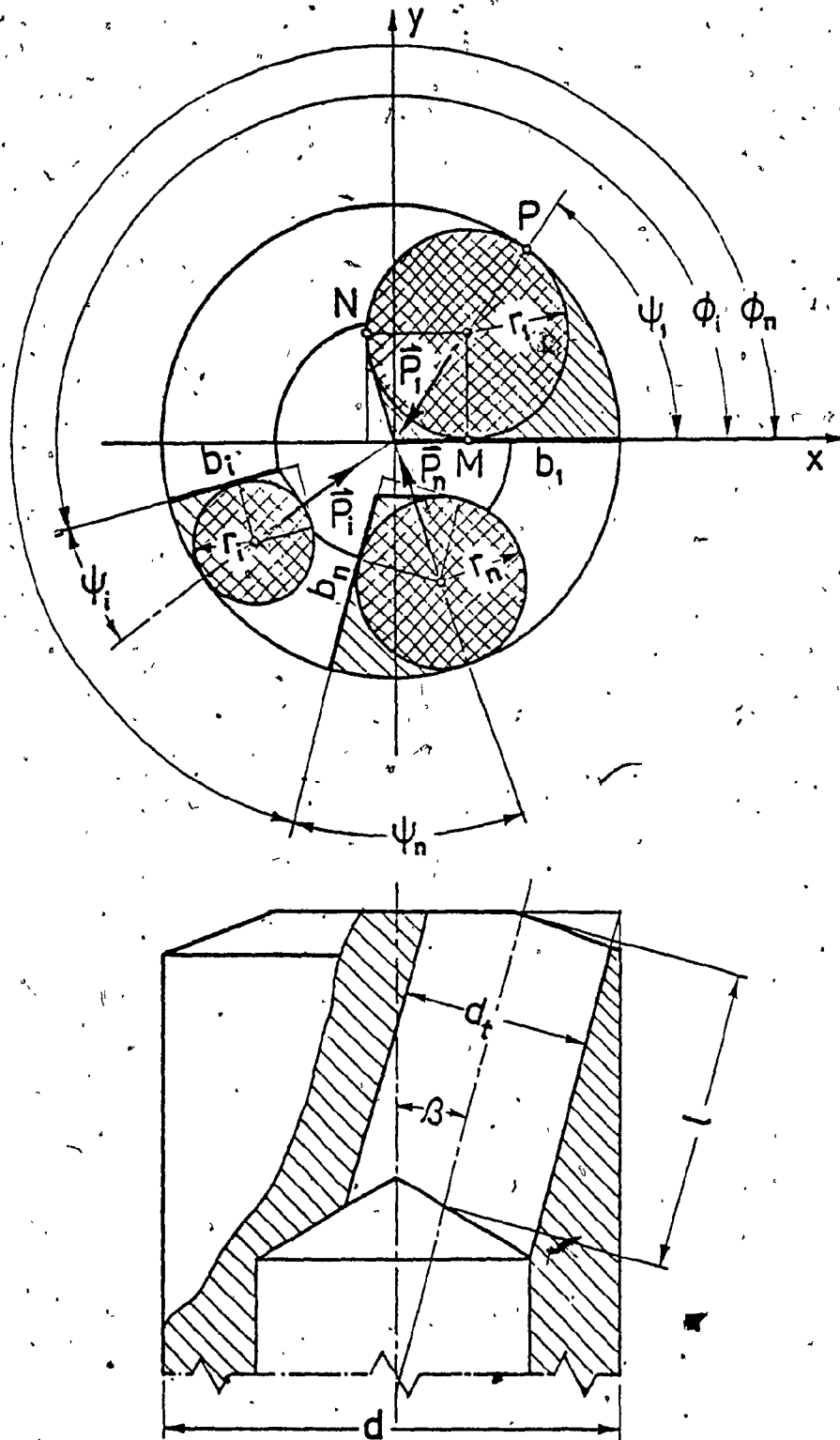
FIG. 4.7 INERTIA FORCES DUE TO IMBALANCE IN
UNSYMMETRIC MULTI-EDGE BORING HEAD

Using the parameters defined by equation (4.23),(4.24) and (4.25) the inertia force due to the imbalance of each cutting edge can be determined.

$$P_i = \eta_i \, e_i \, \frac{\pi d^2_{ti}}{4} \, \ell_\rho \, \omega^2 \qquad i = 1,2,\ldots,n \qquad (4.26)$$

where

ρ = the mass density

ω = the angular velocity

$\eta \leq 1$ = a correction factor which takes care of the incompleteness of the throats due to their intersections.

The inertia forces (4.26) are for the masses that have been removed from the head and they point radially inwards. These forces are due to the removed cylindrical portions of the chipthroats (cross-lined regions in Fig. 4.7) and the rest of the volume (lined regions in Fig. 4.7) is neglected. These portions, however, compensate for the imbalance caused by the difference in mass densities of carbide and steel at the cutter zone.

The correction factor η_i may also take care of the fact that during the cutting operation, the chipthroats are filled out with coolant and chips. This aspect can be separately investigated if it proves necessary.

Having determined the inertia forces, the supporting
reaction of the wear pads is

$$\vec{R}_s = - \sum_{i=1}^{n} (\vec{F}_i + \vec{P}_i) \qquad i = 1,2,\ldots,n \qquad (4.27)$$

If (4.27) is expanded it yields

$$|\vec{R}_s| = \{[\sum_{i=1}^{n} |\vec{F}_i| \cos(\theta_i+\phi_i) + |\vec{P}_i| \cos(\psi_i+\phi_i)]^2 +$$

$$+ [\sum_{i=1}^{n} |\vec{F}_i| \sin(\theta_i+\phi_i) + |\vec{P}_i| \sin(\psi_i+\phi_i)]\}^{\frac{1}{2}} \quad (4.28)$$

with the line of action defined by the angle

$$\lambda = \tan^{-1}\left\{\frac{\sum_{i=1}^{n} |\vec{F}_i| \sin(\theta_i+\phi_i) + |\vec{P}_i| \sin(\psi_i+\phi_i)}{\sum_{i=1}^{n} |\vec{F}_i| \cos(\theta_i+\phi_i) + |\vec{P}_i| \cos(\psi_i+\phi_i)}\right\} \quad (4.29)$$

This analysis shows that the inertia forces due to the
mass imbalance of the head can be expressed in terms of the tool
parameters ϕ_i and b_i only, for a given number of cutters n.
The previous analysis has proven that the cutting forces are a
function of these parameters, also. So, equations (4.28) and
(4.29) can be used for the optimization in defining
the objective function. Before this can be undertaken we
want to assess how much the inertia terms contribute to the
overall force resultant.

This can be achieved if a commonly used single-edge solid boring tool consisting of a cutting edge of $b_1 = d/2$, $\beta = d/2, \beta = 15$ deg. and $\ell = 0.6d$ is analysed. The main geometric parameters can be readily calculated from equations (4.22) to (4.25) to obtain:

$$r_1 = 0.221d; \quad d_{t_1} = 0.427d; \quad r_{c_1} = 0.279d;$$

$$\psi_1 = 52.38^{\circ}(52^{\circ}23'); \quad e_1 = 0.201d; \quad \eta_1 = 1.0$$

If these parameters are substituted into equation (4.26) and the mass density for steel $\rho = 7.86 \times 10^3$ kg/m^3 is used, the inertia force is

$$P_1 = 1.488 \times 10^{-12}d^4n^2 = 1.508 \times 10^{-7}d^2v^2 \text{ [N]} \qquad (4.30)$$

where d is the diameter of the head in mm, n is rpm and v is the cutting speed in m/min.

If a cutting speed of $v = 100$ m/min commonly used for steel, is selected and the tool diameter is $d = 50$ mm, then

$$P_1 = 3.77 \text{ N}(0.85 \text{ lbf})$$

This example demonstrates that the imbalance forces in practice are of three orders of magnitude, less than the cutting forces, and therefore, can safely be ignored in further

analysis of the forces exerted on multi-edge tools.

4.3   OPTIMUM CUTTING FORCE RESULTANT

It has already been stated in the scope of this work in Chapter I, that the cutting force resultant should be chosen in such a way that, on the one hand, enough pressure is exerted onto the machined hole-wall to prevent run-out of the tool; on the other hand, this pressure should be limited to a value that permits a hydrodynamic lubricating action between the supporting pads and the bore-wall. The following analysis is undertaken with the intention of determining the lower limit of the resultant cutting force; this force should exert enough pressure onto the machined hole-wall to ensure the tool guidance.

4.3.1   Variations of Cutting Force Resultant

No doubt, the value of the predetermined cutting force resultant depends on how much variation in its magnitude can be expected, due to the fluctuations of the cutting force components. This value should assure that a minimum positive pressure between the wear pads and the hole-wall is maintained at all times. Moreover, the directional variation of the result-ant force should also be maintained at all times within certain angular limits, in order to ensure that it points between the two wear pads. This is very important for tool

stability and accuracy of the hole size.

To be able to determine any variations of the cutting force resultant, it is necessary to know both the magnitude and the nature of the fluctuations of the cutting force components. Some results on the variation of cutting force components have been reported. They were recorded during the experimental measurement of the cutting force components. The most reliable data seems to be given in [1], which reveals that a fluctuation of the tangential component is ± 8 percent, ± 21.5 per cent for the radial component and ± 2 for the feed component. The boring torque has been reported to vary by ± 14%. Data recently reported [69] indicate that ± 10 per cent variation in the magnitude of both tangential and radial force components is also possible. No information, whatsoever, has been reported on the nature of the cutting force variations in deep-hole machining.

It has been recognized that cutting forces are not steady-state variables but dynamic in nature, with a high degree of randomness. Results in similar metal cutting operations such as turning and drilling, have proven that the cutting forces in these operations are random and Gaussian distributed, particularly in the finishing operations [28, 29, 30, 31]. Since deep-hole machining is a cutting operation very similar to turning and drilling with low feeds, it seems

appropriate to assume that the cutting force components in this operation are also random and Gaussian distributed. Under such an assumption, the problem is tackled analytically in Appendix III, and the exact formulae for the variation of the cutting force resultant in both magnitude and direction are derived.

A calculation of the deviation in magnitude is performed in iterative steps convenient for computer application The deviation represents the difference between the actual magnitude and desired mean magnitude of the resultant force vector

$$\Delta R = \left| \left| \vec{R} \right| - \left| \vec{R}_x \right| \right|. \tag{4.31}$$

and it is calculated from (A3.12)

$$\Delta R = \Delta R_x + \frac{(\Delta R_x)^2 + (\Delta R_y)^2 - (\Delta R)^2}{2R_x} \tag{4.32}$$

Also, the deviation in direction is given by (A3.14)

$$\Delta\lambda = \tan^{-1}\left(\frac{\Delta R_y}{R_x - \Delta R_x}\right) \tag{4.33}$$

Equation (4.32) is used for the calculation of the deviation in the magnitude of the cutting force resultant. Convergence is achieved rapidly after only a few iterations, to three decimal points. Even higher accuracy of up to six decimal points requires about ten iterations. ΔR reflects

very much the cutting force polygon orientation. The same holds for $\Delta\lambda$. The examples given in Fig. 3.5 and Fig. 3.6 best illustrate the trends. While the tool shown in Fig. 3.5 has a large deviation ΔR because of the relatively low value of R, the tool shown in Fig. 3.6 has ΔR small, because of the relatively higher value of R. Both tools, however, have values of R of 6.5 and 7.0 kN. Even more drastic differences in $\Delta\lambda$ are evident from the figures because of the different orientation of the cutting force polygon (here triangle). So, in general, tools with a cutting force polygon oriented in the direction of $\vec{R}$ will have a large deviation ΔR and a small deviation $\Delta\lambda$ and tools with the cutting force polygon oriented perpendicular to $\vec{R}$ will have a large deviation $\Delta\lambda$ and a small deviation ΔR. Evidently, the latter would prove less desirable in practice since a large deviation in the direction of the resultant may cause uneven load of the wear pads and endanger proper tool guidance and stability.

Equation (4.32) is analytical proof of the instability in multi-edge tools with a symmetric location of the cutting edges. Although R_x is theoretically zero, it is never virtually zero; it is small, but indeterminate in value. Since ΔR_x and ΔR_y are changing at random in both magnitude and in sign, it is very likely that tan $(\Delta\lambda)$ assumes values ranging between $-\infty$ and $+\infty$. This means that $\Delta\lambda$ may vary from $-\pi/2$ to $+\pi/2$, i.e., it may assume the completely reverse sense.

This indeterminate character of the cutting force resultant in both magnitude and direction is the main reason of in- stability of the tools with a symmetric location of cutting edges.

The above also indicates what the analytical condition is that the minimal cutting force resultant must satisfy, in order to assure tool guidance and stability is that it must be greater than its deviation ΔR to overcome the boring bar encastré effect and prevent separation of the wear pads from the bore wall. Moreover, the difference $R_x - \Delta R_x$ must be large enough to prevent the deviation in the direction $\Delta \lambda$ to assume a value beyond the maximum value. This maximum value is somewhat flexible in limit, depending on the angular spac- ing of the wear pads.

Two tools, a solid boring head with three cutting edges and a trepanning head with two cutting edges were optimized for various values of the force resultant R. The results are presented graphically in Fig. 4.8 and Fig. 4.9. The diagram in Fig. 4.8 shows how the relative deviation in magnitude of the force resultant $\Delta R/R$ increases by a decrease in the resultant R. The diagram in Fig. 4.9 shows a similar trend for the deviation in direction of the resultant $\Delta \lambda$. While the deviations for the trepanning head are given for the range of R, from 1.5 to 10 kN, the variations for the solid boring head are given only for a range from 5 to 10 kN.
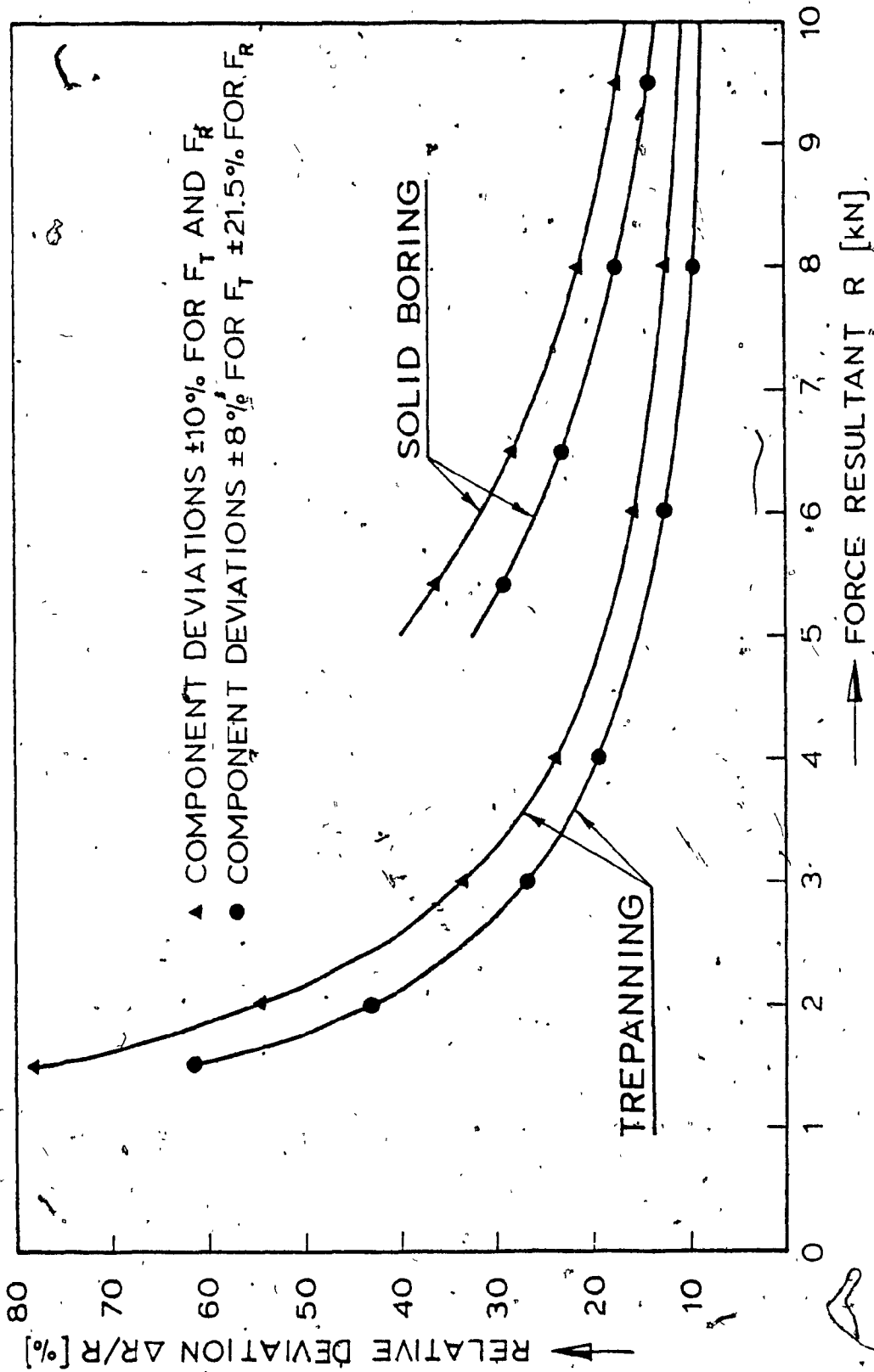
FIG. 4.8 RELATIVE DEVIATION IN MAGNITUDE OF CUTTING FORCE RESULTANT
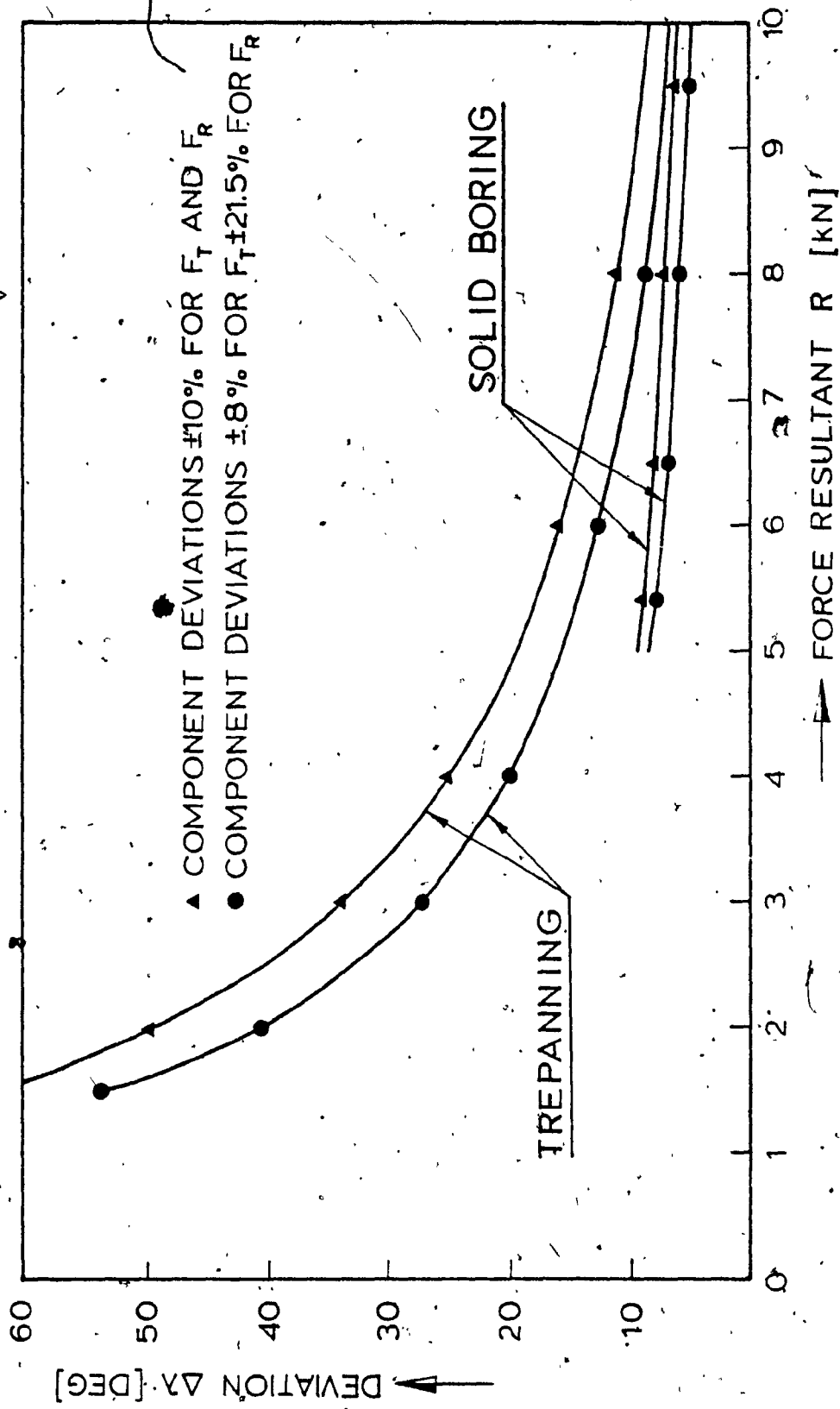
FIG. 4.9 DEVIATION IN DIRECTION OF CUTTING FORCE RESULTANT

It appeared that the solid boring head could not be optimized for values of R less than 5 kN because the limits set upon the width of cut for the tool did not permit values of R below 5 kN.

The most important feature of these two diagrams is that they prove that the tool guidance would not be assured if the tools are optimized for too low values of R, because the deviations in its magnitude and direction will rapidly increase approaching the critical values of 100 per cent and 90 deg. respectively. The diagrams also reveal that the resultant R of the solid boring tool has a larger variation in magnitude and less variation in direction, as compared to the trepanning tool. This confirms what has already been stated about the effect of the cutting force polygon orientation. The diagrams are based on two slightly different data on the fluctuation of cutting force components. The variations in the cutting force components of ± 8 percent in the tangential and ± 21.5 per cent in the radial direction are due to [1], while variations ± 10 in both the tangential and radial components are assumed. No confidence level, however, for these variations has been reported.

It can be concluded that no limit for either deviation can be reliably recommended, but it seems reasonably safe if $\Delta R/R$ is kept below 25 percent and $\Delta\lambda$ below 15 deg.

4.3.2 Hydrodynamic Lubrication of the Supporting Pads

The high frictional forces which develop between the bore-wall and supporting pads can cause the tool to wear out within a few seconds, if no cooling medium is introduced. To reduce the wear on the supporting pads, special additives are mixed with the coolant with the intention of producing a thin lubricating film which remains intact, and withstands high mechanical and termal loads. In spite of the optimal lubricating and cooling conditions provided, wear of the supporting pads is still high, usually occurring on the first third of the legnth of the pads. This wear, and thus the changed geometry of the tool, often produces severe chatter and vibrations, increasing the power consumption and leading to excessive cutting forces. Often, the frictional temperature rises beyond the flash point of the coolant. This can be observed from the carbon deposit on the supporting pads.

The frictional forces can be reduced substantially, if a full hydrodynamic lubricating film is maintained at all times. This, of course, requires special considerations for the exact geometry of the supporting pads. To maintain a stable hydrodynamic film, the following condition must be satisfied [39]:

$$bLN/R_{s_1} > 125 \times 10^{-3} \qquad (4.34)$$

where

μ = absolute viscosity of coolant in P

P = Poise; $1P = (1/6.894757)10^{-4}$ reyns

b = width of the supporting pad in mm

L = length of the supporting pad in mm

N = cutting speed in rps

R_{s_1} = resultant force on each supporting pad in N

N = Newton; 1 N = 0.225 lbf

Considering a coolant such as Shell Garia T, with $\mu = 10^{-6}$ reyns (6.894 cP centipoises) used and a tool where the length of the pad is taken equal to the diameter of the boring head the width of the pad approximately 25 per cent of its length, equation (4.34) can be reduced to

$$R_s \leq \frac{6.89}{3} \, dv \approx \tfrac{3}{4} \, dv \quad [N] \tag{4.35}$$

where

d = tool diameter in mm

v = cutting speed in m/min

R_s = limiting hydrodynamic support force on the pad in N

Fig. 4.10 shows this limiting hydrodynamic support force in relation to the tool geometry, for various cutting speeds. For example, a 40 mm tool cutting at a speed of 100 m/min has a limiting support force R_{s_1} = 3,000 N, at
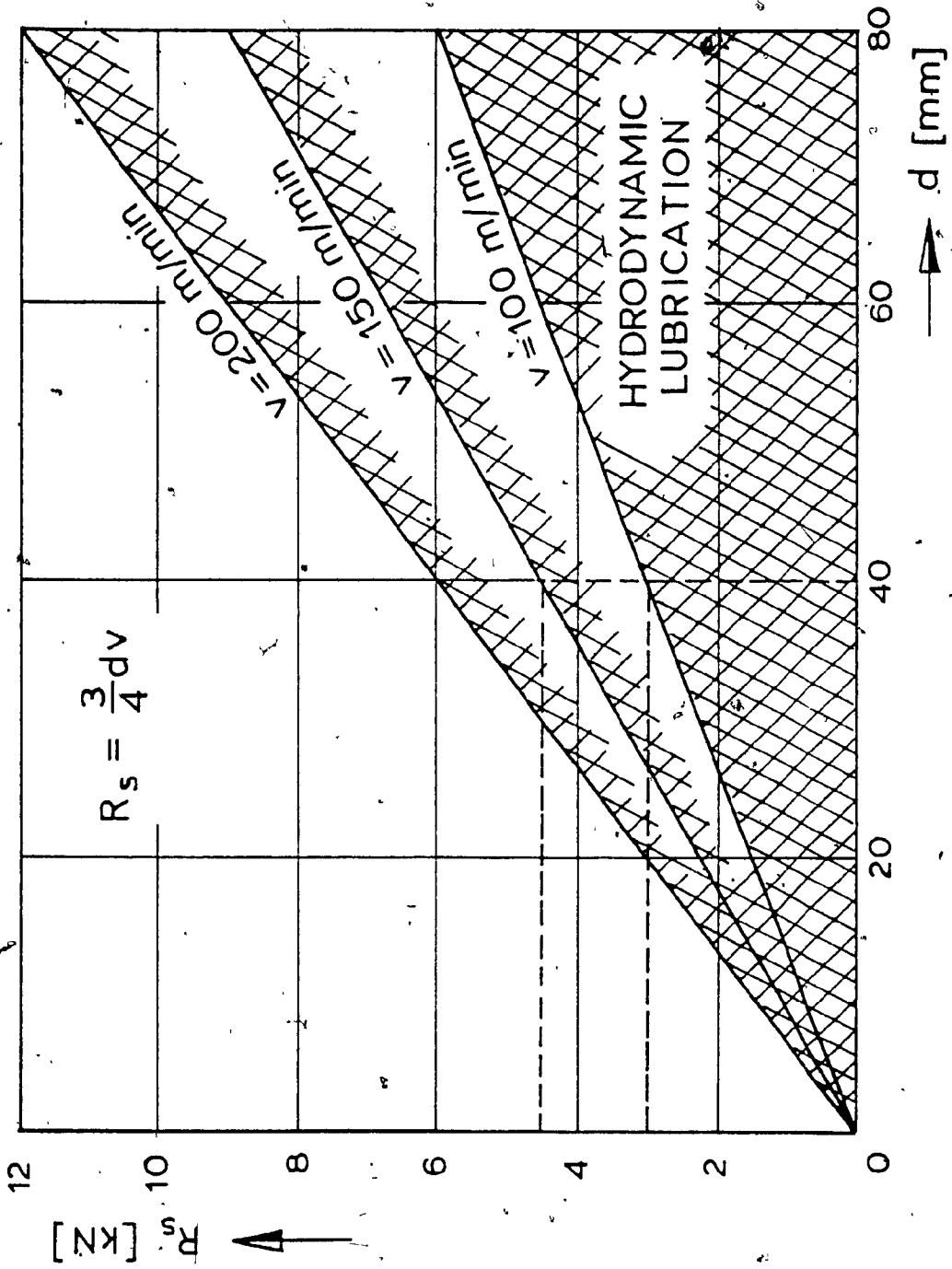
FIG. 4.10 SUPPORTING PAD RESULTANT FORCE FOR HYDRODYNAMIC
LUBRICATION IN RELATION TO BORING DIAMETER

at 150 m/min, R_{S_1} = 4,500 N and at 200 m/min R_{S_1} = 6,000 N. Certainly, these values can be slightly increased when considering the additional hydrostatic effect of the coolant pressure.

Evidently, the cutting force resultant is bounded by a minimum value resulting from the condition of the tool stability and guidance and a maximum value resulting from the hydrodynamic supporting capacity of the wear pads. If any compromise is necessary, it should be borne in mind that equation (4.34) is on the conservative side and that a safety factor of five separates the stable thick film region, set by the equation and the limit of unstable thin film lubrication.

4.4   OPTIMIZATION OF MULTI-EDGE TOOLS

'The analysis given in the previous two sections enables us to set limits for the cutting force resultant as the objective of the optimization similar to that of the staggered tools.

The line of action defined by λ is a variable dependent on independent variables ϕ_i and b_i. To eliminate λ as in the staggered tools, the coordinate system at λ is rotated counter-clockwise, and a new objective function is defined which is identical to that in equation (3.14):

$$Y(\phi_i, b_i) = \left| \sum_{i=1}^{n} (F_{Ri} \cos \phi_i - F_{Ti} \sin \phi_i) \right| - |\vec{R}_s|$$

$$+ k_w \left| \sum_{i=1}^{n} (F_{Ri} \sin \phi_i + F_{Ti} \cos \phi_i \right| \qquad (4.36)$$

where k_w is a positive weighting factor.

The objective function is a multivariable, unconstrained, nonlinear function in ϕ_i and b_i which we wish to be a minimum or preferably zero, under the condition $\lambda = 0$.

Although equations (4.36) and (3.14) are identical, there is a large difference in their evaluation. While the cutting force components in (3.14) are constant in magnitude and are evaluated only once during the optimization procedure, the cutting force components in (4.36) are continuous functions of ϕ_i and b_i and are evaluated in each optimization step. In addition, it is desired that in multi-edge tools, the specific mechanical and thermal load of all cutting edges be as uniform as possible. If the spacing between some of the cutting edges becomes excessive, these edges will carry more load than the remaining ones. This will then result in an uneven wear and tool life of the cutting edges. It is therefore desired that the spacing of the cutting edges be controlled. This can be achieved if the differences in the effective cutting depths are kept to a minimum. Using equation (4.19) a functional relationship for these differences can be defined:

$$\Delta s_i = s_{i+1} - s_i \qquad (4.37)$$

and the objective function

$$Y_3 = \sum_{i=1}^{n} |\Delta s_i| \qquad (4.38)$$

where $i = 1, 2, \ldots, n$, with the subscripts replacement implied.

Using (4.36) and (4.38), the total objective function can be rewritten as follows:

$$Y = -(k_{W1} Y_1 + k_{W2} Y_2 + k_{W3} Y_3) \qquad (4.39)$$

where

$$Y_1 = |R_X - R_S| \qquad (4.40)$$

$$Y_2 = |R_y| \qquad (4.41)$$

and, k_{W1}, k_{W2}, k_{W3} are positive weighting factors.

The objective function (4.39) is to be maximized. It is applicable to both types of tools, solid boring and trepanning. Although the widths of cut are constant in trepanning tools, the magnitudes of the cutting force components are not constant, because these are functions of the angular locations ϕ_i through the cutting depths s_i, as given by equation (4.19).

The number of decision variables for each type of tools are:

Solid boring $\qquad n_v = 2n - 1$

(4.42)

Trepanning $\qquad n_v = n$

where

n_v = the number of decision variables

n = the number of cutters

The decision variables in solid boring are:

$$\phi_i, \quad i = 1,2,\ldots,n; \quad b_i, \quad i = 1,2,\ldots,n-1$$

and in trepanning:

$$\phi_i, \quad i = 1,2,\ldots,n$$

While in staggered tools, the number of cutters and their widths are known in advance, and their angular positions are restricted in a way that the outer cutter is located opposite or nearly opposite to the wear pads, in multi-edge tools, the number of cutters is not known in advance, but is restricted by the strength of the head, and the angular locations of the cutters are bounded and depend on the locations of the two neighbouring cutters. The widths of cut in solid boring vary but are not unrestricted. Their limits are prescribed by the designer and are constant, the upper bound being less

than the tool radius for all but one cutter. These restric-
tions do not require modification of the objective function,
so it remains unconstrained. They can be implemented by
proper bounding of the tool parameters, i.e., by prescribing a
maximum number of cutters and lower and uper limits of the
cutting widths b_i and angular locations of cutters ϕ_i.

First, the limit for the number of cutters is determined.
If equation (4.22) is applied to the average cutting edge, we
have an average radius of the chipmouth circle:

$$r_m = \xi b_m - d + \sqrt{d^2 - \xi d b_m} \qquad (4.43)$$

where b_m is the average cutting width $b_m = \frac{1}{2}(b_L + b_R)$; b_L
and b_R are lower and upper bounds of the widths of the cut,
respectively.

In the solid boring head, one cutter cuts to the center,
and for that cutter $b_m = b = d/2$, and taking $\xi = 1.1$, the
chipmouth radius is calculated

$$r = 0.221d \qquad (4.44)$$

If c designates the part of the chipmouth area re-
served for the cutter pocket, then the total area to be taken
off of the head cross-section is:

$$A_c = (1+c)[(n-1)r_m^2\pi + (0.221d)^2\pi] \qquad (4.45)$$

For a head to be strong enough to withstand the loads exerted on it during the cutting operation, the area A_c should not exceed a certain percent of the head cross-sectional area

$$A_c \leq \zeta \frac{\pi d^2}{4} \tag{4.46}$$

which enables us to determine a maximum number of cutting edges

$$n \leq 1 + \frac{\zeta d^2/4(1+c) - (0.221d)^2}{r_m^2} \tag{4.47}$$

In trepanning tools, however, all cutting widths are identical, i.e., $b_m = b$, $r_m = r$ and hence

$$(1+c)nr^2\pi \leq \zeta(d-b)\pi b \tag{4.48}$$

and a maximum number of cutting edges

$$n \leq \frac{\zeta(d-b)b}{(1+c)r^2} \tag{4.49}$$

It was found that $\zeta = 0.4$ to 0.5 is an optimum for both the solid boring and the trepanning tools. $c = 0.4$ for solid boring and $c = 0.6$ for the trepanning seem to be the best values.

With these values, equations (4.47) and (4.48) can be used for the determination of a maximum number of cutting edges in the solid boring and trepanning tool, respectively.

As discussed in the first section of this chapter, multiple cutting should cover the outer and middle zones of the tool radius. Accordingly, the upper bound for the widths of cut should be around three-quarters of the radius, except for one cutter, which cuts toward the center. In trepanning, the cutting widths are constant and standardized in commercially available inserts.

The angular locations of the cutting edges are specified by the limiting conditions on the angular parameters ϕ_i. However, because the cutter angles and widths of cut are continually changing, and the limits on the cutter angles are dependent on both of these parameters, their limits are continually changing, too. Figure 4.11 shows two cutters arbitrarily located on a solid boring tool. The figure is based on the analytical model of a boring head, shown in Fig.4.7 which was used to approximate the chipmouth. With this approximation, the angle ψ_i, as defined by equation (4.23), is used to express the limits for the location of cutter i; the lower limit is given by

$$\phi_{Li} = \phi_{i-1} + \alpha\psi_{i-1} + \Delta\psi_i \tag{4.50}$$
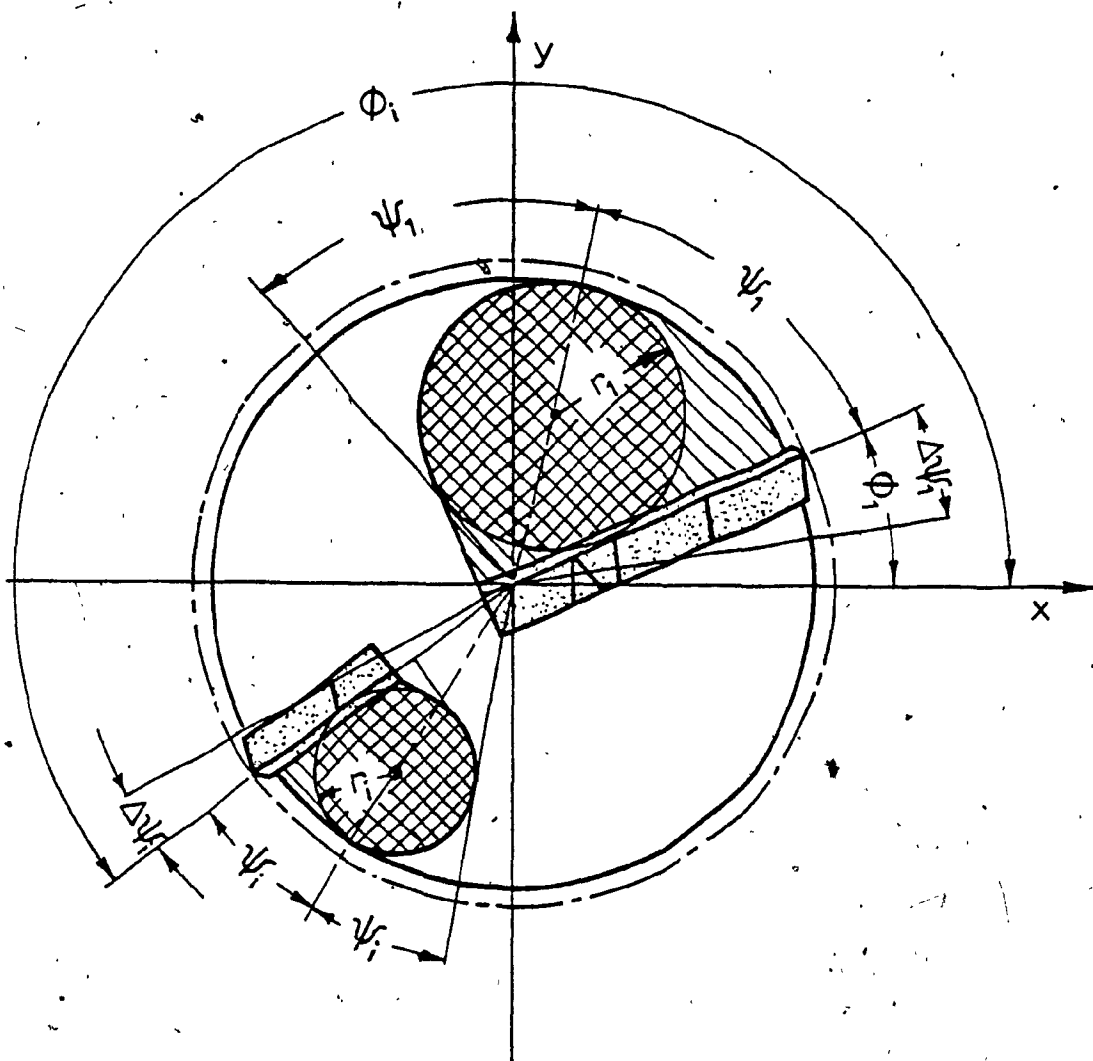
FIG. 4.11   LOWER AND UPPER BOUNDS FOR LOCATION
OF CUTTERS RELATIVE TO EACH OTHER

and the upper limit by

$$\phi_{Ri} = \phi_{i+1} - \alpha\psi_i - \Delta\psi_{i+1} \qquad (4.51)$$

In these equations, the subscripts replacement is implied, so if $i = n+1$ then $i = 1$, and if $i = 0$ then $i = n$; also if $\phi_{Ri} < \phi_{Li}$ and if $\phi_i < \phi_{Li}$ then $\phi_{Li} - 360 \to \phi_{Li}$; if $\phi_{Ri} < \phi_{Li}$ and if $\phi_i > \phi_{Li}$ then $\phi_{Ri} + 360 \to \phi_{Ri}$.

Equations (4.50) and (4.51), as well as equation (4.23), are valid for both the solid boring and the trepanning heads. However, the values of α and Δ are different. and they depend upon how much space expressed in angular units is needed above the cutting edge for the chipmouth and how much space is needed below the cutting edge for the cutter pocket. It was found that $\alpha = 2.0$ and $\Delta = 0.25$ to 0.3 best met the space requirement in the solid boring heads, and $\alpha = 1.5$ and $\Delta = 1.5$ are the values most appropriate to the trepanning heads.

There is no provision in the optimization for the location of wear pads. This has to be determined by the designer. He has the option of standard spacing or a little larger for wear pads, depending upon the magnitude of the cutting force resultant and its deviation in direction, as well as upon the space available for the wear pads, in a given design.

4.5 OPTIMUM TOOL DESIGNS

The method described in Section 3.2 is used to minimize the modified objective function. Since the direct search routine which has been adapted for tool optimization maximizes an objective function, the negative objective function given by (4.39) is maximized, as it was explained in Chapter III.

The computer program consists of a main program and six sub-routines. The direct search itself, is realized in two standard sub-routines, which are readily available in most computer libraries:

(a)   PATRN sub-routine

(b)   EXPLOR sub-routine

The flow charts of these two sub-routines are given in Figures 3.3, 3.4, and 3.5, in Chapter III.

The other three sub-routines developed for the particular problem of tool optimization are:

(c)   LIMITS sub-routine

(d)   CHECK sub-routine

(e)   MERIT sub-routine

(f)   STATS sub-routine

The conversion of program variables into the problem variables, the evaluation of the objective function, and again, the conversion of problem variables into the program variables is performed in the MERIT sub-routine. The detail flow chart of this sub-routine is given in Fig. 4.5. This sub-routine is called by the PATRN and EXPLOR subroutines for the function evaluation after each exploratory or pattern move.

The LIMITS subroutine evaluates the lower and upper bound for the angular parameters and is called by the PATRN and EXPLOR sub-routines after each pattern and exploratory move. No flowchart is given for this sub-routine, since it is relatively simple. The bounds are evaluated by the use of equations (4.50) and (4.51) with the logic required.

The CHECK sub-routine has been separated from both the PATRN and EXPLOR sub-routines. It checks the limits of the variables and it is called by the two sub-routines after the LIMITS sub-routine to check the variable limits.

The STATS sub-routine calculates the deviations in magnitude and direction of the cutting force resultant and in addition, calculates the feed cutting force components and the cutting torque. No flowchart for the evaluation of the deviations is given, since it is simple. For the evaluation of the feed components and the cutting torque, however, the logic given by the flowchart in Fig. 4.5 is used. This part

of the cutting force evaluation is not included in the

MERIT sub-routine for the sake of time saving.

The main program reads in the data, calculates or
reads in the optimal number of cutting edges, calls some of
the sub-routines, and prints out most of the results.

There were several minor changes made to the standard
sub-routines of the direct search routine. These changes are
not of significant importance to be reported. During the pre-
liminary testing of the program, however, a major addition to
the EXPLOR sub-routine was necessary, in order to make it
work efficiently. Namely, during the optimization process,
the cutting edges will slowly rotate in the direction in
which the objective function is approaching the optimum.
Occasionally, two cutters will move towards each other until
their limiting conditions do not allow them to move any
further. This would occur, especially when the cutting head is
overcrowded with cutters for a particular diameter. The
variables would then become 'locked' together. To solve this
problem, an addition was made to the EXPLOR sub-routine in
which the pair of 'locked' cutters would be rotated together,
as a pair, in the direction of approaching the optimum. This
made the sub-routine work in cases when normally they would
not, without this addition. This supplemental section to
the exploratory moves is described in the flow chart given in
Fig. 4.12, and has been implemented into the EXPLOR sub-routine
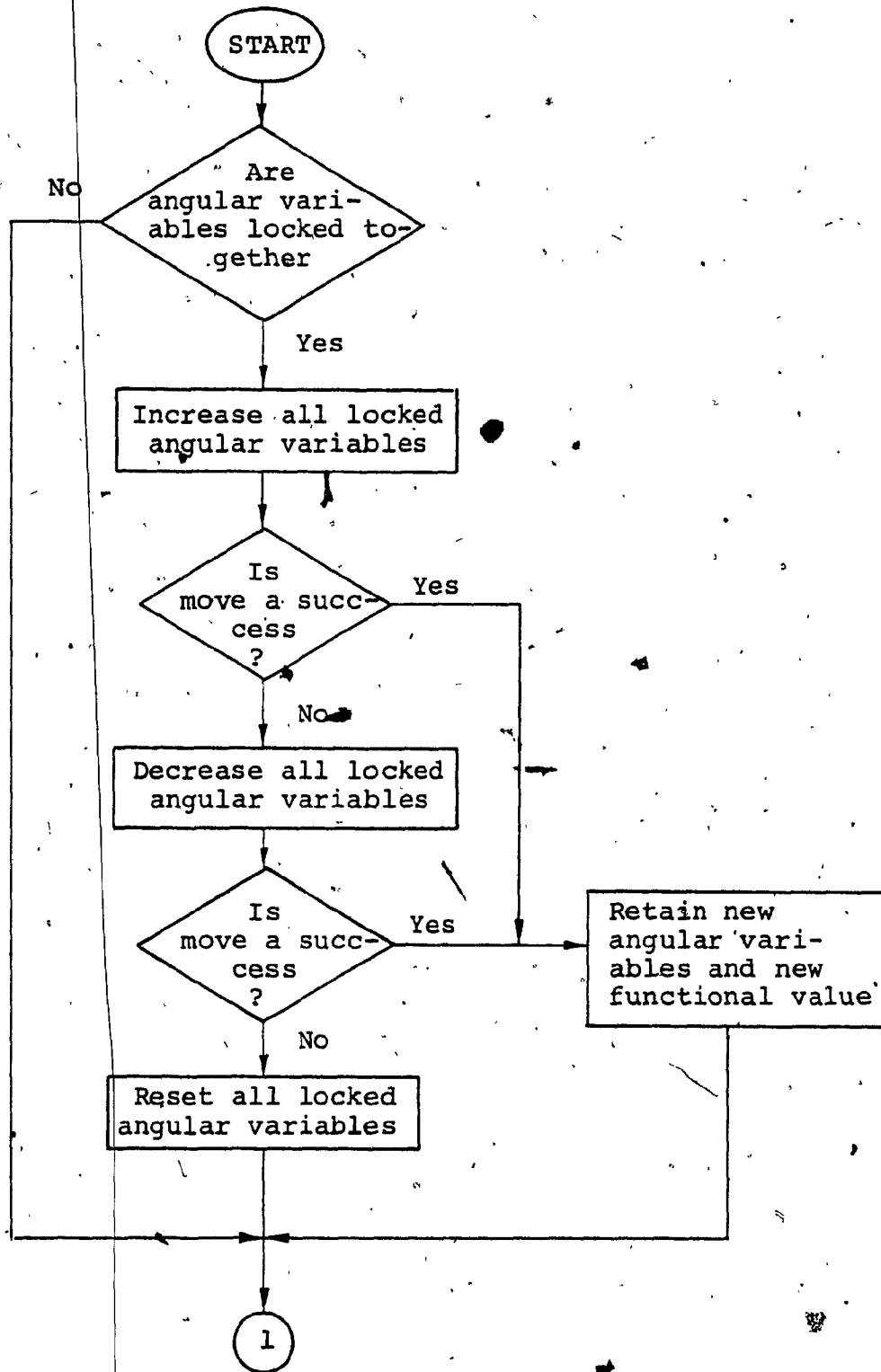
FIG. 4.12   DESCRIPTIVE FLOW CHART OF SUPPLEMENTAL
SECTION OF THE EXPLORATORY MOVES GIVEN
IN FIG.3.3.

described by the flow chart given in Fig. 3.3.

The preliminary testing of the program which primarily was carried out to examine its capability and efficiency, was done with rather hypothetical tool parameters. The exponents to y_1 and y_2 in calculating the cutting force components were not definitely established, at the present values and material constants were more or less selected without serious consideration. The results of this preliminary program testing have proven that the technique represents quite a general and efficient means for the optimization of all types of multi-edge tools, such as staggered tools, solid boring, and trepanning multi-edge tools.

The program listing is given in Appendix IV. The program is written in FORTRAN language and the calculations are performed on a CDC-6400 computer. Five optimal tool designs from the preliminary program testing are presented in Table 4.1. The data sheet for these tools is given in Table A4.1. The typical printouts of these programs reveal that the total number of functional evaluations varied between 195 and 650, the number of base evaluations between 25 and 60, and the central processor time between 4.2 to 11 seconds. The STATS sub-routine was not included in this package, since no routine for statistical analysis was available at that time. The problem had been treated as a deterministic one until the statistical analysis was implemented.

Before the completion of the package by implementing the STATS sub-routine which handles the statistical analysis, the program was used to optimize a trepanning head with three cutting edges, Tool No. 1, in Table 4.2. This tool was aimed toward application in a steel workpiece. The head proto-type was to be manufactured and tested on deep-hole machining facilities that were available for this purpose.

Trepanning Head No. 2, in Table 4.2, was optimized for the same workpiece material after the program package was completed by implementing the STATS sub-routine, and after Tool No. 1 was found likely unstable, due to the large devia-tion in direction of the cutting force resultant. This tool was optimized for a double resultant cutting force which resulted in more than twice less deviation in direction $\Delta\lambda$.

Tool No. 3 in Table 4.2, is a solid boring head optimiz-ed for the same workpiece material as the other two tools.

The tool parameters that are known in advance are the hole diameter, widths of the chip separators p_1 and p_2, and approach angles of the cutting edges κ. These are assumed to be identical for all cutting edges. Constants C_T, C_R and C_F for each cutting zone can be determined from the cutting edge geometry and the ultimate shear strength of the workpiece material, as was described in the first section of this chapter.

TABLE 4.1 — OPTIMAL TOOLS FROM PRELIMINARY PROGRAM TESTING

TABLE 4.1 — OPTIMAL TOOLS FROM PRELIMINARY PROGRAM TESTING

CASE NO.	SOLID BORING			TREPANNING	
	1	2	3	4	5
NC	3	4	5	3	4
RS [kN]		4.50			3.50
R_x [kN]	4.499975	4.500014	4.499991	3.499950	3.499999
R_y [kN]	.000029	.000007	-.000000	.000038	-.000003
$\Sigma\Delta S(I)$	.125499	.196536	.143811	.099068	.086672
Y	-1.255180	-1.965422	-1.438130	-.990982	-.866731
X(1)	72.8844	108.1266	33.4062	28.5438	38.9984
X(2)	162.3695	156.3315	89.7059	175.0094	156.9781
X(3)	268.1000	215.0531	138.4386	262.0344	228.3234
X(4)	14.2605	302.0000	194.6956	28.00*	294.3000
X(5)	18.8807	14.1605	258.3869	28.00*	28.00*
X(6)	28.321*	14.1605	15.4605	28.00*	28.00*
X(7)	-	18.4000	14.8605	-	28.00*

(continued)

	SOLID BORING			TREPANNING	
CASE NO.	1	2	3	4	5
NC	3	4	5	3	4
X(8)	–	28.321*	17.0000	–	28.00*
X(9)	–	–	15.7000	–	–
X(10)	–	–	28.321*	–	–

* PARAMETER CONSTANT

TABLE 4.2   OPTIMAL PARAMETERS FOR THE THREE DESIGNED TOOLS

	TREPANNING		SOLID BORING
TOOL NO.	1	2	3
NC	3	2	3
RS [kN]	3.2792	7.4495	7.0946
RX [kN]	3.2792	7.4495	7.0946
RY [kN]	0.0000	0.0000	0.0000
$\Sigma\Delta S(I)$	0.0465	0.0788	0.03492
Y	-0.4652	-0.7875	-0.3492
RZ [kN]	25.2245	20.3709	21.0952
TQ [kNmm]	964.0965	889.4810	348.8871
ΔR [kN]	0.8729	0.7894	1.2426
$\Delta\lambda$ [DEG]	19.9114	9.5839	4.5262
X(1)	28.0	28.0	.14.700
X(2)	28.0	28.0	18.880
X(3)	28.0	-	28.321

(continued)

TOOL NO.	TREPANNING		SOLID BORING
	1	2	3
X(4)	22.652	-39.291	44.832
X(5)	167.015	174.509	145.932
X(6)	254.351	-	275.132

ρ, δ, k_{w_1}, k_{w_2}, k_{w_3}, and f are the computer program parameters. R_s is the magnitude of the cutting force resultant pre-selected on the basis of a force necessary for the tool guidance and the hydrodynamic lifting force at the wear pads. The feed (denoted in the program by t) is also pre-selected on the basis of the machine tool power and torsional rigidity of the boring bar to be used. Factors ζ and c are pre-selected on the basis of tool strength and space required for the chipmouths. b_L and b_R are lower and upper bounds for the widths of cut. For trepanning heads, the cutters are identical. Factors p and q represent the relative deviations in the radial and tangential cutting force components, respectively. Constant α sets the initial input values for the angular locations of the cutting edges.

The data sheet for these three designed tools is given in Table A4.2.

With these input conditions, the computer program can optimize for two to n cutting edges. The program evaluates the number of cutting edges. The factors that limit the number of cutting edges, are:

(a) The tool diameter - given a certain tool diameter it is possible to attach only a certain number of cutting edges to the tool head, because of the large amounts of space reserved for chipmouths and cutter pockets. The designer can affect the

number of cutters by choice of factor ζ and
the upper limit for the widths of cut, b_R.

(b) Tool strength - the material of the head must be
of sufficient strength to carry the large loads
that are generated. The greater the number of
cutting edges, the larger the loads that are
generated, and the less the mass of cutting head
to support the cutting edges.

(c) Machine capacity - an increased number of
cutting edges would necessarily increase the
feed rate to achieve the optimal chip-forming
conditions. This, however, may require the
torque which is excessive for the boring bar and
for the machine power plant.

The computer print-outs for these three tools are
given in Appendix IV. They show that for the diameters used
three cutting edges were the optimum numbers for both the
solid boring and the trepanning head. However, under the
condition that only 40 percent of the head cross-sectional
area is used for chipmouths and cutter pockets, the number
of cutting edges for the trepanning head was found to be
two.

There is a large number of solutions for any number of cutting edges. These local optimums are dependent on the initial input values and represent the final sets of para- meters closest to the initial sets of input values. This allows a designer the opportunity of partially predetermining the location of the cutting edges. The designer can also choose the optimum result from several of the solutions thus obtained.

Even the optimum result chosen for the design may be subject of minor corrections. These corrections are fine adjustments of the parameters from a practical point of view for the designer's convenience for example, rounding off, the parameters. The effect of these corrections is calculat- ed by a separate computer program called FORCE. This program calculates the resultant force magnitude, while its direction is maintained horizontally and also evaluates the deviations in magnitude and direction of the force result- ant. The program listing and the computer printouts are included in Appendix IV. Actually, the optimal tool designs listed in Table 4.2 are the results of these adjustments and represent the printouts of this program. The difference between the corrected tools and their original optima is, however, insignificant; the corrected tools are free of weak points in terms of stress concentration which cannot be detected by the optimization program itself.

The final step, before the tool design is undertaken, is to locate the wear pads with respect to the direction of the resultant force. This aspect has already been sufficiently investigated in single cutting tools [1,38,55]. The cutting force resultant in multi-edge tools has to be transmitted to the bore-wall in the same way through the two wear pads, as it is transmitted in single-edge tools. This means that the leading wear pad supports most of the resultant force and the trailing wear pad supports the rest of the force. The wear pads are located between 90 and 100 deg. from each other.

Recent research work [61,69] reveals a more qualitative criterion for the wear pad locations. Due to this criterion, the normal supporting force resultant should bisect the angular spacing between the two wear pads. In addition, the angular spacing between the wear pads depends on how much normal force on the wear pad is desired. So, if the wear pad angular spacing tends towards 180 deg., the normal force on the wear pads tends towards infinity and hence, the friction force at the wear pads tends towards infinity. It is also shown that the normal supporting force resultant at the wear pads, varies significantly in direction, due to fluctuation in the friction coefficient. If the friction coefficient is fluctuating between 0.2 and 0.4, the variation in the direction of the normal force resultant will be between 11.3 and 21.8 deg. This variation of ± 5.25 deg.

together with a variation, due to fluctuation in the cutting force components, may in extreme cases, induce intolerable tool instability.

Although the friction coefficient used in this analysis is incompatible with the hydrodynamic theory of lubrication, the procedure seems to lead to the wear pad locations well established in practice, so far. Hence, the tool designs, based on the optimal parameters listed in Table 4.2, have the wear pads located by use of the above described procedure. Namely, the normal supporting force resultant was rotated at the average friction angle of 16.6 deg. clockwise, and the wear pads located so that its line of action bisects the angular spacing between the pads. The angular spacing between the wear pads is greater than 90 deg. and depends on the magnitude of the cutting force resultant and the variation in its direction. The greater the force resultant, the less angular spacing of the wear pads, the greater the variation in the direction of the resultant, the greater the spacing of the wear pads.

The cutting tool optimum designs achieved by the described procedure result from the optimum conditions for the tool in a steady-state cutting operation. However, the tool might work under quite different conditions during the initial cutting into the workpiece. Namely, depending on the order in which each cutting edge begins to cut, the cutting force resultant will increase in magnitude and vary in direction.

This variation in the direction of the resultant force should be within the limits derived from the condition that the line of action of the normal supporting resultant points between the wear pads. This is the principal condition for tool guidance and stability.

In the case of trepanning with multi-edge tools, all cutting edges start cutting into the workpiece simultaneously, with their middle zones. As these zones completely enter the workpiece, the inner zones will begin to cut and before they enter the workpiece, the outer zones will begin to cut. By the time the outer zones completely engage in cutting, the cutting tool reaches the steady state cutting. During this initial cutting, it seems that the period during which the middle zones of the cutters cut alone is most critical for the direction of the cutting force resultant. The approach angles of the inner and outer zones are opposite and the radial forces at these zones cancel out, while the tangential forces increase to their full magnitudes. So, it results in a change of the tangent of θ during this period from approximately 3.3 to 10, which means that the angle changes about 11 deg. If all the cutting forces change direction 11 degs., then the resultant force will change its direction at the same angle. Since 11 deg is not a significant change in direction, it could be considered that the multi-edge trepanning tools will be well supported during the initial cutting by the wear pads; see layouts Z-042-23-0200-0201 and

Z-042-23-0200-0204, in Appendix V.

In the case of the solid boring tool with three cutters, the cutter 1 first begins to cut and it is evident that its cutting force will be supported by the wear pads; see layout Z-041-1000-0051 in Appendix V.

CHAPTER V

EXPERIMENTAL SET-UP

CHAPTER V

EXPERIMENTAL SET-UP

Since it is more convenient to carry out actual tests with trepanning tools, rather than with solid boring ones, only the trepanning heads designed and optimized in the previous chapter were manufactured. The optimal design parameters of these tools are given in Table 4.2. The two and three-cutting edge trepanning heads were then tested using the deep hole installation of Menasco MFG of Canada Ltd., in Montreal with workpieces from the company's production line.

5.1 CUTTING HEADS

The trepanning head with the three cutting edges was designed for a nominal hole diameter of 4.145 inches (105.283 mm) and standard BTA 28 trepanning inserts. The total groove width cut was 28 mm. Also standard wear pads of 16 mm width were used. They were located at 90 deg. from each other, based on the principle described in the previous chapter. The head prototype was manufactured to the detail drawing Z - 042-23-0200-0202 included in Appendix V and was found conforming to the drawing specifications. It is important to state that the cutting edge front geometry specified on the cutting inserts by the approach angles κ is not identical to the geometry of the inserts, as

mounted on the cutting head. Namely, the cutters are tilted
outward 2 deg. to compensate for the wear of the circle land
when regrinding the inserts. This was taken into
account before the design was undertaken and during the tool
optimization, by increasing the approach angles by 2 deg.
The accurate location of the inserts relative to the head
axis was assured by prescribing a close tolerance on the width
of the positional slot and achieving a locational transition
fit of the LT2 push fit class (ASA). In order to avoid any
eccentricity of the positional slots the tool of the slotting
machine was kept at the same position and at the same slope
relative to the machined cutting head which was fixed in a
dividing head and rotated through the desired angular distance.

The head was tested with commercially available
standard BTA 28 carbide inserts. Figure 5.1 shows the tre-
panning head with three standard inserts mounted on it and
two spare inserts in the foreground.

The standard thick-walled boring bar originally plann-
ed for the tool testing phase was not available at the company, so
the next smaller size standard boring bar had to be used. This
bar was only 2 mm less in inner diameter and could be used with
the head provided an adapter was fitted. Such an adapter was
machined and inserted into the head, so that this could be
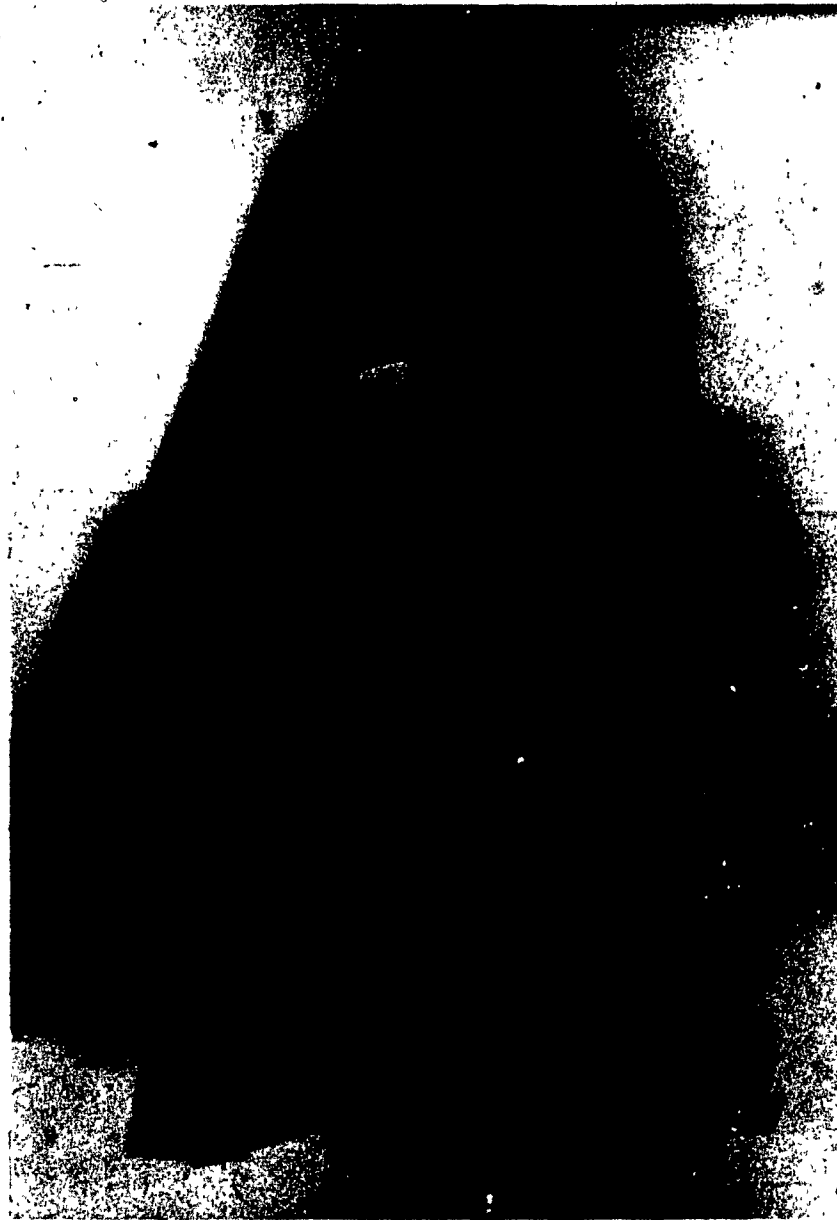
FIG. 5.1 TREPANNING HEAD PROTOTYPE WITH THREE
         CUTTING EDGES
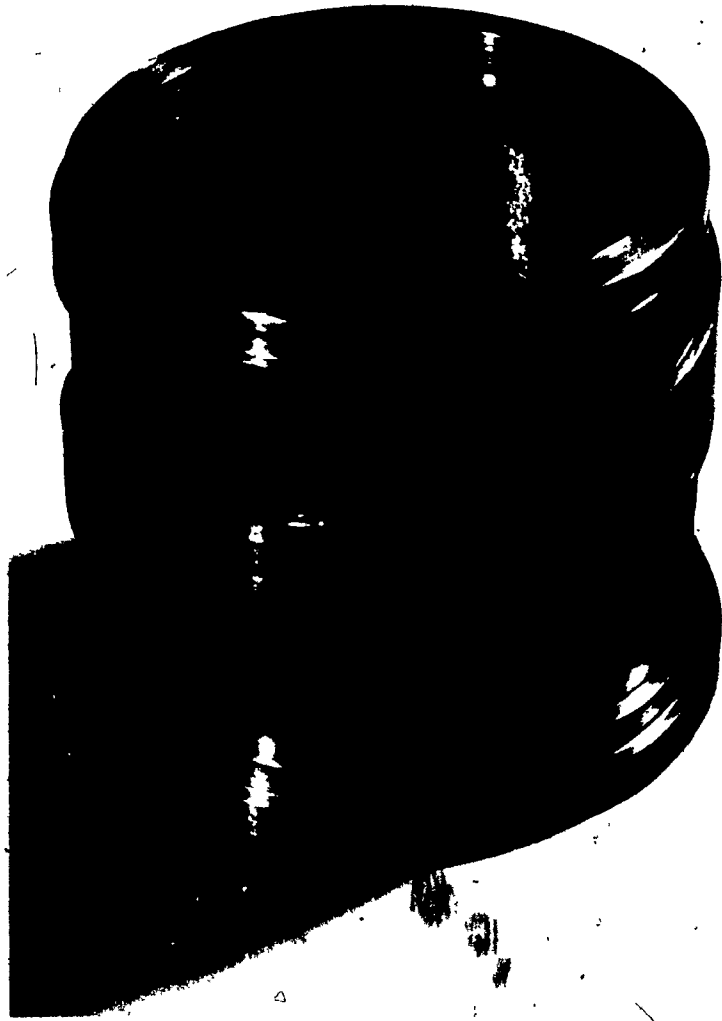
FIG. 5.2 HEAD ADAPTER

attached to the boring bar. The adapter is shown in Fig. 5.2 .
A serious shortcoming of this modification was the fact that
the boring bar used in the tool test had only half the
torsional rigidity of the thick-walled boring bar originally
selected for this purpose. This lower torsional rigidity
was a serious drawback because it did not permit us to take
full advantage of the multi-edge cutting tool by applying
higher feed rates.

The cutting head was not ground to the specifications
of the layout Z-042-23-0200-0201. The three inserts were
levelled to the best possible positions. However, being
commercial inserts, with no regrinding for accuracy, it was
impossible to level them ideally onto the head. The inserts
were set at compromising levels with minimum plus-minus
differences from a mean level. This suggests that the cutting
force components and, hence, the resultant force in such a
head, might have been rather erratic in both magnitude and
direction which might have caused improper tool guidance, and
inaccuracies in the hole size.

After the preliminary tests with the head prototype it was concluded that minor changes were necessary and the head was modified as follows:

(1)   The trailing wear pad was relocated 30 deg. further from the leading pad so that the wear pad angular spacing became 120 deg. This was done with the intension of slightly increasing the supporting forces at the wear pads, and also to make up for an increase in the frictional forces at the wear pads which would tend to shift the resultant supporting force toward the trailing wear pad. But, the main reason for this modification was an excessive variation in the direction of the resultant force which was found after the STATS subroutine had been implemented in the computer package.

(2)   The tool inserts were ground to the specification of the layout:

(a)   the cutting edges were identically ground in the front profile;

(b)   the circle land of the cutter located opposite to the wear pads was ground to the exact hole size; the circle lands of the other cutters were ground inwards for a predetermined clearance;

FIG. 5.3   SET-UP FOR GRINDING TREPANNING
INSERTS

(3)   the chip-breaker grooves were ground as a

function of the effective cutting depth per cutting

edge.

To assure accurate grinding and identical inserts in
both the front profile and the length, a grinding fixture was
made and used for accurate insert positioning during the grind-
ing operation on a universal tool grinder. The location of
the slots in the fixture assured the identical approach
angles for all the inserts, while an adjustable set-screw at
the rear of the fixture assured equal length for the inserts.
The clearance angle of the inserts could be set either on the
grinding head or on the dividing head, to which the fixture was
attached. Grinding of the circle lands of the inserts was
done on a center grinder. All grinding operations were done
with no coolant applied with diamond wheels at speeds from 12
to 18 m/sec (39.4 to 59 fps). The set-up for grinding the
front profile of the inserts is shown in Fig. 5.3.

Besides the trepanning head with three cutting edges,
a head prototype with two cutting edges was also manufactured for
further testing. Having been optimized for a cutting force
resultant of 7.45 kN (1676.25 lbf) this head was expected to be
better guided because of less deviation in the direction of
the force resultant. Also, in order to avoid the use of
excessive feeds, it could be tested with lower feeds and hence,
lower cutting torques without experiencing chip-formation

FIG. 5.4 TREPANNING HEAD PROTOTYPE WITH
TWO CUTTING EDGES

problems. This was supposed to diminish the difficulties caused by the use of a boring-bar of relatively low torsional rigidity.

This trepanning head is of the same nominal diameter and is also aimed at the use of standard trepanning inserts that have been reground to the grinding specifications of Drawing No. Z-042-23-0200-0204, by the use of the same grinding set-up shown in Fig. 5.3. The head with the inserts mounted on it is shown in Fig. 5.4.

5.2 MACHINE TOOL

For the testing of the heads, a modern universal deep-hole boring machine VDF B10 was used. The machine possesses all the characteristics necessary for successful deep-hole machining: sufficient power to overcome cutting torques, sturdiness and rigidity throughout the machine, vibration free power supply   at all speeds, infinitely variable feeds independent of speeds, adjustments in feed possible while machining is in progress, and while chip formation is being observed. It allows the counter-rotating boring operations and has a system of controls and/safety devices to indicate faulty operation, and if necessary, to stop the operation.

Fig. 5.5 shows the front and rear pictorial views of the experimental set-up on VDF B-10 deep-hole boring machines.
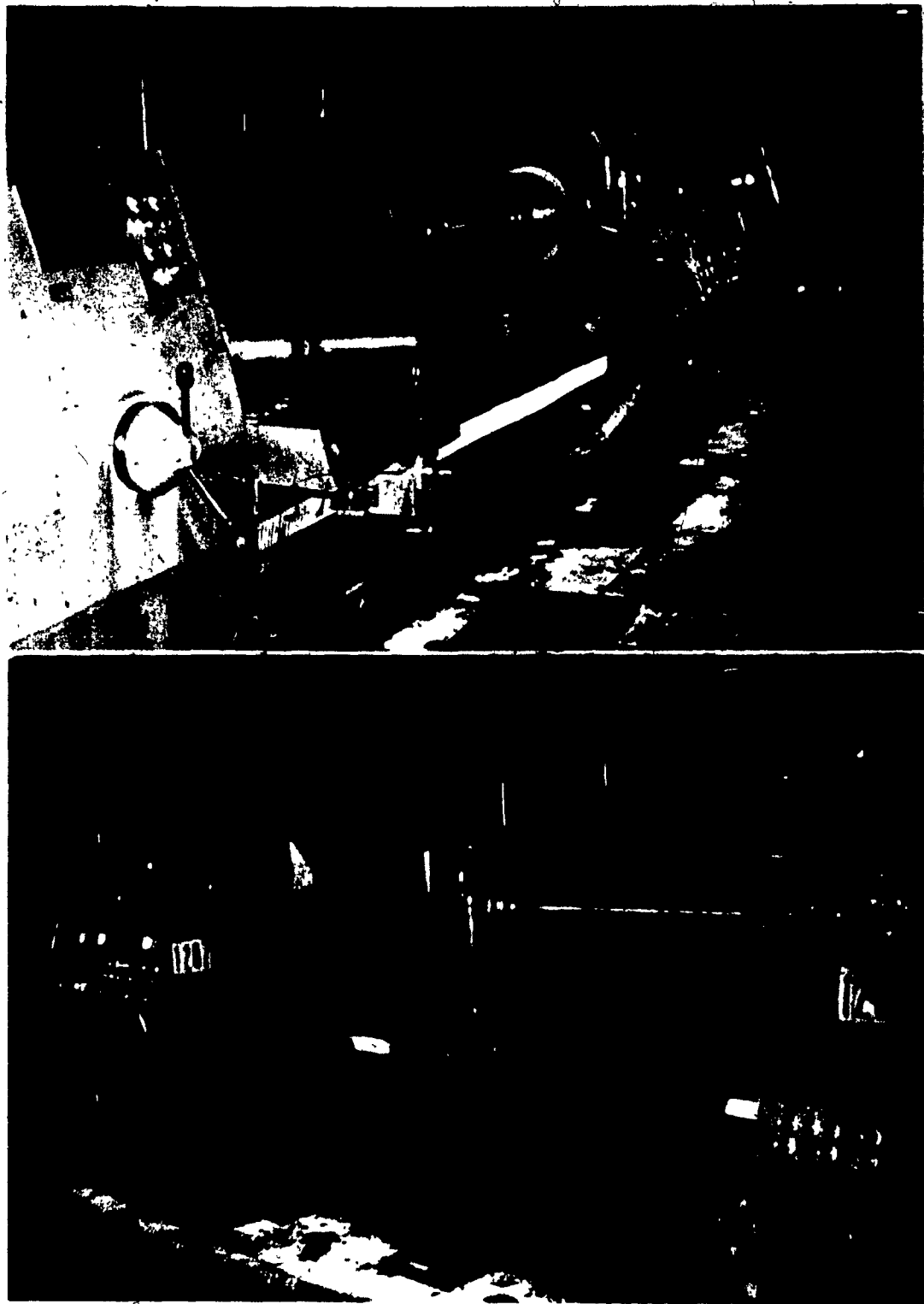
FIG. 5.5 FRONT AND REAR VIEW OF EXPERIMENTAL
SET-UP ON A VDF B10 DEEP-HOLE BORING
MACHINE

The technical data for the VDF B10 deep-hole boring machine is:

Work headstock drive power	74.6 kW(100 HP)
Tool headstock drive power	44.8 kW(60 HP)
Work headstock torque	max. 12.7 kNm(9,375 ft-lb)
Tool headstock torque	max. 7.62 kNm(5,625 ft-lb)
Spindle speed	12 steps 56 to 710 rpm
Boring bar speed	12 steps 56 to 710 rpm
Feed-stepless range	4 to 2,500 mm/min (0.16 to 98.5 ipm)
Fast traverse motion	3,000 mm/min(118 ipm)
Coolant flow range	232 to 855 1/min (51 to 188 gpmP
Coolant pressure range	1,480 to 2,760 kPa (215 to 400 psi)

The carriage of the fluid transfer unit which produces the clamping force on the workpiece located between the reception plate of the pressure head and the work headstock, is seen in the front view of Fig. 5.5. The controls console is attached to the carriage and has the read out indicators located from left-to-right for the following:

1) Clamping thrust force in-lb

2) Feed force in-lb

3) Power of the work headstock in HP.

4) Coolant pressure in psi

5) Power of the tool headstock in HP

6) Coolant flow rate in gpm (located below)

5.2.1 Boring Bar

The boring bar used for the testing of the tools is
a standard thin-walled bar of 82/66 mm hollow cross-section
14 feet long. Since the heads were made for standard thick-wall-
ed   boring bars of 94/68 mm cross-section, they could be
attached to this boring bar by the use of the adapter shown
in Fig. 5.2. The boring bar with the trepanning head attached
to it at its front end, is shown in the front view of
Fig. 5.5 projecting out of the pressure head.

Another view of the boring bar is seen in the rear
view of the same figure. In the foreground, the bar is
clamped to the chuck of the tool headstock; in the middle
it passes through   vibration damper of the Lanchester type;
in the background, it enters the fluid transfer unit.

The boring bar parameters are:

Outer diameter	82 mm (3.228 in)
Inner diameter	66 mm (2.598 in)
Overall length	4,267 mm (14 ft)
Free length	4,089 mm (13 ft-5 in)
Torsional rigidity	$5. \times 10^{9}$ kNcm (442,513 in-lbs)

If the calculated value of the cutting torque of
96.226 kNcm is exerted on the bar, then a twist angle of
0.269 deg. per meter can be expected. If a deflection due to
the frictional torque is added to this value, it results in

the possibility of the twist angle per unit length of the boring bar reaching the value of one-and-a-half times the value allowed for the driving shafts. This indicates that a torsional vibration due to any periodic excitation in the boring bar may reach excessive proportions, and if its frequency is below 1,000 Herz, it would cause the carbide cutters to deteriorate very rapidly.

5.2.2 Vibration Damper

The torsional vibration damper is a standard unit of each deep-hole boring machine, which absorbs torsional vibrations self-excited in the cutting operation. These self-excited vibrations, if excessive, make the cutters chatter, which has a negative effect on the surface finish and tool life, particularly on the tool life of carbide tools. The cutting tool chatter and self-excited vibrations are a phenomena common in metal cutting. The vibrations are non-linear in character, and are attributed to the existence of negative damping in the machine-tool-work-piece system.

The damper is of the Lanchester type vibration absorber. It consists of a flywheel attached to the boring bar by means of a tapered plastic bushing which can be tightened around the bar or loosened, depending on whether we wish to produce more or less Coulomb friction between the bar and the flywheel bushing. The flywheel runs on anti-friction bearings which are fixed in a massive housing. The housing can slide along the

machine sideways for the relocation of the damper at a desired position on the boring bar.

The damper is most efficient when the energy dissipation due to   Coulomb friction between the boring bar and the flywheel is at a maximum. Obviously, this maximum must exist since the energy dissipation is zero when the bushing is entirely loose on the boring bar and no friction exists between them, and when the bushing is firmly tightened on the boring bar and no relative motion between them occurs. An optimum tightening of the bushing around the bar would make the flywheel rotate together with the boring bar allowing a slippage and friction to occur on the contact surface. The best damping effect is achieved when this friction torque becomes a maximum.

Since the Lanchester damper is a displacement damper, it is most efficient when located at the maximum amplitude of the twist angle on the boring bar. The damper located at a nodal point of any vibrating mode will have no damping effect. Although the optimum conditions for   best damping effect of a Lanchester damper can be analytically predicted, uncertainties associated with the friction coefficient and the vibration mode prediction make this analysis impractical. Trial and error searches usually lead to optimal friction and the location of the damper, in each particular application.

The Lanchester damper which is clearly seen in the rear view of Fig. 5.6, besides damping torsional vibra-

tions, has an important role as an extra support in increasing the stability against the buckling of the boring bar. An alternative to the vibration damper in applications where the boring bar does not rotate, is the clamping support. This unit clamps the boring bar at a desired length and it moves with the boring bar, along the slideways during the boring operation. Although the unit can increase multi-fold, the torsional rigidity of the boring bar, its serious shortcoming is that it is applicable only for holes of low length-to-diameter ratios and to a workpiece which can be rotated. This unit is very often mistaken for the vibration damper because it resembles one so much.

5.2.3 Pressure Head

A standard pressure head of UW6 type was used as a fluid transfer unit. It transfers the cooling fluid under high pressure from a stationary unit to a rotating workpiece. A starting bushing which had been built in hardened steel and ground to a clearance of 0.038 mm(0.0015 in) on the diameter provide the cutting head with a necessary guidance during the initial penetration of the cutters until the wear pads enter into the machined hole and support the head against the hole wall. A front view of Fig. 5.6 shows the pressure head with a reception plate ready to receive the workpiece. The trepanning head of the three cutters is seen to be attached to the boring bar which projects from the starting bushing.

FIG. 5.6 CLAMPING OF THE WORKPIECE BETWEEN THE RECEPTION PLATE AND THE HEADSTOCK DEAD CENTER

5.3 WORKPIECE

The workpiece attempted was a component taken from the production line of the company. Its shape is seen in Fig. 5.6 which represents the clamping of the workpiece between the headstock dead-center and the reception plate of the pressure head. The chamfers located at an angle of 30 deg. on the workpiece and in the reception plate, serve to achieve a metal-to-metal sealing between the workpiece and the pressure head and prevent coolant leakage from the fluid transfer unit during the boring operation. The workpiece was rotated and the cutting head counter-rotated, while being fed into the workpiece. The workpiece overall length was 1,295 mm (4 ft, 3 in) and the depth of the blind hole was 1,130 mm (44.5 in). The workpiece material was ductile steel AISI H11, normalized and tempered, between 40 and 42 RC, and with ultimate strength from 110 to 124 kN/cm^2 (160 to 180 ksi). This steel is extremely difficult for chip-breaking and requires careful control of the cutting speed and feed for good chip formation.

CHAPTER VI

TEST RESULTS

CHAPTER VI

TEST RESULTS

The tests of the trepanning heads were conducted in two series. In the first series, the head of three cutting edges was tested, with commercially available cutting inserts. The second series of tests was carried out with the modified head of three cutting edges, and the head of two cutting edges under the conditions described in the previous Chapter.

6.1 PRELIMINARY SERIES OF TESTS

During the preliminary tool testing, five tests were conducted with the tool and workpiece rotating in opposite directions.

Test No. 1

The parameters preselected, as well as those recorded, are listed in Table 6.1. A hole of approximately 2 inches deep was machined and the machine was stopped, for necessary checks. The hole was found to be oversized by approximately 3 mm (0.118 in). The head was found to have rubbed against the bore-wall at the area located a little over 90 deg. behind cutter No. 1. The absence of any carbon deposit on cutters Nos. 2 and 3 suggested that only cutter No. 1 was engaged in cutting.
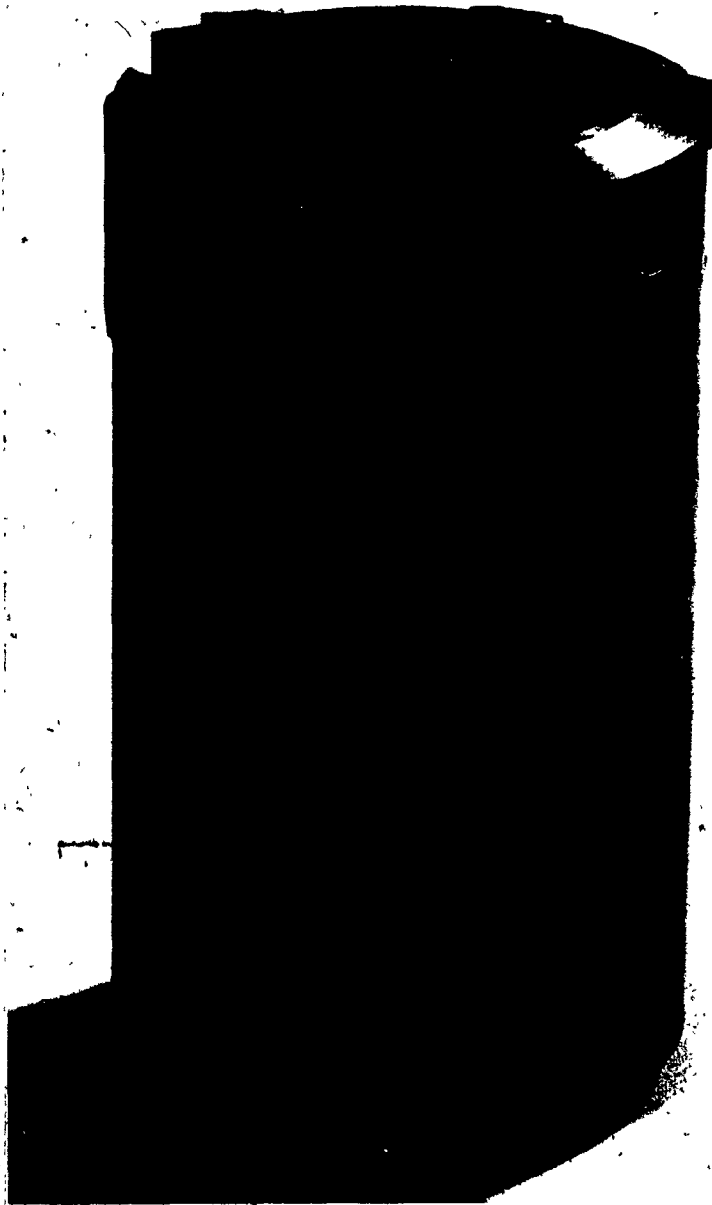
FIG. 6.1 LOCATION OF THE RUBBED AREA OF THE
HEAD IN RELATION TO THE LOCATION
OF THE CUTTERS

TABLE 6.1

CUTTING PARAMETERS PRESELECTED AND RECORDED IN THE FIRST SERIES OF TESTS

CUTTING PARAMETERS		TEST NO.1	TEST NO.2	TEST NO.3	TEST NO.4	TEST NO.5
Workpiece speed	rpm	56	56	56	56	56
Tool speed	rpm	280	224	280	280	280
Tool cutting speed	rpm	336	280	336	336	336
Surface cutting Speed	m/min	111.1	92.6	111.1	111.1	111.1
	fpm	364.6	303.9	364.6	364.6	364.6
Feed rate	mm/min	50.8	80.0	80.0	80.0	111.125
	ipm	2.0	3.15	3.15	3.15	4.375
Feed per revolution	mm/rev	0.151	0.286	0.238	0.238	0.331
	ipr	0.006	0.0112	0.0094	0.0094	0.0130
Coolant flow	1/min	500	855	855	855	855
	gpm	110	188	188	188	188
Coolant pressure	kPa	2,200	1,580	1,580	1,580	1,580
	psi	320	230	230	230	230
Clamping force	N	22,220	22,220	22,220	22,200	22,220
	lb	5,000	5,000	5,000	5,000	5,000

(continued)

TABLE 6.1

CUTTING PARAMETERS PRESELECTED AND RECORDED IN THE FIRST SERIES OF TESTS

CUTTING PARAMETERS		TEST NO.1	TEST NO.2	TEST NO.3	TEST NO.4	TEST NO.5
Feed force	N	15,111	19,556	19,556	19,556	19,556
	lb	3,400	5,100	4,400	4,400	5,300
Work headstock Power	kW	6.7	10.8	10.8	10.8	---
	HP	9	14.5	14.5	14.5	---
Tool headstock Power	kW	32.0	42.46	44.7	44.7	---
	HP	43.0	57.0	60.0	60.0	---

way which could significantly affect the cutting head to slightly slip aside, and make the cutting edge located in that direction to cut at a larger radius.

Test No. 4

The test could not resume with the head set-up from the previous trial because the inserts were damaged. So, a new set of inserts was levelled on the head, as given in Table 6.2. However, the set of parameters used in the previous test, was maintained with the hope that it would result in a chatter-free operation.

As the initial hole was machined and the machine was stopped for the usual checks, it was found that the hole size was accurate. The surface finish and the chip removal were also satisfactory. Chip Sample No. 4 in Fig. 6.2 was taken during this short trial.

Test No. 5

This test was undertaken with the same tool set-up and the same parameters as the previous test except for the feed. The feed rate was increased to create better conditions for chip-breaking and to increase the cutting force resultant. This was supposed to create better tool stability and cut down the torsional vibration of the boring bar and the chatter of cutters.

This change brought a significant improvement in the operation. The chatter was cut down but not completely eliminated. The chips were removed successfully although they were not optimal in shape and length. Sample No. 5 in Fig. 6.2 represents chip forms achieved in this test. A hole of approximately 1 foot was machined before the problems with the chip removal occurred, resulting in the automatic stoppage of the machine.

It appeared that the stopage in the operation was due to a failure of Cutter No. 3. A solid block of the jammed chips shown in the foreground of Fig. 6.2, No.5, was found stuck in the chipthroat. This blockage in the chip passage was itself, enough to cause the stopage in the operation.

Since this attempt failed to produce a hole of the required depth, it was decided to resume the tests after these preliminary results were studied, and the necessary improvements to the head had been implemented. The results of this first series of tests could be summarized as follows:

(1) The tool proved capable of cutting accurate holes of good surface finish at higher material removal rates with feeds between 2 and 4.375 ipm and surface cutting speeds between 304 and 365 fpm, which is a significant increase, compared with the values of 1 ipm feed and 215 fpm surface-cutting speed used in the single-edge trepanning of the same workpiece material.

(2)   Commercially available standard trepanning inserts
      are not accurate enough to assure the identical cutting
      profile of the cutting edges. The difference in the
      effective cutting depths caused by this inaccuracy,
      is of the same order of magnitude as the cutting
      depths, themselves, which results in a distorted cutt-
      ing force system and an erratic force resultant, in-
      stead of the predetermined one.

(3)   The tool exhibited a tendency to chatter due to a self-
      excited torsional vibration of the boring bar at fre-
      quencies below 1,000 Hz. The carbide inserts deter-
      iorate rapidly if worked at these frequencies; so either
      a boring bar of higher torsional rigidity or more
      efficient vibration damping are essential if the tool
      is to be saved from premature deterioration.

(4)   The chipmouth and chipthroat areas of the head should
      be slightly increased in order to facilitate the chip-
      removal and prevent any blockage in the chip-passages.

6.2   SECOND SERIES OF TESTS

During this series nine tests were attempted;
the first seven with the new trepanning head of two cutters,
and the last two with the modified trepanning head of three
cutters. The standard trepanning carbide inserts were reground
to the specifications required in the tools' layouts and stated

in the previous chapter. Values of the cutting parameters used, both preselected before and recorded during the tests, are listed in Table 6.3. The tests were conducted with the same boring facilities and the same workpiece as the first series. Tests No. 5 and on, were done with an aluminum bushing inserted in the pressure head behind the starting bushing with the intention of dampening the torsional vibration of the boring bar. Apparently, this helped in damping out the vibration, but it is unclear just how much.

Since a standard thick-wall boring bar could not be assured to increase the rigidity of the system, attention was paid to the best utilization of the vibration damper to damp down the torsional vibrations of the bar and prevent chatter of the cutters. It appeared that the chatter was a major obstacle to successful tool performance; the more intensive the chatter, the more rapidly the cutters deteriorated.

The damping effect of the damper was controlled by sliding the damper along the slideways until the location of maximum amplitude of the vibration of the boring bar had been found. Similarly, the amount of Coulomb friction generated by the damper was controlled by tightening or loosening the tapered bushing around the boring bar. This trial-and-error procedure required very careful observation in order to achieve the best efficiency of the damper. It took a couple of tests

TABLE 6.3

CUTTING PARAMETERS PRESELECTED AND RECORDED IN THE SECOND SERIES OF TESTS

CUTTING PARAMETERS		TEST NO.1	TEST NO.2	TEST NO.3	TEST NO.4	TEST NO.5
Workpiece speed	rpm	56	56	71	71	71
Tool speed	rpm	140	180	180	180	180
Total cutting speed	rpm	196	236	251	251	251
Surface cutting Speed	m/min	64.8	78.1	83.0	83.0	83.0
	fpm	212.7	256.1	272.4	272.4	272.4
Feed rate	mm/min	45.72	50.8	31.75	40.64	40.64
	ipm	1.8	2.0	1.25	1.6	1.6
Feed per revolu-tion	mm/rev	0.233	0.215	0.127	0.162	0.162
	ipr	0.0092	0.0085	0.0050	0.0064	0.0064
Coolant flow	l/min	618	855	855	855	855
	gpm	136	188	188	188	188
Coolant pressure	kPa	1,992	1,580	1,580	1,580	1,580
	psi	290	230	230	230	230
Clamping force	N	22,220	22,220	22,220	22,220	22,220
	lb	5,000	5,000	5,000	5,000	5,000

(continued)

TABLE 6.3

CUTTING PARAMETERS, PRESELECTED AND RECORDED IN THE SECOND SERIES OF TESTS

CUTTING PARAMETERS		TEST NO. 1	TEST NO. 2	TEST NO. 3	TEST NO. 4	TEST NO. 5
Feed force	N	19,556	18,667	13,333	15,556	15,556
	lb	4,400	4,200	3,000	3,500	3,500
Work headstock Power	kW	8.9	8.2	6.7	8.9	8.9
	HP	12.0	11.0	9.0	12.0	12.0
Tool headstock power	kW	22.4	26.1	17.9	20.9	20.9
	HP	30.0	35.0	24.0	28.0	28.0
Machined depth	mm	50.8	203.2	50.8	50.8	101.6
	in	2.0	8.0	2.0	2.0	4.0

(continued)

TABLE 6.3

CUTTING PARAMETERS PRESELECTED AND RECORDED IN THE SECOND SERIES OF TESTS

CUTTING PARAMETERS		TEST NO.6	TEST NO.7	TEST NO.8	TEST NO.9
Workpiece speed	rpm	71	65	65	65
Tool speed	rpm	180	140	140	140
Tool cutting speed	rpm	251	205	205	205
Surface cutting Speed	m/min	83.0	67.8	67.8	67.8
	fpm	272.4	222.5	222.5	222.5
Feed rate	mm/min	40.64	38.1-50.8	50.8-76.2	63.5
	ipm	1.6	1.5 to 2.0	2.0 to 3.0	2.5
Feed per revolution	mm/rev	0.162	0.186 - 0.248	0.248 - 0.372	0.310
	ipr	0.0064	0.0073 - 0.0098	0.0098 - 0.0146	0.0122
Coolant flow	1/min	855	855	855	855
	gpm	188	188	188	188
Coolant pressure	kPa	1,580	1,580	1,580	1,580
	psi	230	230	230	230
Clamping force	N	22,220	22,220	22,220	22,220
	lb	5,000	5,000	5,000	5,000

(continued)

TABLE 6.3

CUTTING PARAMETERS PRESELECTED AND RECORDED IN THE SECOND SERIES OF TESTS

CUTTING PARAMETERS		TEST NO.6	TEST NO.7	TEST NO.8	TEST NO.9
Feed force	N	15,556	16,889-20,444	20,444-26,667	23,556
	lb	3,500	3,800-4,600	4,600-6,000	5,300
Work headstock power	kW	8.9	8.9	11.2-14.9	12.7
	HP	12.0	12.0-15.0	15.0-20.0	17.0
Tool headstock power	kW	20.9	17.9-23.1	23.1-31.3	28.3
	HP	28.0	24.0-31.0	31.0-42.0	38.0
Machined depth	mm	71.2	127.0	76.2	101.6
	in	28.0	5.0	3.0	4.0

before the results of the damping control became evident. The
chatter was significantly cut down although not completely
eliminated. This resulted in an extended tool life.
Finally, a hole of reasonable length was machined in
Test No. 6, shown in the center of Fig. 6.4.

The hole machined in Test No. 6 proved to have a good
surface finish and no run-outs. It was found to be accurate
within the prescribed tolerance. The chips formed in this
test were slightly longer, but shaped conveniently and removed
successfully. A sample of the chips formed in the test are
shown in Fig. 6.5.

In order to cut down the chatter of the cutters and
achieve good chip formation, the cutting speeds and feeds were
slightly varied, which is evident from Table 6.3.

The results of this series of tests can be summarized
as follows:

(1) All nine tests, regardless of the amount of chatter
present and the length of the hole machined, produced
holes accurate in size, within the prescribed toler-
ance.

(2) The feeds could be increased up to 60 percent for the
head of two cutters and up to 100 per cent for the
head of the three cutters compared to a single-edge
trepanning head.

FIG. 6.4   HOLES MACHINED IN THE TESTS
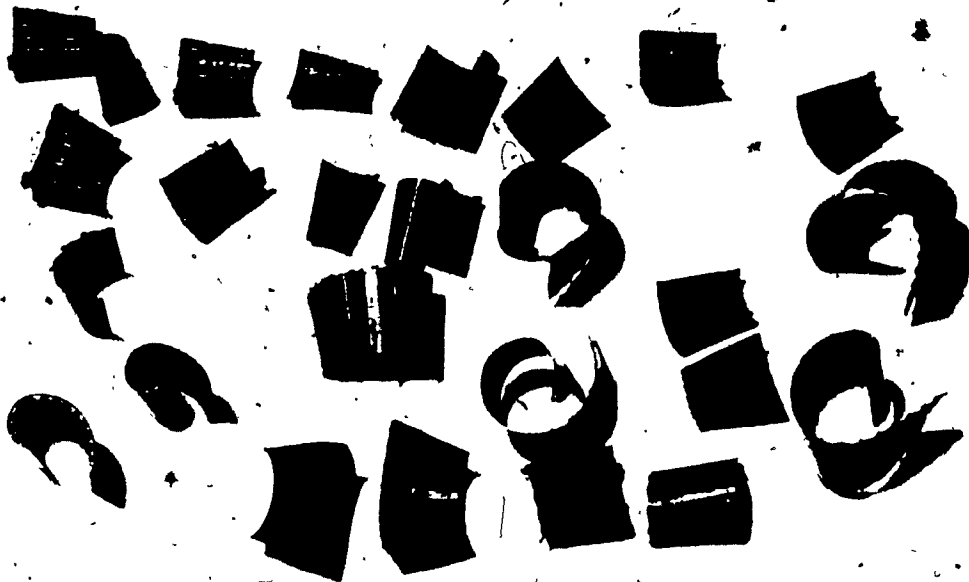
FIG. 6.5   CHIP SAMPLE FROM TEST NO. 6

(3) The surface finish of holes machined during all the tests was good.

(4) Both the new head of the two cutters and the modified head of the three cutters were properly supported by the wear pads which is evident from the carbon deposits accumulated on the leading and trailing wear pad. Fig. 6.6 clearly shows this deposit of carbon on the wear pads of the head with the two cutters. It seems that the leading wear pad has a little more carbon deposited on it, which means that this wear pad was taking more load than the trailing one, which primarily, was the objective. A similar deposit of carbon was found on the wear pads of the head with the three cutters. Because of a fewer number of trials attempted with this head, the amount of carbon deposit was much less.

(5) The hole size control was performed, as predicted by the cutting edge located opposite to the wear pads. This cutter has a carbon deposit behind its circle land while the other cutters have no such carbon deposits. This is evident from Fig. 6.7, which shows the two standard inserts photographed after Test No. 6 had been completed. Insert '14' was located opposite the wear pads and was assigned to the hole size control, while the circle land of insert '24' was
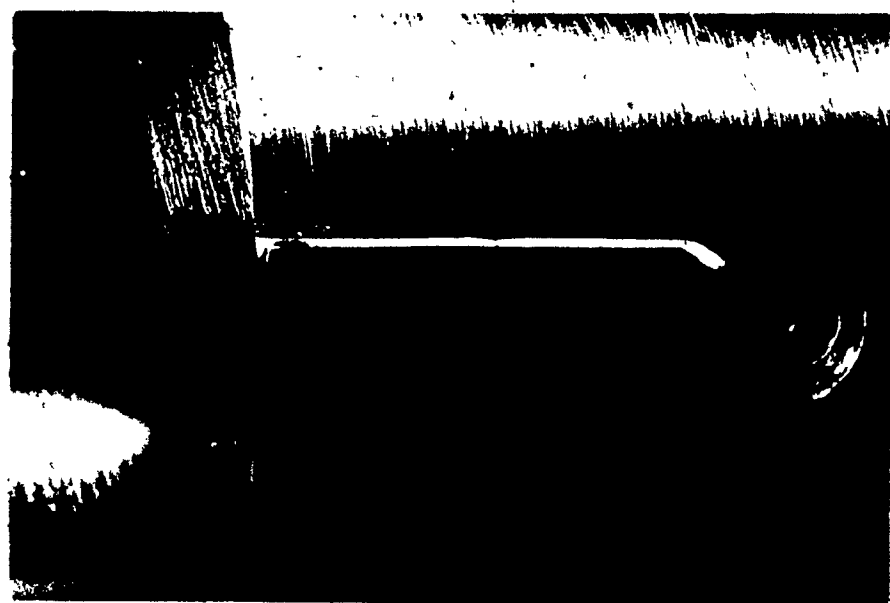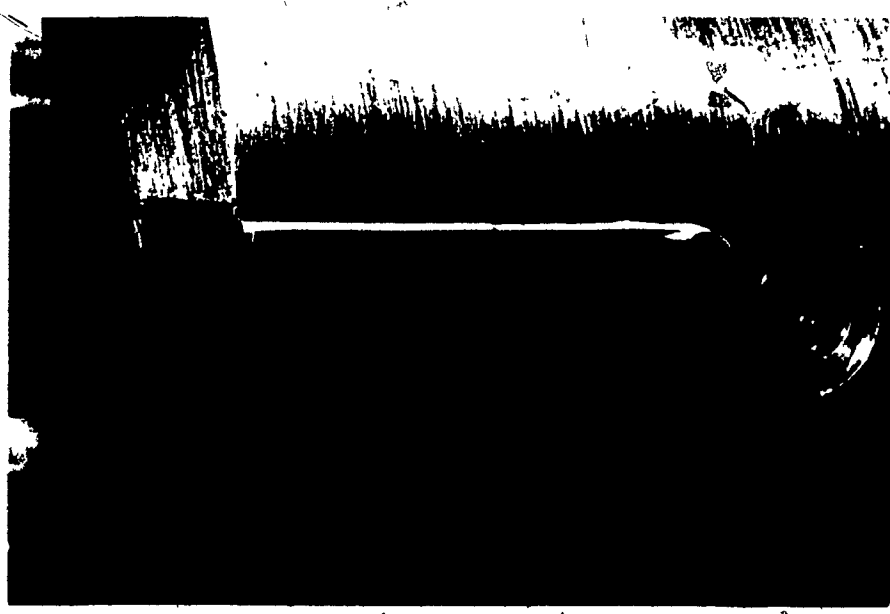
FIG. 6.6. WEAR PADS OF THE HEAD WITH TWO CUTTERS (a) TRAILING PAD
(b) LEADING PAD
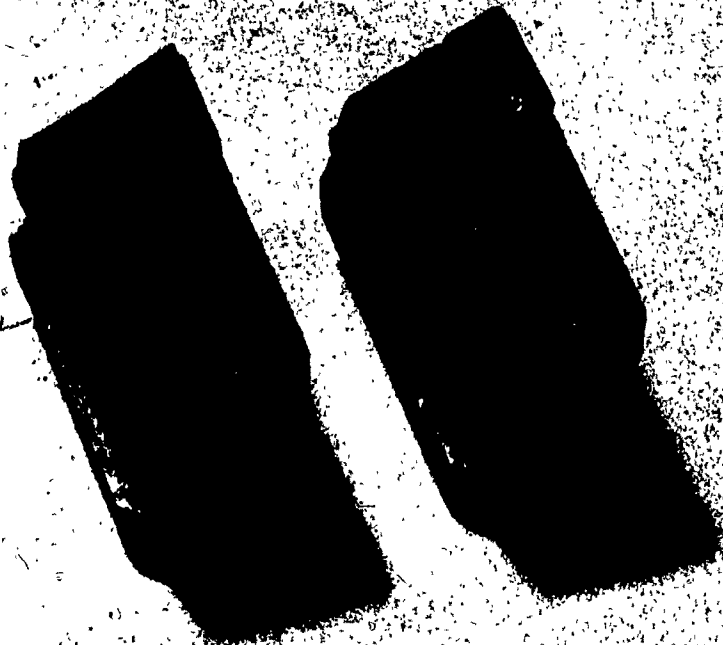
FIG. 6.7 CUTTING INSERTS OF THE HEAD WITH TWO
CUTTERS AFTER TEST NO. 6
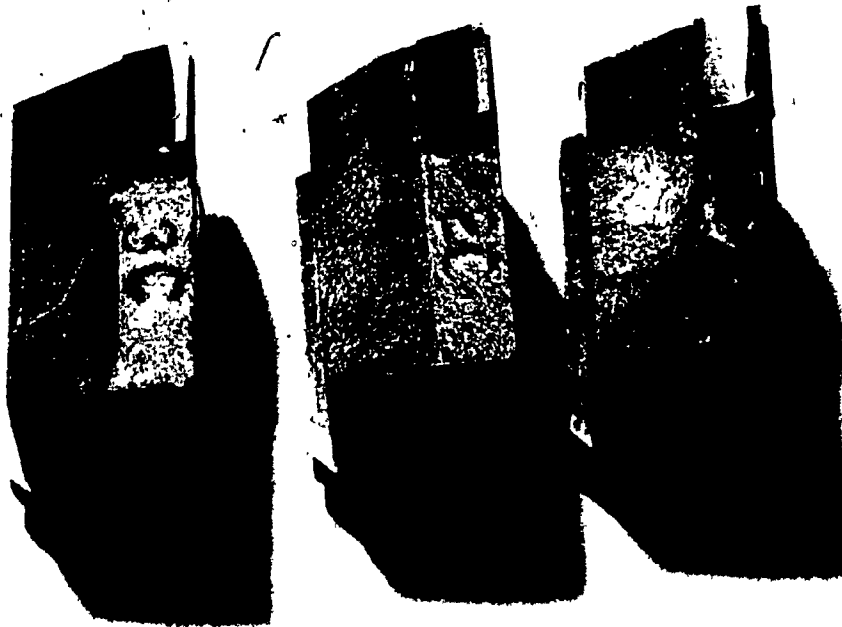
FIG. 6.8 CUTTING INSERTS OF THE HEAD WITH THREE
CUTTERS AFTER TEST NO. 8

ground inwards for a clearance of 0.1 mm (0/.004 in).
The same was observed on the tool with the three
cutters. The photograph taken after Test No.8 had
been completed is shown in Fig. 6.8. It reveals a
trace of carbon at the edge of the circle land of the
insert '1C' which was assigned to control the hole
size while no carbon deposit on the other two inserts
'2C' and '3C', was found. The inserts were ground
inwards for the same clearance. This proves that the
principle of hole size control, so important in single-
edge tools, can be maintained in multi-edge tools
only if the cutter located opposite the wear pads is
ground accurately to the hole size; the other
cutters should be ground inwards for a certain clear-
ance. This principle is essential in deep-hole
machining and was pointed out in the basic concept of
multi-edge BTA tools set in the Introduction.

(6) The readings of the power and feed force, given in
Table 6.3, reveal that the cutting torques and, hence,
the tangential force components, calculated by the
computer and measured on the machine during the tests,
agree within five percent. However, the feed forces
measured on the boring bar seem to be in disagreement
with those calculated by the computer. The
difference in some cases, is as large as 20 per
cent. The results are not considered too reliable

since the measuring devices set on such machines
are not very precise instruments.

(7) The aspect of the coolant flow was also considered as
possible cause of the tool's premature deteriora-
tion. It was found, however, that the coolant velocity
at the chipmouths of the tool, is between 8 to 10 times
larger than the cutting speed, which should be sufficient
for flushing the chips, since it conformed to the
recommendations.

(8) Chip-removal was successful throughout the tests and
the chip form optimal. It is uncertain, however,
whether this would have been the case if the chatter
had not been present. Nevertheless, grinding of the
chip-breakers, as a function of the effective cutting
depth per cutting edge, proved to result in a much
better chip-form and uniform chip lengths.

(9) The tests could have been more successful if they
had not been conducted under pressing production
conditions and strict 'no scrap allowed' restrictions.
Five workpieces were used in nine tests, and none
was scrapped. However, they had to be finished by a
conventional single-edge trepanning tool.

CHAPTER VII

SUMMARY, CONCLUSIONS AND RECOMMENDATIONS FOR
FUTURE WORK

CHAPTER VII

SUMMARY, CONCLUSIONS AND RECOMMENDATIONS FOR FUTURE WORK

7.1 SUMMARY

In this thesis, a new design concept and analysis of multi-edge BTA deep-hole machining tools are given. The main feature of the design is that the cutting head consists of multi-cutting edges unsymmetrically located with respect to the rotational axis on the cutting head. This provides a means of maximizing the metal removal rate per revolution and hence the productivity without sacrificing those advantages provided by single-edge cutting tools.

To investigate these objectives the following analytical and experimental work has been carried out.

7.1.1 Mathematical Model of the Cutting Tool

A mathematical model describing the three cutting force components - tangential, radial and feed - as well as the cutting torque has been developed in terms of certain fundamental cutting parameters and properties of the workpiece material.

The model represents a generalized form which is applicable to all types of deep-hole machining tools. In particular, the model is suitable for solid boring, trepanning and counter-

boring cutting operations. It is based on empirical testing results in conjunction with a consideration of cuting mechanics. In this approach, the cutting operation is basically an orthogonal model with two major cutting force components - the tangential and the thrust force. The latter was resolved into radial and feed components to form a rotating right-hand tried with respect to the cutting edge. For a given number of cutting edges and feed rate, the equations of the cutting-force components are written as a function of width of cut and angular location of cutting edge.

To verify the validity of this model, the cutting forces were evaluated again based on six established shear-angle theories and compared with the calculated values from the developed model. The results were within the range predicted by theories and compared particularly well with the Oxley Shear-angle theory.

7.1.2 Optimization and Design Strategy

Based on the mathematical model developed for the cutting forces, an objective function for the design of the cutting head was formulated. The design strategy of the optimization procedure is to minimize the variation of the cutting edge pressure of the tool cutters for a predetermined wear-pad force necessary for tool self-guidance.

The objective function is of a multivariable non-linear form modified to an unconstrained type with bounded decision variables.

A numerical direct search technique, accelerated in distance, has been used to minimize the objective function. This procedure ensures, on the one hand, a predetermined cutting force resultant, necessary for the tool guidance, and on the other hand, it minimizes the differences in the cutting force per unit width of the cutting edge for all cutters distributed on the cutting head. A relatively fast computer routine has been adapted to provide optimal tool parameters which could be used to design the cutting head prototypes. The optimization routine allows a large number of local optima, depending on the initial set of decision variables, which gives a designer the opportunity of partially predetermining the optimal set of parameters. The designer has an opportunity to make minor corrections to the parameters to eliminate any inconvenient shape of cutting edges undetectable for the computer. These corrections are carried out by a separate program.

Several minor changes have been made to the standard routine of the direct search method. A major addition to the exploratory routine has been implemented to make it work when two or more angular variables become 'locked' together; a case which otherwise ends with failure of the optimization.

The computer program can optimize for two to n cutting edges. The program evaluates the number of cutting edges based on:

(a) tool diameter and the lower and upper limits of the width-of-cut prescribed by the designer,

(b) the strength of the head and/or chip-coolant passages,

(c) the machine tool and/or boring bar capacity.

The criteria for optimal value of the resultant, transmitted to the bore-wall have been established based on:

(a) the upper limit that ensures a hydrodynamic lubricating action between the supporting pads and the bore-wall, and

(b) the lower limit that ensures tool guidance and prevents the separation of the supporting pads from the bore-wall.

The latter aspect has been investigated by considering the cutting forces as random with Gaussian distribution. Based on these assumptions, exact expressions for the devitions of the resultant force in both their magnitude and direction have been derived. The results show that as the force resultant decreases, these deviations increase, so that the deviation in magnitude tends to infinity and the deviation in direction approaches ± 90 deg. This case may be identified as 'indeterminate' as far as the force resultant is concerned

and it must be avoided during the selection of the force resultant as a basis for the optimization.

Several tools have been optimized of both solid boring and trepanning types. Computer printouts for three heads were produced to illustrate the major advantages of the procedure. These tools were then detail-designed and two of them actually manufactured for the experimental testing.

To cover the total range of multi-edge tools, the so-called staggered multi-edge tools are also investigated in this work. The means of analysis and optimization of these tools have been developed separately from the unsymmetrical multi-edge solid boring and trepanning tools.

Three cutting heads with staggered cutting edges, two trepanning and one solid boring have been designed using an optimization program for this type of tool. Two of the tools have been tested on the production line. The cutting torque and the feed force measured during the testing were in agreement with those calculated by the computer program within five percent or less.

7.2 CONCLUSIONS

Based on the experimental results of this investigation, the following conclusions can be drawn:

(1)   Commercially available standard trepanning inserts
        have proven to be unacceptable for use in multi-edge
        tools because of intolerable differences in the front
        profile of the cutting edges. This has resulted in
        a distorted cutting force system and an erratic force
        resultant which caused improper tool guidance and hole-
        size control.

(2)   An advantage of the staggered multi-edge BTA tools over
        single-edge tools, can also be sought in the possibili-
        ty of combining carbide grades of the cutters in order
        to achieve higher feeds without sacrificing the tool
        life.

(3)   In order to assure proper tool guidance and hole size
        control, the following conditions must be fulfilled:

        (a)   the cutting edges should be identically ground
              in the front profile,

        (b)   the circle land of the cutter located opposite
              to the wear pads should be ground to exact hole
              size, the circle lands of the other cutters
              should be ground inwards for a predetermined small
              clearance,

        (c)   the chip-breaker grooves should be ground as a
              function of the effective cutting depth per cutting
              edge.

By ensuring these conditions, all holes machined during the experimental part of this work were accurate within the tolerance prescribed and have a good surface finish.

(4)   Tools with multi-cutting edges are capable of delivering higher feed rates. The head with two cutters delivered up to 60 per cent and the head with three cutters delivered up to 100 percent higher feed, compared to those with single-edge cutting heads.

(5)   The evident presence of intolerable chatter seems to be a major obstacle to the successful performance of the tested tools. A general shortcoming associated with this multi-edge tool seems to be a tendency to chatter, due to a self-excited torsional vibration of the boring bar. The standard boring bars, particularly thin-walled, seem to have insufficient torsional rigidity. High torsional rigidity of boring bars are essential when multi-edge cutting heads are used.

In the final conclusion, it should be pointed out that the major objective of this thesis, i.e., the feasibility of unsymmetrical multi-edge deep-hole machining, has been accomplished. An analytical means for the complex cutting force system of a multi-edge tool has been provided; an optimization procedure based on this model has been formulated; and experimental evidence on the overall performance of the

designed tools and the other important aspects, such as tool guidance, hole-size control, hole straightness, chip forma-tion and tool stability, has been furnished. The fact that only the trepanning tools have been experimented with in this work does not affect the generality of the model and the feasibility of the design method for other types of multi-edge tools.

Since the implementation of the unsymmetrical multi-edge tools would require an increase in the direct tool cost, an economical assessment of such an implementation shows, in an illustrative way, that the machining cost per unit length of a hole, using multi-edge cutting tools, is significantly decreased. It can be concluded therefore, that the proposed method should in fact, if adapted on production lines, not only increase the productivity of the hole machining, but also decrease the hole production cost.

7.3 RECOMMENDATIONS FOR FUTURE WORK

Although all the major aspects of a multi-edge tool with unsymmetric locations of the cutters have been dealt with, theoretical and experimental results show that further research work is needed before these tools are put into mass production. These can be summarized as follows:

(1) Due to the level of tool instability and chattering observed during the experimental testing it is recommended that a detailed dynamic analysis of the machine-tool-workpiece system and its stability be carried out in the future. The condition where no chatter occurs must be secured by investigating the torsional behaviour of the boring bar.

(2) Due to high levels of stresses with multi-edge cutting tools compared to those with single-edge cutters, the optimization program should be extended to select design parameters that will provide a safe stress level within the cutting head. The stress analysis should also take into account, in addition to the cutting forces, the thermal effects and frictional forces on the supporting pads.

(3) The chip ratio-chip thickness relationship should be investigated in order to establish an analytical expression for a range of chip thicknesses, feasible in application of deep-hole machining operations. This relationship, coupled with Oxley's shear-angle relationship, would constitute a base for the use of a cutting mechanics' approach, in predicting the cutting forces in deep-hole machining.

(4)   Since there is no provision in the optimization pro-
gram for the location of wear pads, it may be possible
to implement the restrictions on the wear pad locations
through the selection of a tool optimum out of many
optima achieved by changing the initial set of
decision parameters. It may be possible to make
computer programs perform this selection, based on
criteria set by the designer. In the present procedure,
it is the designer who makes this selection, by using his
own judgement.

(5)   The data obtained from empirical testing were fully
investigated only for steel workpieces, while other
workpiece materials are not covered. Hence, more work
is required to determine such a data for aluminum, as
well as for copper alloys.

(6)   Further experimental work is needed, using solid boring
heads. Some additional problems with this type of
tools are expected, particularly the cutting edge over-
load in the zone of the secondary cutting edge. This
problem may be overcome by grinding the cutting edge
with a -10 deg rake angle, instead of a -30 deg and
making this portion of the cutting edge out of carbide
with higher toughness.

(7)   In order to secure identical front profiles of
        cutters for multi-edge cutting tools at relatively low
        cost, new grinding methods for these types of tools
        need to be developed.

REFERENCES

REFERENCES

[1] Greuner, B., "Beitrag zür Frage der Kräfte an Schneide und Führungsleisten an einscheidigen hartmetallbestuckfen Tiefbohrwerkzeugen", Diss.TH. Hannover, 1970.

[2] Gildemeister-Heidenreich and Harbeck, "Was bietet modernes Tiefbohren der Fertigungstechnik heute?", Vortragsveranstaltung, Remscheid, May, 1973.

[3] Dibner, B., "Machines and Weaponry", The Unknown Leonardo, McGraw-Hill Book Co., 1974, p.174.

[4] Encyclopedia Britannica, W. Benton-Publisher, 1970, pp.526-529.

[5] Steeds, W., A History of Machine Tools 1700-1910, Oxford at Clarendon Press, 1969, pp.1-24.

[6] Thorne, W.H., "Twist Drills", ASME Trans. Vol.VII, 1886, pp.130-137.

[7] Bird, W.W., and Fairfield, H.P., "A Twist Drill Dynamometer", ASME Trans., Vol.XXVI, 1905, pp.355-366.

[8] Boston, O.W., and Oxford, C.J., "Performance of Cutting Fluid in Drilling Various Metals", ASME Trans., Vol.55-1, 1933, pp.1-29.

[9] Boston, O.W., and Oxford, C.J., "Power Required to Drill Cast Iron and Steel," ASME Trans., Vol.52-2, 1930, pp.5-26.

[10] Boston, O.W., and Gilbert, W.W., "The Torque and Thrust of Small Drills Operating in Various Metals", ASME Trans., Vol.58-2, 1936, pp.79-89.

[11]   Merchant, M.E., "Basic Mechanics of Cutting Process",
       J. Applied Mechanics, Vol.11,1944, pp.168-175.

[12]   Merchant, M.E., "Mechanics of the Metal Cutting Process
       in Orthogonal Cutting and the Type 2 Chip", J. Applied
       Physics, Vol.16, No.5, 1945, pp.267-275.

[13]   Shaw, M.C., Cook,N.H., and Smith, P.A., "The Mechanics
       of Three-Dimensional Cutting Operations," ASME Trans.
       Vol.74, 1952, pp.1055-1067.

[14]   Oxford, C.J.Jr., "On the Drilling of Metals, 1-Basic
       Mechanics of Process", ASME Trans. Vol.77, 1955,
       pp.103-114.

[15]   Shaw, M.C., and Oxford, C.J.Jr., "On the Drilling of
       Metals, 2-The Torque and Thrust in Drilling," ASME
       Trans., Vol.79, 1957, pp.139-148.

[16]   Smith,J.D., and Tobias, S.A., "The Dynamic Cutting of
       Metals," Int.J. Machine Tool Design and Res., Vol.1,
       Pergamon Press 1961,pp.283-292.

[17]   Albrecht,P., "Dynamics of the Metal-Cutting Process",
       ASME Trans., J. Eng. for Industry, 1965, pp.429-441.

[18]   Hahn,R.S., "The Design of the Lanchester Damper for the
       Elimination of Metal Cutting Chatter", ASME Trans.
       Vol.73, 1951,pp.33-41.

[19]   Williams, R.A., "Dynamic Geometry of a Twist Drill",
       Int.J. Production Res., Vol.7, No.4, 1969, pp.253-267.

[20]   Fuji,S., DeVries,M.F., and Wu,S.M., "An Analysis of
       Drill Geometry for Optimum Drill Design by Computer,
       Part I - Drill Geometry Analysis, Part II - Computer
       Aided Design", ASME Trans., J. Eng. for Industry,
       1970, pp.647-666.

[21] Stankovic, P., "Mašinska obrada I - Obrada rezanjem"
(Metalworking, Vol.1 - Metal Cutting) Gradjevinska
knjiga - 1962.

[22] Zorev, N.N., Metal Cutting Mechanics, Pergammon
Press, 1966. Transl. from Russian by Massey,H.S.H.

[23] Kronenberg, M., Machining Science and Application,
Pergammon Press, 1966.

[24] Amarego,E.J.A., and Brown, R.H., The Machining of
Metals, Prentice-Hall,Inc., 1969.

[25] Bhattacharyya, A., and Ham,I., "Design of Cutting
Tools - Use of Metal Cutting Theory", ASTME, Dearborn,
Mich., 1969.

[26] Pal, A.K., Bhattacharyya, A., and Sen,G.C., "Investi-
gation of the Torque in Drilling Ductile Materials",
Int.J. Machine Tool Des. and Res., Vol.4, Pergamon
Press, 1965, pp.205-221.

[27] Mansour, W.M., Osman, M.O.M., and Gladwell, G.M.L.,
"Stability and Kinematic Accuracy of Hydraulic Copy-
ing Mechanism in Metal Cutting", ASME Trans. J. of Eng.
for Industry, Vol.95, No.3, 1973, pp.787-793.

[28] Osman, M.O.M., and Sankar, T.S., "Short-Time Acceptance
Test for Machine Tools Based Upon Random Nature of
Cutting Forces", ASME Trans., J. of Eng.for Industry,
Vol.94, No.4, 1972, pp.1020-1024.

[29] Maragos, S.K., "Measurement and Modeling of the Cutting
Force Fluctuations During Machining", M.Eng.Thesis,
Sir George Williams Univ., Montreal, 1973.

[30] Rakhit, A.K., Sankar, T.S., and Osman, M.O.M., "The
Effect of Stochastic Response of Machine-Tool-Work-
piece on Formation of Surface Texture in Turning", ASME
Vibration Conf., Cincinnati, 1973.

[31] Chahil, G.S., "Measurement and Modeling of Torque and Thrust in Twist Drilling Operation", M.Eng.Thesis, Concordia Univ., Montreal, 1976.

[32] Pearson,H.J., "High-Speed Boring" - Parts 1, 2, 3 and 4. Production Technology, March, April, July 1962 and May 1963.

[33] Swinehart, H.J., "Gundrilling, Trepanning and Deep-Hole Machining", ASTME, Dearborn,Mich., 1967.

[34] Hutson,G.A., "Modernization of Gun Tube Boring Facilities", Bent R & E Laboratories, Technical Report WVT-7016, New York, 1970.

[35] Griffiths, B.J., "The Machining Action During Deep-Hole Boring and the Resultant Hole Form and Force System", Proc. 2nd Int.Conf. on Production Res., Copenhagen, 1973.

[36] Osman, M.O.M., and Greuner, B., "Entwicklunstendenzen eines BTA - Werkzeuges zum Bohren ins Volle", TZ fur praktische Metallbearbeitung, Vol.68,No.5,1974,pp.166-168.

[37] Osman,M.O.M., "BTA Deep-Hole Boring: An Economic Way for Hole Machining", Tooling and Production, Feb.1975, pp.49-52.

[38] Osman, M.O.M., and Latinovic, V., "On the Development of Multi-Edge Cutting for BTA Deep-Hole Machining", ASME Trans.,J. Eng. for Industry,Vol.98,No.2, 1976, pp.474-480.

[39] Osman, M.O.M., and Mansour, W.M., "Lubrication of Journal Bearings", Design Engineering,Vol.15,No.10, Oct.1969,pp.56-60.

[40] Griffiths,B.J., "An Introduction to Deep Hole Drilling and Boring", Int.Conf. on Deep Hole Drilling and Boring, Brunel Univ., May 1975.

[41] Greuner, B., "Deep Hole Boring and Finishing Techniques and Their Application to the Manufacture of Hydraulic Cylinders", Int.Conf. on Deep Hole Drilling and Boring, Brunel Univ., May 1975.

[42] Faber, K., "Deep Hole Drilling Using the Ejector System", Int.Conf. on Deep Hole Drilling and Boring, Brunel Univ., May 1975.

[43] Renz, M., and Cawdery, D.O., "The Concept of Gun Drilling, Design and Development of Machines and Tools", Int.Conf. on Deep Hole Boring and Drilling, Brunel Univ., May 1975.

[44] Buck, G., "Chip Forms in Drilling With Gun Drills", Int.Conf. on Deep Hole Drilling and Boring, Brunel Univ., May 1975.

[45] Streicher, P., "Drilling With Long Gun Drills", Int. Conf. on Deep Hole Drilling and Boring, Brunel Univ., May 1975.

[46] Lundgren, E., "The Role of the Cutting Geometry in Deep-Hole Drilling", Int.Conf. on Deep Hole Drilling and Boring, Brunel Univ., May 1975.

[47] Fink,P., "Economic Efficiency of Deep Hole Boring: Optimum Cutting Conditions", Int.Conf. on Deep Hole Drilling and Boring, Brunel Univ., May 1975.

[48] Griffiths, B.J., "The Surface Integrity of Holes Produced by the BTA Deep Drilling Process", Int.Conf. on Deep Hole Drilling and Boring, Brunel Univ., May 1975.

[49] Turner, C.F., "Practical Aspects of Producing Holes", Int.Conf. on Deep Hole Drilling and Boring, Brunel Univ., May 1975.

[50] Tuffentsammer, K., "Feasability of Controlled Adaption in Deep Hole Boring", Int.Conf.on Deep Hole Drilling and Boring, Brunel Univ., May 1975.

[51] Zwingmann,G., "Cooling Lubricants for Deep Drilling", Int.Conf. on Deep Hole Drilling and Boring, Brunel Univ., May 1975.

[52] Davies, J., "Deep Hole Boring Within Rolls Royce (1971) Ltd., Small Engine Division", Int.Conf.on Deep Hole Drilling and Boring, Brunel Univ., May 1975.

[53] Dicken,T.E.A., "Applications of Deep Hole Boring at Royal Ordnance Factory, Nottingham", Int.Conf.on Deep Hole Drilling and Boring, Brunel Univ., May 1975.

[54] Trinkaus, W.H., "A High-Powered Tool for King-Sized Drilling", Manufacturing Engineering, August 1975, From SME Tech.Paper TE 75-451, presented at Upper Midwest Conf., St. Paul,Minnesota, May 1975.

[55] Latinovic, V., and Osman,M.O.M., "Unsymmetrical Multi-Edge Cutting in Deep-Hole Machining-Design Concept and Analysis", Proc. NAMRC-IV, May 1976,pp.255-262.

[56] Whitney,T., "Sandvik Ejector Drill System Aids Productivity at Heroux", Canadian Machinery and Metalworking, August 1976, pp.48-49.

[57] Doolan,P., Phadke, M.S., and Wu,S.M., "Computer Design of Vibration-Free Face Milling Cutter", ASME Trans. J. of Eng. for Industry,Vol.97,No.3,1975,pp.925-930.

[58] Saravanja-Fabris,N., and D'Souza, A.F., "Identification of Dynamic Metal Cutting Process With Reference to Chatter", Proc.NAMRC-IV, May 1976, pp.428-435.

[59] Colwell,L.V., and Mazur, J.C., "Tool Wear Tracking in the Production Shop", Proc. NAMRC-IV, May 1976, pp.420-427.

[60] Weber, U., "Leistungsaufteilung und Energiebilanz beim Tiefbohren" (Power Distribution and Energy Balance During Deep-Hole Boring), Tiefbohren, Dortmund Univ., April 1976, pp.9-12.

[61] Stockert, R., "Optimierung von Tiefbohrwerkzeugen hinsichtlich Konstruktion,Funktion und Wirtschaftlichkeit", <u>Tiefbohren</u>, Dortmund Univ., April 1976, pp.13-15.

[62] Stockert, R., "Zerspankraftverteilung über der Schneide von BTA-Vollbohrköpfen Zerspankraftverlauf über dem Bohrweg", <u>Tiefbohren</u>, Dortmund Univ., April 1976, pp.16-19.

[63] Hooke,R., and Jeeves, T.A., "Direct Search Solution of Numerical and Statistical Problems",<u>J.Assoc.Comp. Mach.</u>, <u>Vol.8,No.2</u>,1961,pp.212-229.

[64] Beveridge, G.S.G., and Schechter, R.S., <u>Optimization Theory and Practice</u>, McGraw-Hill Series in Chemical Engineering, 1970.

[65] Kuester, J.L., and Mize, J.H., <u>Optimization Technique With FORTRAN</u>", McGraw-Hill Book Co., 1973.

[66] Papoulis, A., <u>Probability, Randon Variables and Stochastic Processes</u>, McGraw-Hill Book Co., 1965.

[67] Jeffery,L.R., "Drilling Cost Analysis", <u>Sandia Laboratories Report SAND 75 - 0197</u>, May 1975.

[68] VDF - "Waggerecht Tiefbohrmaschinen,VDF - Prospect Nr. 148D(Horizontal Deep-Hole Machines", <u>VDF-Catalogue No.148D</u>) Verbrindliche Ausführung, Sept.1969, p.24.

[69] Cronjäger,L., "Entwicklungsstand des Tiefbohrens Metallisher Werkstoffe", <u>Tiefbohren'77</u>, <u>VDI-Berichte Nr.301</u>,1977,pp.5-11.

[70] Weber, U., "Messen der Zerspankraft beim Tiefbohren" <u>VDI-Berichte Nr.301</u>,1977,pp.27-35.

APPENDIX I

BASIC ECONOMICAL ASSESSMENT

APPENDIX I

BASIC ECONOMICAL ASSESSMENT

The purpose of this brief analysis is not to give a complete economic analysis of deep-hole machining, or to estimate the productivity and economic efficiency of deep-hole machining relative to other maching operations. These aspects have already been investigated [46,47]. The analysis presented here inquires into the way in which changes in some parameters influence deep-hole machining costs. The emphasis is placed on the tool life and the feed rate. An assessment of how these parameters affect the total cost of the machining is possible from the cost per unit length of a hole, as it has been done in soil drilling [66].

To simplify the problem, it is assumed that all other costs not included in the analysis are essentially fixed, and independent of both the feed rate and the tool life. Under these conditions, the cost per unit length, say in dollars per foot, is given by

$$c_L = \frac{(T_{CH} + T) c_M + C_T}{FT} \qquad (A1.1)$$

where

$c_M \ [\$ T^{-1}]$ = machine cost per unit time

$C_T \ [\$]$ = direct tool cost

F $[LT^{-1}]$ = feed rate

T_{CH} $[T]$ = tool replacement time

T $[T]$ = tool life

If the tool life is given in terms of the length of the hole machined between the grinds L, then

$$L = FT \qquad (A1.2)$$

Equation (A1.1) can be rearranged to give

$$c_L = \frac{c_M}{F}\left(1 + \frac{T_{CH} + C_T/c_M}{T}\right) \qquad (A1.3)$$

where the term C_T/c_M is commonly called the relative direct tool cost [46] and expressed in units of machine time; it decreases with the rising machine cost.

If a nondimensional tool life t is introduced as

$$t = \frac{T}{T_{CH} + C_T/c_M} \qquad (A1.4)$$

then the cost per unit length given by (A1.3) can be rewritten as

$$C_L = \frac{C_M}{F}\left(1 + \frac{1}{t}\right) \qquad (A1.5)$$

To inquire into the way in which changes in the feed rate influence the cost per unit length, Equation (A1.5) is differentiated with respect to the feed rate, keeping in mind that both the machine cost c_M and the tool life t are functions of the rate. The result is

$$\frac{dF}{dR} = \frac{dc_M}{RdR}\left(1 + \frac{1}{t}\right) - \frac{c_M}{R}\left(1 + \frac{1}{t}\right) - \frac{c_M}{R}\frac{dt}{t^2 dR} \qquad (A1.6)$$

Using (A1.5) and rearranging (A1.6) to relate the fractional changes in each of the parameters of interest, it becomes

$$\frac{dF}{F} = \frac{dc_M}{c_M} - \frac{dR}{R} - \frac{1}{t+1}\frac{dt}{t} \qquad (A1.7)$$

Equation (A1.7) is convenient for a qualitative analysis and assessment of the influence of fractional changes in the major parameters on the cost per unit length. It shows that the changes in the machine cost c_M and feed rate F change the cost per unit length by equal and possibly compensating amounts. On the other hand, a similar fractional change in tool life t, will always result in a smaller effect. The additional multiplier $1/(1 + t)$ is responsible for that. In fact, only if t approaches zero with a given fractional change in the tool life will it result in an equal change in the cost per unit length.

This case, however, is unlikely to occur in practice. It should be noted that a tool which is very expensive relative to the machine cost per unit time could result in a small value of t for somewhat moderate tool-replacement time.

To provide the means for a quantitative analysis, equation (A1.7) can be integrated directly from an initial set of parameters denoted by a subscript '0' to a final set of parameters indicated by no subscript, resulting in

$$\frac{c_L}{c_{L_0}} \frac{c_{M_0}}{c_M} \frac{F}{F_0} = \frac{1 + 1/t}{1 + 1/t_0} = \phi \qquad (A1.8)$$

where parameter ϕ is a nondimensional 'cost-rate factor' which also could be obtained directly, if equation (A1.5) written for the final conditions, was divided by the same equation written for the initial conditions.

Several special cases can be derived from equation (A1.8). As a first example, the cost break-even occurs when the cost per unit length remains constant. In this case $c_L/c_{L_0} = 1$ and ϕ becomes

$$\phi_C = \frac{c_{M_0}}{c_M} \frac{F}{F_0} \qquad (A1.9)$$

which shows that for the constant cost per unit length, doubling of the machine cost, for example, requires twice the higher feed rate. For many situations, the improvement in

deep-hole machining has little or no influence on the total machine cost, thus $C_{M_0}/c_M = 1$ and ϕ is

$$\phi_M = \frac{c_L}{c_{L_0}} \frac{F}{F_0}$$ (A1.10)

It is of particular interest to examine the direct economic relation between the feed rate and the tool life. In fact, this aspect has prompted the present analysis. Here, ϕ becomes a combination of the above two cases, i.e., both the cost per unit length and the machine cost are taken as constant, which gives

$$\phi_{CM} = \frac{F}{F_0}$$ (A1.11)

Any of these cases can be examined by using equation (A1.8) but, as it has been stated, the direct relation between the feed rate and the tool life is of a particular interest.

The analysis can be best tested through an example. Consider a trepanning situation with the following operating parameters: Machine cost $c_{M_0} = \$40$ per hour, direct tool cost $C_{T_0} = \$40$, calculated on the basis of $\$2,000$ - cost per head, $\$36$ cost per insert and 500 inserts per head life; feed rate $F_0 = 1$ in/min, tool replacement time $T_{CH} = 5$ min., and tool life $T_0 = 60$ min.

Suppose the set of parameters is for a single-edge tool. If it is replaced by a new set for a tree-edge trepanning tool which allows a feed rate of $F = 2$ in/min, and requires a higher direct tool cost of 15 percent per each additional cutting edge, we can examine the economic feasibility of such an implementation under the condition that the tool life and the tool-replacement time remain the same.

The cost per unit length for the single-edge tool calculated from (A1.1) is $c_{L_0} = \$16.67$ per foot, and the non-dimensional tool life from (A1.4) $t_0 = 0.923$. The nondimensional tool life for the three-edge tool is $t = 0.723$.

For the cost break-even situation from (A1.9) we get $c_M / c_{M_0} = 0.572$, which shows that this implementation would allow 75 per cent increase in the machine cost or an additional cost of \$30 per hour on top of the present cost of \$40 per hour.

If the machine cost, however, remains unchanged, which practically means that the same machining facilities are to be used, then $c_M / c_{M_0} = 1$ and from (A1.10) it follows that $c_L = 0.572 \, c_{L_0}$ or 42.8 per cent decrease in the cost per unit length, hence, \$9.53 per foot instead of \$16.67 per foot.

From the direct relation between the feed rate and tool life given by (A1.11), the nondimensional tool life is $t = 0.3243 t_0$, which shows that it could be decreased by a

factor of 2.64. Since it already was decreased by a factor of 0.783 due to the increase in the direct tool cost, it results in a net factor of 0.414 reduction in tool life, which can be accepted with no increase in cost per unit length.

On the other hand, suppose we somehow double the tool life without increasing its direct tool cost and suppose all other operating parameters are not changed, then $t = 1.846$.

The cost break-even situation from (Al.9) yields $(c_{M_0}F/c_MF_0) = 0.74$, which for the same machine cost $(c_{M_0}/c_M) = 1$ gives $F = 0.74$, F_0, requiring the new feed rate to be within 74 per cent of the original value. If machining is to be at the same feed rate then $c_M = 1.35 \, c_M$ shows that the machine cost could be increased by 35 per cent only.

If, however, the machine cost and feed rate are kept the same, then the cost per unit length will be $c_L = 0.74$, c_{L_0}. This makes the cost per unit length \$12.34 per foot, instead of the initial value of \$16.67 per foot.

It is evident, from the example, that in terms of deep-hole machining economics, the feed rate is substantially more important than the tool life. If both the tool life and the feed rate are increased by the same factor, the cost per unit length will decrease faster by the increase in the feed rate than it will decrease by the increase in the tool life. This clearly suggests that any future research work in

deep-hole machining should be directed toward methods which allow increased feed rates.

APPENDIX II

CUTTING FORCE EVALUATION FROM VARIOUS
SHEAR-ANGLE RELATIONS

APPENDIX II

CUTTING FORCE EVALUATION FROM VARIOUS SHEAR ANGLE RELATIONS

In addition to Stabler's shear-angle relationship, given by (2.4), other most characteristic relations selected for cutting force computation are as follows.

Lee and Shaffer's shear-angle relationship

$$\phi = 45 - (\tau - \alpha) \qquad \text{(A2.1)}$$

Ernest and Merchant's shear-angle relationship based on the principle of minimum energy

$$\phi = 45 - \tfrac{1}{2}(\tau - \alpha) \qquad \text{(A2.2)}$$

Merchant's shear angle relationship based on a slightly modified model

$$2\phi = c - (\tau - \alpha) \qquad \text{(A2.3)}$$

where

$$c = \cot^{-1}(K)$$

K = material constant

Weisz's shear-angle relationship

$$\phi = 54.7 - (\tau - \alpha) \qquad (A2.4)$$

Kronenberg's shear-angle relationship

$$\phi = 45 + \frac{\alpha}{2} - (0.75 + 0.045\alpha)\tau \qquad (A2.5)$$

Oxley's shear-angle relationship (approximation)

$$\phi = 50 - 0.8(\tau - \alpha) \qquad (A2.6)$$

These relations can be used to determine the shear angle provided the rake angle and the shear angle are known. The rake angle is known from the tool geometry and it represents the normal or true rake. The shear angle should be known from an experimental data. This seems to be an indirect way of solving the problem. To solve it directly, it seems necessary to find the chip ratio by measuring the cutting speed (v) and the chip velocity (v_c) and computing their ratio

$$r_t = \frac{v_c}{v} \qquad (A2.7)$$

Once the chip ratio is known, the shear angle ϕ can be determined from (2.3). With the shear angle known, any of the shear-angle relations can be used to determine the friction angle τ. With these fundamental variables known, the cutting force components can be computed from (2.7) to (2.11). This means that the values of the cutting force components computed

from the different shear-angle relations will differ from each other. To estimate which values are likely to be the most realistic, it seems to be best to compute the force components from all the preselected shear-angle relations and compare the values with the experimental data available.

Before this computation is undertaken, we shall recall the fact that the chip ratio is greatly affected by the chip cross-sectional area, cutting speed and cutting fluid used. This means that if the equations (2.7) to (2.11) should hold for any chip cross-sectional area and the cutting speeds and fluids common to deep-hole machining, experimental data is needed. Since such data is not available at the present time, it does not seem feasible to use this approach for cutting force prediction in deep-hole machining. Nevertheless, data for turning can be utilized for the purpose of assessing the order of magnitudes and the trends of the cutting force components resulting from the preselected shear-angle relations.

Such data is taken from reference [22] for the turning of steel, similar to that of SAE 1035, with 10 deg rake angle carbide tool at the cutting speed of 110 m/min. The data is plotted on log-log grid shown in Fig. A2.1. The straight line fit permits a simple analytical relation to be established

$$r_t = 0.53 \; s^{0.2} \qquad (A2.8)$$

Equations (2.1) and (2.2) can be rewritten in the form of equation (2.12) as follows:

$$F_p = A \, K_p \qquad \text{(A2.9)}$$

$$F_q = A \, K_q \qquad \text{(A2.10)}$$

where the tangential and thrust unit cutting forces are, according to equation (2.6), given by

$$K_p = \frac{S_0 \, \csc\phi}{(1 - K \, \tan(\phi+\tau-\alpha)} \, \frac{\cos(\tau-\alpha)}{\cos(\phi+\tau-\alpha)} \qquad \text{(A2.11)}$$

$$K_q = \frac{S_0 \, \csc\phi}{(1 - K \, \tan(\phi+\tau-\alpha)} \, \frac{\sin(\tau-\alpha)}{\cos(\phi+\tau-\alpha)} \qquad \text{(A2.12)}$$

Trends of change of the unit cutting forces can be best assessed from the normalized unit cutting forces $K_p(S)/K_p(0.1)$ and $K_q(S)/K_q(0.1)$. Normalizing is done with respect to the unit cutting force at $s = 0.1$ mm since the depths of cut in deep-hole machining are likely to be in the vicinity of this value. A simple computer program was used to compute these normalized unit cutting forces over a range of 0.05 to 1.0 mm which plots are given in the diagram in Fig. A2.1. Full lines show the tangential forces and dashed lines the thrust forces. The lines evaluated from the empirical expressions with $Y = 0.8$ for the tangential and $Y = 0.65$ for the trust force are drawn heavier. All lines are almost straight and the trends from an empirical approach

seem to be in good agreement with those resulting from the mechanics of cutting. These values are for a tool with 10 deg rake angle. Using a rake angle - chip ratio relationship [22] it was possible to estimate a corresponding steeper but rather hypothetical line for 0 deg. rake angle

$$r_t = 0.53 \ s^{0.15} \qquad (A2.13)$$

The results obtained in the identical way, such as those for a 10 deg rake angle, are plotted in the diagram shown in Fig. A2.2. As it may be seen, the lines diverge faster but the trends remain more or less the same. It should be noted that similar diagrams were not attempted for a 30 deg. negative rake angle, which is used in the inner zone of the solid boring cutter. This was not possible because of a lack of sufficient data. For this small zone, however, the multipliers ζ_p and ζ_q were evaluated under the assumption that the chip ratio is the same as that in the 0 deg. rake angle tool.

The three cutting force components are computed for two solid boring heads. The results for a tool of 50 mm diameter cutting in a steel similar to SAE 9255 at a feed of 0.14 mm per rev. are given in Table A2.1. The results for the other tool, of 35 mm diameter cutting in the same material at a feed of 0.16 mm per rev. are tabulated in Table A2.2.

Since the tool geometry was available for both tools, it was possible to compute the cutting force components and compare them with the experimental results reported [1,70].

TABLE A2.1

CUTTING FORCE COMPONENTS FOR 50 MM DIAMETER SOLID BORING HEAD

NO.	s mm	r_t	ζ_p	ζ_q	K_p N/mm²	K_q N/mm²	F_T N	F_R N	F_F N	θ DEG
1	0.14	0.358	1.36	2.33	2190.2	1036.2	8162.3	193.4	4312.6	88.6
2	0.14	0.358	1.53	2.00	5211.7	6353.6	19981.2	1343.4	25202.6	86.2
3	0.14	0.358	1.23	1.53	3133.3	2696.0	11420.4	1125.0	11556.7	84.4
4	0.14	0.358	1.12	1.24	2663.4	1869.1	9523.3	787.9	6573.1	85.3
5	0.14	0.358	1.58	2.75	2582.1	1725.9	9980.7	166.0	7612.5	89.0
6	0.14	0.358	1.13	1.29	2871.6	2235.5	10285.8	918.2	7927.8	84.9
7	0.14	—	1.16	1.28	2568.9	2247.9	9250.0	928.2	7958.6	84.3
8	0.14						9250.0	1040.0	7500.0	83.6

EXPERIMENTAL VALUES. [68]

TABLE A2.2

CUTTING FORCE COMPONENTS FOR 35 MM DIAMETER SOLID BORING HEAD

No.	s	r_t	ζ_p	ζ_q	K_p	K_q	F_T	F_R	F_F	θ
	mm				N/mm^2	N/mm^2	N	N	N	DEG
1	0.16	0.367	1.36	2.36	2165.2	1001.8	6511.5	131.2	3423.2	88.8
2	0.16	0.367	1.52	2.01	4959.3	5839.5	15371.4	1167.2	18847.4	85.7
3	0.16	0.367	1.25	1.56	3036.4	2527.2	8939.2	729.2	7541.2	85.3
4	0.16	0.367	1.12	1.17	2618.7	1805.8	7513.4	659.8	5007.3	85.0
5	0.16	0.367	1.56	2.75	2528.6	1650.2	7895.7	89.3	5987.1	89.4
6	0.16	0.367	1.14	1.30	2809.3	2140.9	8092.6	727.4	5739.5	84.9
7	0.16	-	1.16	1.28	2511.2	2145.3	7262.7	737.3	6076.5	84.2
8	0.16						5000.0	2800.0	5300.0	60.8

EXPERIMENTAL VALUES [1]
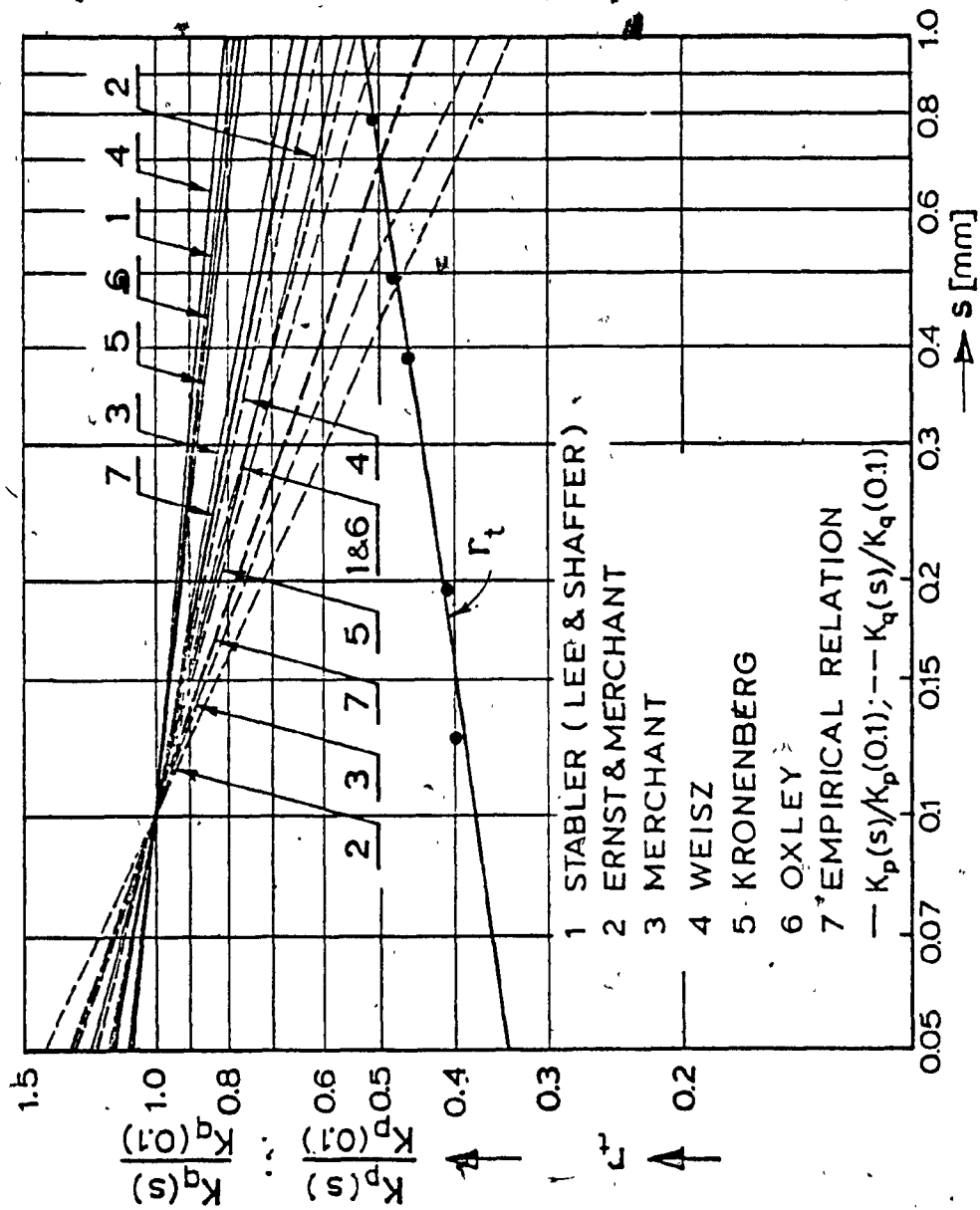
FIG. A2.1 TRENDS OF NORMALIZED UNIT CUTTING FORCE K_p AND K_q FOR 10 DEG RAKE
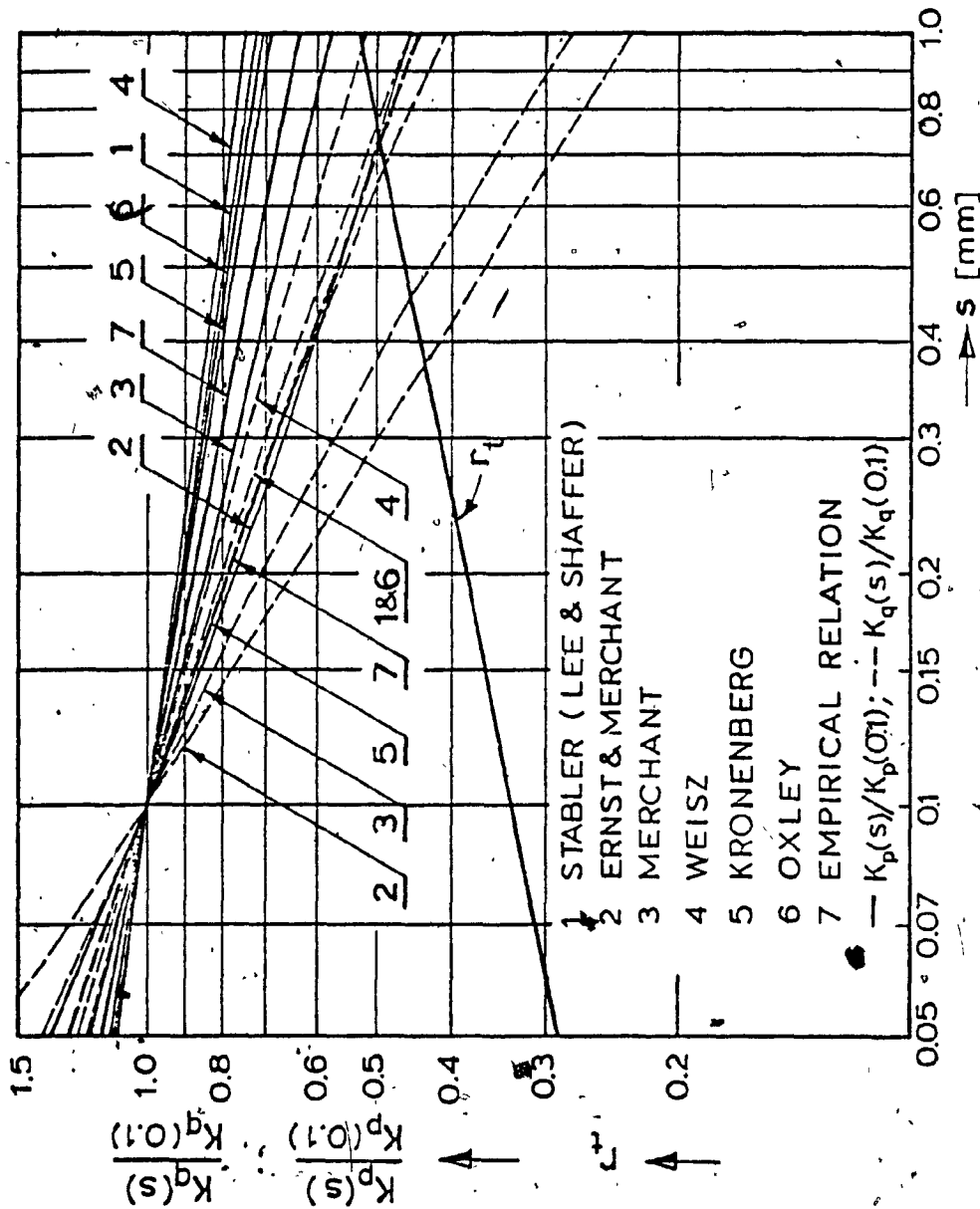
FIG. A2.2   TRENDS OF NORMALIZED UNIT CUTTING FORCES K_p AND K_q FOR ZERO RAKE

APPENDIX III

VARIATIONS IN MAGNITUDE AND DIRECTION OF THE
CUTTING FORCE RESULTANT

APPENDIX III

VARIATIONS IN MAGNITUDE AND DIRECTION OF THE
CUTTING FORCE RESULTANT

The supporting reaction R_s is given by equation (3.9). An identical equation would have resulted from (4.23) if the inertia terms had been neglected. Since R_s and R are identical in magnitude it follows that

$$R^2 = R_x^2 + R_y^2$$

$$= (\sum_{i=1}^{n} F_{Ri} \cos\phi_i - F_{Ti} \sin\phi_i)^2$$

$$+ (\sum_{i=1}^{n} F_{Ri} \sin\phi_i + F_{Ti} \cos\phi_i)^2 \qquad (A3.1)$$

where $i = 1,2,\ldots,n$, and the subscript i denotes the order of cutting edges counted from a positive x-axis in counter-clockwise direction.

In this analysis, the individual cutting forces entering into the summation, are considered to be uncorrelated and furthermore, the peak heights in each of the constituent forces are assumed to be sample functions of a stochastic stationary process, with possibly a Gaussian distribution. Equation (A3.1) is then valid provided that R, F_{Ri} and F_{Ti} are taken to represent the mean value of the respective variables. The upper limit of the cutting force resultant squared, may be written as

$$(R + \Delta R)^2 = [\sum_{i=1}^{n} (F_{Ri}+\Delta F_{Ri})\cos\phi_i - (F_{Ti}+\Delta F_{Ti})\sin\phi_i]^2$$

$$+ [\sum_{i=1}^{n} (F_{Ri}+\Delta F_{Ri})\sin\phi_i + (F_{Ti}+\Delta F_{Ti})\cos\phi_i]^2$$

$$(A3.2)$$

where the symbol Δ designates the deviation from the mean. These deviations may be both positive or negative, depending on the actual behaviour of the particular variable.

Subtracting (A3.1) from (A3.2) yields

$$2R\Delta R + (\Delta R)^2 = [\sum_{i=1}^{n} (F_{Ri}+\Delta F_{Ri})\cos\phi_i - (F_{Ti}+\Delta F_{Ti})\sin\phi_i]^2$$

$$+ [\sum_{i=1}^{n} (F_{Ri}+\Delta F_{Ri})\sin\phi_i + (F_{Ti}+\Delta F_{Ti})\cos\phi_i]^2$$

$$- (\sum_{i=1}^{n} F_{Ri}\cos\phi_i - F_{Ti}\sin\phi_i)^2$$

$$- (\sum_{i=1}^{n} F_{Ri}\sin\phi_i + F_{Ti}\cos\phi_i)^2 \qquad (A3.3)$$

Using the identity $A^2 - B^2 = (A+B)(A-B)$ equation (A3.3) can be rewritten as

$$2R\Delta R + (\Delta R)^2 = [\sum_{i=1}^{n} (2F_{Ri} + \Delta F_{Ri})\cos\phi_i - (2F_{Ti} + \Delta F_{Ti})\sin\phi_i]$$

$$* (\sum_{i=1}^{n} \Delta F_{Ri}\cos\phi_i - \Delta F_{Ti}\sin\phi_i)$$

$$+ [\sum_{i=1}^{n} (2F_{Ri} + \Delta F_{Ri})\sin\phi_i + (2F_{Ti} + \Delta F_{Ti})\sin\phi_i]$$

$$* (\sum_{i=1}^{n} \Delta F_{Ri}\sin\phi_i + \Delta F_{Ti}\cos\phi_i) \qquad (A3.4)$$

Using the identity

$$\sum_{i=1}^{n} 2A_i + a_i \pm (2B_i + b_i) = 2\sum_{i=1}^{n} A_i \pm B_i + \sum_{i=1}^{n} a_i \pm b_i$$

equation (A3.4) can be rearranged as follows:

$$2R\Delta R + (\Delta R)^2 = (\sum_{i=1}^{n} \Delta F_{Ri}\cos\phi_i - \Delta F_{Ti}\sin\phi_i)$$

$$* (\sum_{i=1}^{n} \Delta F_{Ri}\cos\phi_i - \Delta F_{Ti}\sin\phi_i$$

$$+ 2\sum_{i=1}^{n} F_{Ri}\cos\phi_i - F_{Ti}\sin\phi_i)$$

$$+ (\sum_{i=1}^{n} \Delta F_{Ri}\sin\phi_i + \Delta F_{Ti}\cos\phi_i)*$$

$$* (\sum_{i=1}^{n} \Delta F_{Ri}\sin\phi_i + \Delta F_{Ti}\cos\phi_i$$

$$+ 2\sum_{i=1}^{n} F_{Ri}\sin\phi_i + F_{Ti}\cos\phi_i) \qquad (A3.5)$$

Equation (A3.5) reduces to

$$2R\Delta R + (\Delta R)^2 = \Delta R_x(\Delta R_x + 2R_x) + \Delta R_y(\Delta R_y + 2R_y) \qquad (A3.6)$$

where R_x and R_y are defined by (A3.1) and ΔR_x and ΔR_y represent the deviation from the mean in the two Cartesian components of the cutting force resultant and are given by

$$\Delta R_x = \sum_{i=1}^{n} (\Delta F_{Ri} \cos\phi_i - \Delta F_{Ti} \sin\phi_i) \qquad (A3.7)$$

$$\Delta R_y = \sum_{i=1}^{n} (\Delta F_{Ri} \sin\phi_i + \Delta F_{Ti} \cos\phi_i) \qquad (A3.8)$$

The quantity ΔR_x represents the deviation from the mean of the cutting force resultant along the x-axis. In practice, measurements of the cutting forces are commonly specified in terms of the maximum and minimum values encountered in a given time interval. It appears reasonable to assume that in such measurements, the two extreme values are the $\pm 3\sigma$ values which for a Gaussian distribution of the peak heights encompasses 99.73 percent of all possible instantaneous values likely to occur within the measurement of interest. In this contest, then, ΔR_x becomes synonymous with a multiple of the standard deviations of the cutting force component along the x-axis and we can, in general, assume that the same confidence level applies to the measurements of the forces associated with each cutting edge. Equation (A3.7) gives the relationship for 3σ of the force resultant, in terms of the 3σ values of the forces

at the contributing cutting edges. Obviously, this relation-
ship holds for one standard deviation and since the variables
appearing in (A3.7) are uncorrelated and normal, the variance
may be written as

$$(\Delta R_x)^2 = \sum_{i=1}^{n} (\Delta F_{Ri})^2 \cos^2\phi_i + (\Delta F_{Ti})^2 \sin^2\phi_i \qquad (A3.9)$$

$$(\Delta R_y)^2 = \sum_{i=1}^{n} (\Delta F_{Ri})^2 \sin^2\phi_i + (\Delta F_{Ti})^2 \cos^2\phi_i \qquad (A3.10)$$

To find the deviation of the resultant force ΔR, the quadratic
equation (A3.6) is solved by an iteration of the correspond-
ing difference equation

$$\Delta R = \frac{1}{R}(R_x \Delta R_x + \Delta R_y \Delta R_y) + \frac{(\Delta R_x)^2 + (\Delta R_y)^2 - (\Delta R)^2}{2R} \qquad (A3.11)$$

Equation (A3.11) can be further simplified to fit the
special rotated coordinate system selected in the optimization
procedure. Namely, the system is selected so that a predetermin-
ed force resultant points horizontally to the left ($\lambda=0$).
Consequently $R_y = 0$, $R_x = R$ and equation (A3.11) reduces to

$$\Delta R = \Delta R_x + \frac{(\Delta R_x)^2 - (\Delta R_y)^2 - (\Delta R)^2}{2R_x} \qquad (A3.12)$$

Starting with $\Delta R = 0$ the iteration is repeated until
the difference between the two last approximations is less than
a prescribed amount. Equation (A3.12) has been found to

converge rapidly and furthermore, it can be readily solved by digital computer techniques.

A graphical representation of equation (A3.12) is depicted in Fig. A3.1 and the corresponding graphical solution for ΔR is

$$\Delta R = ||\vec{R}| - |\vec{R}_x|| \qquad \text{(A3.13)}$$

For an assessment of the tool-guidance and stability, besides the deviation from the mean magnitude of the cutting force resultant, it is equally important to know the deviation from the mean direction of the cutting force resultant. This can be accomplished from Fig. A3.1 as follows

$$\Delta \lambda = \tan^{-1}\left(\frac{\Delta R_y}{R_x - \Delta R_x}\right) \qquad \text{(A3.14)}$$

Since $\lambda = 0$ has been selected in the optimization procedure, it follows that the direction of the cutting force resultant is defined by a normal random variable λ with zero mean.

Since the system is linear and R_x and R_y have been assumed to be Gaussian, it follows that R and λ are both normally distributed.
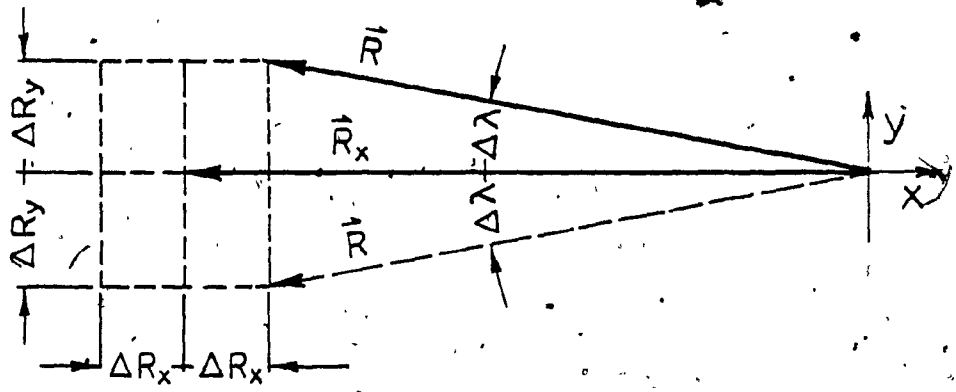
FIG. A3.1 GRAPHICAL REPRESENTATION OF DEVIATIONS OF THE CUTTING FORCE RESULTANT

APPENDIX IV

LISTING OF COMPUTER PROGRAMS, DATA SHEETS
AND PRINTOUTS OF TYPICAL RESULTS

```
      PROGRAM ME990 (INPUT,OUTPUT,TAPE 60=INPUT,TAPE 61=OUTPUT)
C
C        PATTERN SEARCH FOR MULTIVARIABLES
C
C        CALLING PROGRAM REQUIREMENTS
C
C        N        NUMBER OF INDEPENDENT VARIABLES (MAXIMUM 10)
C        NC       NUMBER OF CUTTING EDGES
C        NP       CONVERGENCE MONITOR
C        NP=0     WILL NOT PRINT
C          =1     WILL PRINT EVERY ITERATION
C          =2     WILL PRINT EVERY SECOND ITERATION
C        DELTA    CURRENT STEP SIZE
C        F        MINIMUM STEP SIZE
C        XL       LOWER BOUND OF SEARCH DOMAIN
C        XR       HIGHER BOUND OF SEARCH DOMAIN
C        X        CURRENT BASE POINT
C        XX       BASE POINT RESULTING FROM CURRENT MOVE
C        XXX      PREVIOUS BASE POINT
C        Y        FUNCTIONAL VALUE AT BASE POINT
C        YY       FUNCTIONAL VALUE RESULTING FROM CURRENT SET
C        YYY      FUNCTIONAL VALUE RESULTING FROM CURRENT MOVE
C                 OF EXPLORATORY MOVES OR PATTERN MOVE
C        ROW      REDUCTION FACTOR FOR STEP SIZE LESS THAN 1
C        NN       NUMBER OF ITERATIONS
C
      DIMENSION X(5),XX(5),XXX(5),XL(5),XR(5),S(5),B(5),FR(5),
     /FT(5),FF(5),TQ(5),R(5)
      COMMON NC,O,B,N,P1,P2,P12,P22,CR1,CR2,CR3,CT1,CT2,CT3,CF1,
     /CF2,CF3,RS,KW1,KW2,T,DELTA,Y1,Y2,RX,RY,RZ,RTQ,FR,FT,FF,TQ
    3 FORMAT (4I5)
    5 FORMAT (6F10.5)
      READ 3, NC,N,NP,NR
      READ 5,D,P1,P2,P12,P22,CR1,CR2,CR3,CT1,CT2,CT3,CF1,CF2,CF3,
     /ROW,DELTA,(X(I),I=1,N),(B(I),I=1,NC),RS,KW1,KW2,T,F,P,Q
      CALL PATRN (N,NC,NP,NR,NN,NO,DELTA,F,XL,XR,Y,X,ROW,O)
      CALL MERIT(X,Y)
      WRITE (61,10)    X(1),Y
      CALL STATS (FI,X,P,Q)
      WRITE (61,6) RX
      WRITE (61,7) RY
      WRITE (61,8) RZ
      WRITE (61,9) RTQ
      WRITE (61,12)(FR(I),I=1,NC)
      WRITE (61,14)(FT(I),I=1,NC)
      WRITE (61,16)(FF(I),I=1,NC)
      WRITE (61,18)(TQ(I),I=1,NC)
    6 FORMAT (5X,* RX CUTTING FORCE COMPONENT = *,F15.6)
    7 FORMAT (5X,* RY CUTTING FORCE COMPONENT = *,F15.6)
    8 FORMAT (5X,* RZ CUTTING FORCE COMPONENT = *,F15.6)
    9 FORMAT (5X,* RESULTANT TORQUE RTQ       = *,F15.6)
   10 FORMAT (5X,2F11.5)
   12 FORMAT (5X,* RADIAL CUTTING FORCES    FR(I) = *,3F10.6)
   14 FORMAT (5X,* TANGENTIAL CUTTING FORCES FT(I) = *,3F10.6)
   16 FORMAT (5X,* FEED CUTTING FORCES FF(I)       = *,3F10.6)
   18 FORMAT (5X,* CUTTING TORQUES               = *,3F10.6)
      STOP
```

```
      SUBROUTINE PATON (N,NC,NP,NR,NN,NO,DELTA,F,XL,XR,Y,X,ROW,O)
      DIMENSION X(5),XX(5),XXX(5),XL(5),XR(5)
      NF=0
      N1=0
      N2=0
      NN=0
      DELTA1=DELTA
      IF (NP) 5,5,6
6     WRITE (61,7)
      WRITE (61,4)
7     FORMAT (1H1,////,10X,* C O N V E R G E N C E    M O N I T O R
     /  P A T T E R *////)
4     FORMAT ( 7X, NN        DELTA         Y          X(1)       X(2)
     /   X(3) */)
5     CALL MERIT (X,Y)
      IF (NN-NP) 8,13,13
8     NF=NF+1
      NN=NN+1
      IF(NP)31,31,32
32    WRITE(61,33)NN,DELTA,Y,(X(I),I=1,N)
33    FORMAT(5X,I4,8F12.5)
31    CONTINUE
1     YY=Y
      DO 10 K=1,N
      XX(K)=X(K)
10    CONTINUE
      CALL LIMITS(XX,XL,XR)
      CALL EXPLOR (N,NC,XX,YY,XL,XR,DELTA,ROW,NF,O)
      A=YY-Y-0.000001
      IF (A) 3,3,2
2     DO 12 K=1,N
      XXX(K)=X(K)
      X(K)=XX(K)
12    CONTINUE
      Y=YY
      DO 20 I=1,N
      XX(I)=2.0*XX(I)-XXX(I)
20    CONTINUE
      DO 30 I=1,N
      CALL LIMITS(XX,XL,XR)
      IF(XX(I)-XL(I))41,42,42
41    XX(I)=XL(I)
42    IF(XX(I)-XR(I))30,30,44
44    XX(I)=XR(I)
30    CONTINUE
      CALL LIMITS(XX,XL,XR)
      CALL MERIT (XX,YYY)
      IF (NN-NR) 25,13,13
25    NF=NF+1
      NN=NN+1
      YY=YYY
      IF(N2)21,22,21
21    N2=N2+1
      IF(N2-NP)22,23,22
22    WRITE (61,33) NN,DELTA,Y,(Y(I),I=1,N)
      IF (NN.EQ.50) WRITE (61,107)
      IF (NN.EQ.105) WRITE (61,107)
```

```
107   FORMAT (1H1)
      N2=0
23    CALL EXPLOR (N,NC,XX,YY,XL,XR,DELTA,ROW,NF,O)
      B=YY-Y-0.000001
      IF (B) 1,1,2
3     DDELTA=DELTA-F
      IF(DDELTA)13,15,15
15    DELTA=ROW*DELTA
      GO TO 1
13    WRITE (61,100) NF
      WRITE (61,101)Y
      WRITE (61,102)NN
      WRITE (61,103)DELTA 1
      WRITE (61,104)DELTA
      WRITE(61,105)ROW
      WRITE(61,106)F
100   FORMAT(///,5X,* TOTAL NO OF FUNCTIONAL EVALUATIONS = *,I6)
101   FORMAT(5X, * LARGEST MERIT ORDINATE = *,2X,F15.6)
102   FORMAT(5X, * NUMBER OF BASE EVALUATIONS = *,2X,I5)
103   FORMAT(5X, * ORIGINAL STEP SIZE = *,2X,F15.6)
104   FORMAT(5X, * FINAL STEP SIZE = *,2X,F15.6)
105   FORMAT(5X,* REDUCTION FACTOR FOR STEP SIZE = *,2X,F15.6)
106   FORMAT(5X,* FRACTIONAL REDUCTION OF UNCERTAINTY = *,F15.6)
      RETURN

      SUBROUTINE EXPLOR (N,NC,XX,YY,XL,XR,DELTA,ROW,NF,O)
      DIMENSION XX(5),XL(5),XR(5),F(5)
      DO 10 K=1,N
      A=XX(K)
      XX(K)=XX(K)+DELTA
      IF(XX(K)-XL(K))21,22,22
21    XX(K)=XL(K)
22    IF(XX(K)-XR(K))24,24,23
23    XX(K)=XR(K)
24    CONTINUE
      CALL MERIT (XX,YYY)
      NF=NF+1
      B=YYY-YY-0.000001
      IF (B) 1,1,2
2     YY=YYY
      CALL LIMITS(XX,XL,XR)
      GO TO 10
1     XX(K)=A-DELTA
      IF(XX(K)-XL(K))25,26,26
25    XX(K)=XL(K)
26    IF(XX(K)-XR(K))28,28,27
27    XX(K)=XR(K)
28    CONTINUE
      CALL MERIT (XX,YYY)
      NF=NF+1
      C=YYY-YY-0.000001
      IF (C) 3,3,4
4     YY=YYY
      CALL LIMITS(XX,XL,XR)
      GO TO 10
3     XX(K)=A
      CALL LIMITS(XX,XL,XR)
10    CONTINUE
      RETURN
      END
```

234

```fortran
      SUBROUTINE LIMITS(XX,XL,XR)
      DIMENSION XX(5),XL(5),XR(5),FI(5),FIL(5),FIR(5)
      COMMON NC,D,B,N,P1,P2,P12,P22,CR1,CR2,CR3,CT1,CT2,CT3,CF1,
     /CF2,CF3,PS,KW1,KW2,T,DELTA,Y1,Y2,RX,RY,RZ,RTQ,FR,FT,FF,TQ
      DO 5 J=1,NC
      FI(J)=XX(J)
    5 CONTINUE
      FIL(1)=330.0
      FIR(1)=30.0
      FIL(2)=0.0
      FIR(2)=360.0
      FIL(3)=255.0
      FIR(3)=295.0
      DO 20 I=1,NC
      IF(FIR(I).LT.0)FIR(I)=FIR(I)+360.0
      IF (FIR(I)-FIL(I)) 8,18,18
    8 IF (FI(I)-FIL(I)) 10,10,15
   10 FIL(I)=FIL(I)-360.0
      GO TO 18
   15 FIR(I)=FIR(I)+360.0
   18 XL(I)=FIL(I)
      XR(I)=FIR(I)
   20 CONTINUE
      RETURN
      END


      SUBROUTINE MERIT (X,Y)
      DIMENSION X(5),XX(5),XXX(5),XL(5),XR(5),B(5),FI(5),PSI(5)
     /,FR(5),FT(5),FF(5),CRO(5),CTO(5),CFO(5),R(5),TQ(5)
      REAL KW1,KW2
      COMMON NC,D,B,N,P1,P2,P12,P22,CR1,CR2,CR3,CT1,CT2,CT3,CF1,
     /CF2,CF3,PS,KW1,KW2,T,DELTA,Y1,Y2,RX,RY,RZ,RTQ,FR,FT,FF,TQ
      PI=3.1415926
      RAD = PI/180.0
      DO 10 J=1,NC
      FI(J)=X(J)
   10 CONTINUE
      CRO(1)=CR1*B(1)
      CRO(2)=CR2*B(2)
      CRO(3)=CR3*B(3)
      DO 20 I=1,NC
      CTO(I)=CT1*B(I)
   20 CONTINUE
      DO 30 I=1,NC
      FR(I)=CRO(I)*T**0.65
      FT(I)=CTO(I)*T**0.80
   30 CONTINUE
      DO 100 I=1,NC
      FI(I)=FI(I)*RAD
  100 CONTINUE
      I=0
      RX=0.0
      RY=0.0
  105 I=I+1
      RX=RX+FR(I)*COS(FI(I))-FT(I)*SIN(FI(I))
      RY=RY+FR(I)*SIN(FI(I))+FT(I)*COS(FI(I))
      IF(I-NC)105,110,110
  110 CONTINUE
      Y1 = ABS(RX-PS)
      Y2 = ABS(RY)
      Y = -(KW1*Y1+KW2*Y2)
      RETURN
      END
```

```
      SUBROUTINE STATS (FI,X,P,Q)
      DIMENSION FI(5),X(5),R(5),B(5),CRO(5),CTO(5),CFO(5),FR(5),
     /FT(5),FF(5),TO(5),DELFR(5),DELFT(5)
      COMMON NC,D,R,N,P1,P2,P12,P22,CR1,CR2,CR3,CT1,CT2,CT3,CF1,
     /CF2,CF3,PS,KW1,KW2,T,DELTA,Y1,Y2,RX,RY,RZ,RTQ,FR,FT,FF,TO
      PI=3.1415995
      RAD=PI/180.0
      R(1)=D/2
      R(2)=R(1)-B(1)
      R(3)=R(2)-B(2)
      CFO(1)=CF1*R(1)
      CFO(2)=CF2*R(2)
      CFO(3)=CF3*R(3)
      DO 11 I=1,NC
      FF(I)=CFO(I)*T**0.65
      TQ(I)=FT(I)*(R(I)-B(I)/2.0)
11    CONTINUE
      I=0
      RZ=0.0
      RTQ=0.0
12    I=I+1
      RZ=RZ+FF(I)
      RTQ=RTQ+TQ(I)
      IF(I-NC) 12,14,14
14    CONTINUE
      DO 20 I=1,NC
      FI(I)=X(I)
      FI(I)=FI(I)*RAD
      DELFR(I)=P*FR(I)
      DELFT(I)=Q*FT(I)
20    CONTINUE
      I=0
      VARX=0.0
      VARY=0.0
30    I=I+1
      VARX=VARX+((DELFR(I))**2)*((COS(FI(I)))**2)+
     /((DELFT(I))**2)*((SIN(FI(I)))**2)
      VARY=VARY+((DELFR(I))**2)*((SIN(FI(I)))**2)+
     /((DELFT(I))**2)*((COS(FI(I)))**2)
      IF (I-NC) 30,40,40
40    CONTINUE
      DELRX=SQRT(VARX)
      DELRY=SQRT(VARY)
      EPS=0.000001
      K=0
      SUM=0.0
50    SM=SUM
      K=K+1
      SUM=DELRX+(DELRX**2+DELRY**2-SM**2)/(2.0*RX)
      IF (ABS(SUM-SM).GT.EPS) GO TO 50
      DELR=SUM
      DELLA=ATAN(DELRY/(RX-DELRX))/RAD
      WRITE (61,5) K
      WRITE (61,6) DELR
      WRITE (61,7) DELLA
      WRITE (61,8) DELRX,DELRY
5     FORMAT (5X,* K = *,I5)
6     FORMAT (5X,* R VARIATIN IN MAGNITUDE KN = *,F10.6)
7     FORMAT (5X,* R VARIATIN IN DIRECTION DEG =*,F10.6)
8     FORMAT (5X,2E15.6)
      RETURN
      END
```

TABLE A4.1

DATA SHEET FOR OPTIMIZATION OF THREE STAGGERED TOOLS

	TREPANNING	SOLID BORING	TREPANNING
TOOL NO	1	2	3
NC	3	2	2
N	3	2	2
NP		1	
NR		200	
D [mm]	85.725	85.725	298.704
P1 [mm]	8.0	8.0	10.333
P2 [mm]	8.0	8.0	10.333
P12 [mm]	0.0	5.431	3.0
P22 [mm]	0.0	8.0	7.0
CR1	0.2924	0.3114	0.3114
CR2	− 0.2924	0.2325	0.2325
CR3	0.0	0.3136	0.3136
CT1	1.734	1.734	1.734
CT2	1.734	0.0	0.0
CT3	1.734	0.0	0.0
CF1	1.0911	1.0858	1.0858
CF2	1.0911	0.041	0.041
CF3	1.1296	0.02193	0.02193
ROW	0.5	0.5	0.5
DELTA	0.1	0.1	0.1
X(1) [DEG]	0.0	300.0	300.0
X(2) [DEG]	200.0	180.0	180.0
X(3) [DEG]	320.0	−	−
B(1) [mm]	8.0	24.0	31.0
B(2) [mm]	8.0	18.862	17.0
B(3) [mm]	8.0	−	−
RS [kN]	4.5	6.5	7.0
KW1	2.0	2.0	2.0
KW2	5.0	2.0	2.0
T [mm]	0.15	0.33	0.17
F	0.001	0.001	0.001
P	0.1	0.215	0.215
Q	0.1	0.08	0.08

C O N V E R G E N C E   M O N I T O R   P A T T E R N

NN	DELTA	Y	X(1)	X(2)	X(3)
1	.10000	-14.09644	0.00000	200.00000	320.00000
2	.10000	-7.59771	-.10000	199.90000	285.00000
3	.10000	-3.45093	-.10000	199.90000	255.10000
4	.10000	-3.42846	.90000	201.00000	255.10000
5	.10000	-3.36178	.20000	200.20000	255.20000
6	.10000	-3.24954	.50000	200.50000	255.40000
7	.10000	-3.09191	.90000	200.90000	255.70000
8	.10000	-2.88452	1.40000	201.40000	256.10000
9	.10000	-2.63894	2.00000	202.00000	256.60000
10	.10000	-2.34263	2.70000	202.70000	257.20000
11	.10000	-1.99898	3.50000	203.50000	257.90000
12	.10000	-1.61373	4.40000	204.40000	258.70000
13	.10000	-1.60035	4.50000	204.30000	258.70000
14	.10000	-1.57121	4.70000	204.30000	258.70000
15	.10000	-1.53545	5.00000	204.20000	258.70000
16	.10000	-1.48580	5.40000	204.10000	258.70000
17	.10000	-1.42280	5.90000	204.00000	258.70000
18	.10000	-1.34713	6.50000	203.90000	258.70000
19	.10000	-1.25961	7.20000	203.80000	258.70000
20	.10000	-1.16121	8.00000	203.70000	258.70000
21	.10000	-1.05447	8.90000	203.60000	258.70000
22	.10000	-.93677	9.90000	203.50000	258.70000
23	.10000	-.91262	11.10000	203.40000	258.70000
24	.10000	-.67915	12.20000	203.40000	258.70000
25	.10000	-.53640	13.50000	203.40000	258.70000
26	.10000	-.39431	14.90000	203.40000	258.70000
27	.10000	-.24225	16.40000	203.50000	258.80000
28	.10000	-.06220	19.00000	203.50000	258.90000
29	.10000	-.05055	19.10000	203.50000	258.90000
30	.10000	-.03417	18.70000	203.50000	258.90000
31	.10000	-.01799	18.50000	203.50000	258.90000
32	.10000	-.00597	18.60000	203.60000	258.90000
33	.05000	-.00129	18.65000	203.60000	258.90000
34	.01250	-.00085	18.63750	203.60000	258.90000
35	.00625	-.00079	18.64375	203.60000	258.90000
36	.00313	-.00035	18.64062	203.59687	258.90000
37	.00313	-.00007	18.63750	203.59687	258.90000

TOTAL NO OF FUNCTIONAL EVALUATIONS =   289
LARGEST MERIT ORDINATE =   -.000075
NUMBER OF BASE EVALUATIONS =   37
ORIGINAL STEP SIZE =   .100000
FINAL STEP SIZE =   .000781
REDUCTION FACTOR FOR STEP SIZE =   .500000
FRACTIONAL REDUCTION OF UNCERTAINTY =   .001000
    18.63750   -.00007
K =   6
R VARIATIN IN MAGNITUDE KN =   .365421
R VARIATIN IN DIRECTION DEG =   5.593771
        .348400   .406612
RX CUTTING FORCE COMPONENT =   4.500002
RY CUTTING FORCE COMPONENT =   .000014
RZ CUTTING FORCE COMPONENT =   7.719931
RESULTANT TORQUE RTQ   =   281.555779
RADIAL CUTTING FORCES   FR(I) =   .681595   -.681595   0.000000
TANGENTIAL CUTTING FORCES FT(I) =   3.040970   3.040970   3.040970
FEED CUTTING FORCES FF(I)   =   2.543395   2.543395   2.633140
CUTTING TORQUES   = 118.179683 93.951926 69.524169

CONVEGENCE MONITOR PATTERN

NH	DELTA	Y	X(1)	X(2)
1	.10000	-27.12907	300.00000	180.00000
2	.10000	-26.99924	300.10000	179.90000
3	.10000	-26.73920	300.30000	179.70000
4	.10000	-26.34824	300.60000	179.40000
5	.10000	-25.82529	301.00000	179.00000
6	.10000	-25.16893	301.50000	179.50000
7	.10000	-24.37748	302.10000	177.90000
8	.10000	-23.44894	302.80000	177.20000
9	.10000	-22.38110	303.60000	176.40000
10	.10000	-21.17154	304.50000	175.50000
11	.10000	-19.81772	305.50000	174.50000
12	.10000	-15.31698	306.60000	173.40000
13	.10000	-16.66666	307.80000	172.20000
14	.10000	-14.86416	309.10000	170.90000
15	.10000	-12.90699	310.50000	169.50000
16	.10000	-10.79289	312.00000	168.00000
17	.10000	-8.51991	313.60000	166.40000
18	.10000	-6.08652	315.30000	164.70000
19	.10000	-3.49173	317.10000	162.90000
20	.10000	-.73518	319.00000	161.00000
21	.10000	-.58965	319.10000	160.90000
22	.10000	-.51638	319.30000	160.70000
23	.10000	-.42638	319.60000	160.40000
24	.10000	-.39630	319.70000	160.30000
25	.10000	-.37020	319.70000	160.20000
26	.10000	-.34810	319.60000	160.10000
27	.10000	-.32595	319.50000	160.00000
28	.10000	-.30376	319.40000	159.90000
29	.10000	-.28153	319.30000	159.80000
30	.10000	-.25926	319.20000	159.70000
31	.10000	-.23696	319.10000	159.60000
32	.10000	-.21461	319.00000	159.50000
33	.10000	-.19222	318.90000	159.40000
34	.10000	-.16979	318.80000	159.30000
35	.10000	-.14732	318.70000	159.20000
36	.10000	-.12481	318.60000	159.10000
37	.10000	-.10226	318.50000	159.00000
38	.10000	-.07967	318.40000	158.90000
39	.10000	-.05704	318.30000	158.80000
40	.10000	-.03437	318.20000	158.70000
41	.10000	-.02279	318.10000	158.60000
42	.05000	-.01954	318.15000	158.60000
43	.02500	-.01126	318.12500	158.60000
44	.01250	-.01105	318.13750	158.60000
45	.00313	-.01089	318.13750	158.59687
46	.00313	-.01018	318.13437	158.59375
47	.00313	-.00876	318.12812	158.58750
48	.00313	-.00663	318.11875	158.57812
49	.00313	-.00380	318.10625	158.56562
50	.00313	-.00096	318.09375	158.55312

```
51      .00156      -.00039     318.09219   158.55312
52      .00078      -.00038     318.09297   158.55312


TOTAL NO OF FUNCTIONAL EVALUATIONS =      292
LARGEST MERIT ORDINATE =                -.000392
NUMBER OF BASE EVALUATIONS =              52
ORIGINAL STEP SIZE =              .100000
FINAL STEP SIZE =                  .000781
REDUCTION FACTOR FOR STEP SIZE =           .500000
FRACTIONAL REDUCTION OF UNCERTAINTY =        .001000
  318.09297,    -.00039
K. =        0
R VARIATIN IN MAGNITUDE KN =    1.142825
R VARIATIN IN DIRECTION DEG =  14.633982
       1.007036       1.434295
RX CUTTING FORCE COMPONENT =          6.500021
RY CUTTING FORCE COMPONENT =           .000170
RZ CUTTING FORCE COMPONENT =         23.082654
RESULTANT TORQUE RTQ       =        656.122975
RADIAL CUTTING FORCES     FR(I) =       .605527      .509677
TANGENTIAL CUTTING FORCES FT(I) =     17.142395    13.472494
FEED CUTTING FORCES FF(I)       =     12.910143    10.172511
CUTTING TORQUES TQ(I)           =    529.057152   147.065323



11.21.52.ME890.
11.21.52.** V.LATINOVIC ***
11.21.52.ACCOUNT,CABSK55,.
11.21.52.FTN,OPT=0.
11.22.10.      3.796 CP SECONDS COMPILATION TIME
11.22.11.LGO.
11.22.19.     STOP
11.22.20.       .927 CP SECONDS EXECUTION TIME
11.22.20.UEAD.      0.001KUNS.
11.22.20.UEMS,     0.736KUNS,
11.22.20.UECP,     5.988SECS.
11.22.20.AESP,     7.768UNTS,
11.25.22.UCLP, 23,      0.773 KLNS.
```

CONVEGENCE MONITOR PATTERN

NN	DELTA	Y	X(1)	X(2)
1	.10000	-11.30709	300.00000	180.00000
2	.10000	-11.22084	300.10000	179.90000
3	.10000	-11.04810	300.30000	179.70000
4	.10000	-10.78841	300.60000	179.40000
5	.10000	-10.44111	301.00000	179.00000
6	.10000	-10.00531	301.50000	178.50000
7	.10000	-9.47994	302.10000	177.90000
8	.10000	-8.86376	302.80000	177.20000
9	.10000	-8.15538	303.60000	176.40000
10	.10000	-7.35330	304.50000	175.50000
11	.10000	-6.58432	305.40000	174.50000
12	.10000	-6.44046	306.20000	173.40000
13	.10000	-6.25233	306.90000	172.20000
14	.10000	-6.05408	307.50000	170.90000
15	.10000	-5.81976	308.00000	169.50000
16	.10000	-5.56330	308.40000	168.00000
17	.10000	-5.28892	308.70000	166.40000
18	.10000	-4.99916	308.90000	164.70000
19	.10000	-4.69884	309.00000	162.90000
20	.10000	-4.39109	309.00000	161.00000
21	.10000	-4.07939	308.90000	159.00000
22	.10000	-3.76708	308.70000	156.90000
23	.10000	-3.45748	308.40000	154.70000
24	.10000	-3.15376	308.00000	152.40000
25	.10000	-2.85905	307.50000	150.00000
26	.10000	-2.80860	306.90000	147.70000
27	.10000	-2.71097	306.80000	147.80000
28	.10000	-2.53319	306.60000	147.90000
29	.10000	-2.53707	306.30000	147.90000
30	.10000	-2.47929	305.90000	147.80000
31	.10000	-2.39870	305.40000	147.60000
32	.10000	-2.29403	304.80000	147.30000
33	.10000	-2.15384	304.10000	146.90000
34	.10000	-2.00658	303.30000	146.40000
35	.10000	-1.82055	302.40000	145.80000
36	.10000	-1.60394	301.40000	145.10000
37	.10000	-1.35484	300.30000	144.30000
38	.10000	-1.07123	299.10000	143.40000
39	.10000	-.88587	298.00000	142.40000
40	.10000	-.81000	298.10000	142.30000
41	.10000	-.80067	298.10000	142.10000
42	.10000	-.76600	298.00000	141.80000
43	.10000	-.70622	297.80000	141.40000
44	.10000	-.64308	297.60000	140.90000
45	.10000	-.57753	297.40000	140.30000
46	.10000	-.48856	297.10000	139.60000
47	.10000	-.39903	296.80000	138.80000
48	.10000	-.28759	296.40000	137.90000
49	.10000	-.17801	296.00000	136.90000
50	.10000	-.07213	295.60000	135.80000

51	.10000	-.05207	295.10000	134.80000
52	.10000	-.05192	295.10000	134.90000
53	.10000	-.02724	295.20000	135.10000
54	.10000	-.01711	295.30000	135.30000
55	.05000	-.00981	295.35000	135.35000
56	.02500	-.00969	295.35000	135.32500
57	.02500	-.00359	295.32500	135.30000
58	.01250	-.00353	295.32500	135.28750
59	.01250	-.00084	295.31250	135.27500
60	.00313	-.00047	295.31250	135.27187
61	.00078	-.00028	295.31172	135.27109
62	.00078	-.00012	295.31094	135.27031

```
TOTAL NO OF FUNCTIONAL EVALUATIONS =      345
LARGEST MERIT ORDINATE =                -.000117
NUMBER OF BASE EVALUATIONS =          62
ORIGINAL STEP SIZE =              .100000
FINAL STEP SIZE =                 .000781
REDUCTION FACTOR FOR STEP SIZE =              .500000
FRACTIONAL REDUCTION OF UNCERTAINTY =         .001000
   295.31094    -.00012
 K =       9
R VARIATIN IN MAGNITUDE KN =    1.048502
R VARIATIN IN DIRECTION DEG =    5.836906
        1.025293        .610782
RX CUTTING FORCE COMPONENT =           7.000050
RY CUTTING FORCE COMPONENT =           -.000008
RZ CUTTING FORCE COMPONENT =          16.802488
RESULTANT TORQUE RTQ        =       2528.021337
RADIAL CUTTING FORCES       FR(I) =       .508118      -.049434
TANGENTIAL CUTTING FORCES FT(I) =      13.024755     7.142614
FEED CUTTING FORCES FF(I)      =      10.835257     5.967231
CUTTING TORQUES TQ(I)          =    1743.390956   784.630381
```

```
10.40.20.MER90.
10.40.20.** V.LATINOVIC ***
10.40.21.ACCOUNT,CABSK55,.
10.40.22.FTN,OPT=0.
10.40.40.     3.791 CP SECONDS COMPILATION TIME
10.40.40.LGO.
10.40.50.     STOP
10.40.50.     1.065 CP SECONDS EXECUTION TIME
10.40.50.UEAD,      0.001KUNS.
10.40.50.UEMS,      0.738KUNS.
10.40.50.UECP,      6.108SECS.
10.40.50.AESR,      7.897UNTS.
10.42.49.UCLP, 23,      0.763 KLNS.
```

```
      PROGRAM ME890 (INPUT,OUTPUT,TAPE 60=INPUT,TAPE 61=OUTPUT)
C
C      PATTERN SEARCH FOR MULTIVARIABLES
C
C      CALLING PROGRAM REQUIREMENTS
C
C      N          NUMBER OF INDEPENDENT VARIABLES (MAXIMUM 10)
C      NP         CONVERGENCE MONITOR
C      NP=0       WILL NOT PRINT
C        =1       WILL POINT EVERY ITERATION
C        =2       WILL PRINT EVERY SECOND ITERATION
C      DELTA      CURRENT STEP SIZE
C      F          MINIMUM STEP SIZE
C      XL         LOWER BOUND OF SEARCH DOMAIN
C      XR         HIGHER BOUND OF SEARCH DOMAIN
C      X          CURRENT BASE POINT
C      XX         BASE POINT RESULTING FROM CURRENT MOVE
C      XXX        PREVIOUS BASE POINT
C      Y          FUNCTIONAL VALUE AT BASE POINT
C      YY         FUNCTIONAL VALUE RESULTING FROM CURRENT SET
C      Y.YY       FUNCTIONAL VALUE RESULTING FROM CURRENT MOVE
C             OF EXPLORATORY MOVES OR PATTERN MOVE
C      ROW        REDUCTION FACTOR FOR STEP SIZE LESS THAN 1
C      NN         NUMBER OF ITERATIONS
C
      DIMENSION X(10),XX(10),XXX(10),XL(10),XR(10),S(5),B(5),FR(5),
     /FT(5),FF(5),TQ(5)
      REAL KSI,KW1,KW2,KW3
      COMMON NC,D,KSI,N,P1,P2,CR1,CR2,CR3,CT1,CT2,CT3,CF1,CF2,
     /CF3,KW1,KW2,KW3,RS,T,DELTA,Y1,Y2,Y3,S,RX,RY,RZ,FR,FT,FF,TQ
     /,RTQ
    3 FORMAT (2I5)
    5 FORMAT (6F10.5)
      READ 3,NP,NR
      READ 5,D,P1,P2,KSI,CR1,CR2,CR3,CT1,CT2,CT3,CF1,CF2,CF3,
     /ROW,DELTA,RS,KW1,KW2,KW3,T,F,ZETA,C,BL,BR,P,Q,ALFA
      BA=(BL+BR)/2.0
      RA=KSI*BA-D+SQRT(D**2-KSI*D*BA)
      NC=1+((ZETA*D**2)/(4.0*(1.0+C))-(0.221*D)**2)/RA**2
      ND=2*NC
      N=ND-1
      DO 2 J=1,NC
      JM1=J-1
      AA=JM1
    2 X(J)=360.0*AA/NC+ALFA
      NCM1=NC-1
      DO 11 K=1,NCM1
      KC=K+NC
      XL(KC)=BL
      XR(KC)=BR
   11 X(KC)=XL(KC)
      X(ND)=0.5*D
      WRITE (61,20) NC,ND,N
   20 FORMAT (3I5)
      CALL PATEN (N,NC,NP,NR,NN,ND,DELTA,F,XL,XR,Y,X,ROW,D)
      CALL MERIT(X,Y)
      WRITE (61,10)     X(1),Y
```

```
      CALL STATS (FI,X,P,Q)
      WRITE (61,6) PX
      WRITE (61,7) RY
      WRITE (61,8) PZ
      WRITE (61,9) RTQ
      WRITE (61,12) (FR(I),I=1,NC)
      WRITE (61,14) (FT(I),I=1,NC)
      WRITE (61,16) (FF(I),I=1,NC)
      WRITE (61,19) (TQ(I),I=1,NC)
      WRITE (61,19) (S(I),I=1,NC)
6     FORMAT (5X,* RX CUTTING FORCE COMPONENT = *,F15.6)
7     FORMAT (5X,* RY CUTTING FORCE COMPONENT = *,F15.6)
8     FORMAT (5X,* RZ CUTTING FORCE COMPONENT = *,F15.6)
9     FORMAT (5X,* RESULTANT TORQUE RTQ      = *,F15.6)
10    FORMAT (5X,2F11.5)
12    FORMAT (5X,* RADIAL CUTTING FORCES     FR(I) = *,5F12.6)
14    FORMAT (5X,* TANGENTIAL CUTTING FORCES FT(I) = *,5F12.6)
16    FORMAT (5X,* FEED CUTTING FORCES FF(I)       = *,5F12.6)
18    FORMAT (5X,* CUTTING TORQUES TQ(I)           = *,5F12.6)
19    FORMAT (5X,* EFFECTIVE CUTTING DEPTHS S(I)   = *,5F12.6)
      STOP
      END



      SUBROUTINE PATON (N,NC,NP,NR,NN,NO,DELTA,F,XL,XR,Y,X,ROW,D)
      DIMENSION X(10),XX(10),XXX(10),XL(10),XR(10)
      NF=0
      N1=0
      N2=0
      NN=0
      DELTA 1=DELTA
      IF(NP) 5,5,6
6     WRITE (61,7)
      WRITE (61,4)
7     FORMAT (1H1,////,15X,* C O N V E R G E N C E    M O N I T O R
     / P A T T E R N *////)
4     FORMAT ( 7X,*NN       DELTA       Y       X(1)        X(2)
     / X(3)       X(4)        X(5)       X(6) */)
5     CALL MERIT (X,Y)
      IF (NN-NR) 8,13,13
8     NF=NF+1
      NN=NN+1
      IF(NP)31,31,32
32    WRITE (61,33) NN,DELTA,Y,(X(I),I=1,NO)
33    FORMAT(5X,I4,8F12.5)
31    CONTINUE
      XX(NO)=0.5*D
1     YY=Y
      DO 10 K=1,N
      XX(K)=X(K)
10    CONTINUE
      CALL EXPLOR (N,NC,XX,YY,XL,XR,DELTA,ROW,NF,NO,D)
      A=YY-Y-0.000001
```

```
        IF (A) 3,3,2
2       DO 12 K=1,N
        XXX(K)=X(K)
        X(K)=XX(K)
12      CONTINUE
        X=YY
        DO 20 I=1,N
        A=XX(I)
        XX(I)=2.0*XX(I)-XXX(I)
        IF (I.LE.NC) GO TO 20
        IN=I-NC
        CALL LIMITS (XX,XL,XR)
        IF (XX(IN).GT.XR(IN).OR.XX(IN).LT.XL(IN)) XX(I)=A
20      CONTINUE
        CALL CHECK (XX,XL,XR)
        CALL MERIT (XX,YYY)
        IF (NN-NR) 25,13,13
25      NF=NF+1
        NN=NN+1
        YY=YYY
        IF(N2)21,22,21
21      N2=N2+1
        IF(N2-NP)22,23,22
22      WRITE (61,33) NN,DELTA,Y,(X(I),I=1,ND)
        IF (NN.EQ.35) WRITE (61,107)
        IF (NN.EQ.75) WRITE (61,107)
107     FORMAT (1H1)
        N2=0
23      CALL EXPLOP (N,NC,XX,YY,XL,XR,DELTA,ROW,NF,ND,0)
        B=YY-Y-0.000001
        IF (B) 1,1,2
3       DDELTA=DELTA-F
        IF(DDELTA)13,15,15
15      DELTA=ROW*DELTA
        GO TO 1
13      WRITE (61,100) NF
        WRITE (61,101)Y
        WRITE (61,102)NN
        WRITE (61,103)DELTA 1
        WRITE (61,104)DELTA
        WRITE(61,105)ROW
        WRITE(61,106)F
100     FORMAT(///,5X,* TOTAL NO OF FUNCTIONAL EVALUATIONS = *,I6)
101     FORMAT(5X, * LARGEST MERIT ORDINATE = *,2X,F15.6)
102     FORMAT(5X, * NUMBER OF BASE EVALUATIONS = *,2X,I5)
103     FORMAT(5X, * ORIGINAL STEP SIZE = *,2X,F15.6)
104     FORMAT(5X, * FINAL STEP SIZE = *,2X,F15.6)
105     FORMAT(5X,* REDUCTION FACTOR FOR STEP SIZE = *,2X,F15.6)
106     FORMAT(5X,* FRACTIONAL REDUCTION OF UNCERTAINTY = *,F15.6)
        RETURN
        END
```

```
      SUBROUTINE EXPLOR(N,NC,XX,YY,XL,XR,DELTA,ROW,NF,ND,D)
      DIMENSION XX(10),XL(10),XR(10)
      CALL CHECK(XX,XL,XR)
      DO 34 I=1,NC
      IF (XX(I)-XL(I)-0.0000001) 34,34,15
15    IF (XR(I)-XX(I)-0.0000001) 30,30,34
30    IDELTA=0
      IP1=I+1
      IF(IP1.GT.NC) IP1=IP1-NC
      IP2=I+2
      IF(IP2.GT.NC)IP2=IP2-NC
      IP3=I+3
      IF (IP3.GT.NC) IP3=IP3-NC
      IP4=I+4
      IF(IP4.GT.NC) IP4=IP4-NC
      B1=XX(I)
      B2=XX(IP1)
      IDELTA=IDELTA+1
      C1=XR(IP1)-XL(IP1)-0.000001
      IF(C1)31,31,45
31    B3=XX(IP2)
      IDELTA=IDELTA+1
      C2=XR(IP2)-XL(IP2)-0.000001
      IF(C2)32,32,45
32    B4=XX(IP3)
      IDELTA=IDELTA+1
      C3=XR(IP3)-XL(IP3)-0.000001
      IF(C3)33,33,45
33    B5=XX(IP4)
      IDELTA=IDELTA+1
45    CONTINUE
      ADELTA=0.0
      BDELTA=0.0
      N1=I+IDELTA
      IF (N1.GT.NC) N1=N1-NC
      XX(N1)=XX(N1)+DELTA
      IF (XX(N1).GT.XR(N1)) ADELTA=XX(N1)-XR(N1)
      XX(I)=B1+DELTA-ADELTA
      XX(IP1)=B2+DELTA-ADELTA
      IF (IDELTA .GE. 2) XX(IP2)=B3+DELTA-ADELTA
      IF (IDELTA.GE.3) XX(IP3)=B4+DELTA-ADELTA
      IF(IDELTA.GE.4) XX(IP4)=B5+DELTA-ADELTA
      CALL MERIT(XX,YYY)
      NF=NF+1
      AA=YYY-YY-0.0000001
      IF(AA)5,5,6
6     YY=YYY
      CALL LIMITS(XX,XL,XR)
      GO TO 35
5     XX(I)=B1-DELTA
      IF (XX(I).LT.XL(I)) BDELTA=XL(I)-XX(I)
      XX(I)=B1-DELTA+BDELTA
      XX(IP1)=B2-DELTA+BDELTA
      IF (IDELTA.GE.2) XX(IP2)=B3-DELTA+BDELTA
      IF (IDELTA.GE.3) XX(IP3)=B4-DELTA+BDELTA
      IF (IDELTA.GE.4) XX(IP4)=B5-DELTA+BDELTA
      CALL MERIT(XX,YYY)
```

```
      NF=NF+1
      AA=YYY-YY-0.0000001
      IF (AA)7,7,8
    8 YY=YYY
      CALL LIMITS(XX,XL,XR)
      GO TO 35
    7 XX(I)=B1
      XX(IP1)=B2
      IF (IDELTA.GE.2) XX(IP2)=B3
      IF (IDELTA.GE.3) XX(IP3)=B4
      IF (IDELTA.GE.4) XX(IP4)=B5
      CALL LIMITS(XX,XL,XR)
   35 CONTINUE
   34 CONTINUE
      DO 10 K=1,N
      A=XX(K)
      XX(K)=XX(K)+DELTA
      IF (K.LE.NC) GO TO 50
      KN = K-NC
      CALL LIMITS(XX,XL,XR)
      IF (XX(KN).GT.XR(KN).OR.XX(KN).LT.XL(KN)) GO TO 1
   50 CALL CHECK(XX,XL,XR)
      CALL MERIT (XX,YYY)
      NF=NF+1
      B=YYY-YY-0.000001
      IF (B) 1,1,2
    2 YY=YYY
      CALL LIMITS(XX,XL,XR)
      GO TO 10
    1 XX(K)=A-DELTA
      CALL CHECK(XX,XL,XR)
      CALL MERIT (XX,YYY)
      NF=NF+1
      C=YYY-YY-0.000001
      IF (C) 3,3,4
    4 YY=YYY
      CALL LIMITS(XX,XL,XR)
      GO TO 10
    3 XX(K)=A
      CALL LIMITS(XX,XL,XR)
   10 CONTINUE
      RETURN
      END




      SUBROUTINE LIMITS(XX,XL,XR)
      DIMENSION XX(10),XL(10),XR(10),FIL(5),FIR(5),PSI(5),B(5),FI(5)
      REAL KSI
      COMMON NC,D,KSI,N,P1,P2,CR1,CR2,CR3,CT1,CT2,CT3,CF1,CF2,
     /CF3,KW1,KW2,KW3,RS,T,DELTA,Y1,Y2,Y3,S,RX,RY,RZ,FR,FT,FF,TQ
     /,RTQ
      PI=3.1415926
      DEG=180.0/PI
```

```
      DO 5 J=1,NC
      JC=J+NC
      FI(J)=XX(J)
      B(J)=XX(JC)
      R=KSI*B(J)-O+SQRT(O**2-KSI*O*B(J))
      RC=O/2-R
      PSI(J)=ASIN(R/RC)*DEG
5     CONTINUE
      DO 20 I=1,NC
      IM1=I-1
      IP1=I+1
      IF(IM1.LT.1)IM1=IM1+NC
      IF(IP1.GT.NC)IP1=IP1-NC
      FIL(I)=FI(IM1)+2.0*PSI(IM1)+0.25*PSI(I)
      FIR(I)=FI(IP1)-2.0*PSI(I)-0.25*PSI(IP1)
      IF(FIR(I).LT.0)FIR(I)=FIR(I)+360.0
      IF (FIR(I)-FIL(I)) 8,15,18
8     IF (FI(I)-FIL(I)) 10,10,15
10    FIL(I)=FIL(I)-360.0
      GO TO 18
15    FIR(I)=FIR(I)+360.0
18    XL(I)=FIL(I)
      XR(I)=FIR(I)
20    CONTINUE
      RETURN
      END




      SUBROUTINE CHECK(XX,XL,XR)
      DIMENSION XX(10),XL(10),XR(10)
      REAL KSI,KW1,KW2,KW3
      COMMON NC,O,KSI,N,P1,P2,CR1,CR2,CR3,CT1,CT2,CT3,CF1,CF2,
     /CF3,KW1,KW2,KW3,RS,T,DELTA,Y1,Y2,Y3,S,RX,RY,RZ,FR,FT,FF,TQ
     /,RTQ
      IF (NC.EQ.N) GO TO 9
      CALL LIMITS(XX,XL,XR)
      NCP1=NC+1
      DO 5 I=NCP1,N
      IF (XX(I)-XL(I)) 6,7,7
6     XX(I)=XL(I)
7     IF (XX(I)-XR(I)) 5,5,8
8     XX(I)=XR(I)
5     CONTINUE
9     CALL LIMITS (XX,XL,XR)
      DO 10 I=1,NC
      IF (XX(I)-XL(I)) 11,10,10
11    XX(I)=XL(I)
      CALL LIMITS(XX,XL,XR)
10    CONTINUE
      DO 15 I=1,NC
      IF (XX(I)-XR(I)) 15,15,16
16    XX(I)=XR(I)
      CALL LIMITS(XX,XL,XR)
15    CONTINUE
      RETURN
      END
```

```
      SUBROUTINE MERIT (X,Y)
      DIMENSION X(10),XX(10),XXX(10),XL(10),XR(10),B(5),FI(5),S(5)
     /,PSI(5),FIL(5),FIR(5),FR(5),FT(5),FF(5),TQ(5),DELFI(5),DELS(5)
     /,CRO(5),CTO(5),CFO(5)
      REAL KSI,KW1,KW2,KW3
      COMMON NC,D,KSI,N,P1,P2,CR1,CR2,CR3,CT1,CT2,CT3,CF1,CF2,
     /CF3,KW1,KW2,KW3,RS,T,DELTA,Y1,Y2,Y3,S,RX,RY,RZ,FR,FT,FF,TQ
     /,RT3
      PI=3.1415926
      RAD=PI/180.0
      DO 10 J=1,NC
      JC=J+NC
      FI(J)=X(J)
      B(J)=X(JC)
   10 CONTINUE
      DO 16 I=1,NC
      IP1 = I + 1
      IF (IP1.GT.NC)IP1=IP1-NC
      DELFI(I)=FI(IP1)-FI(I)
      IF (DELFI(I)) 12,15,15
   12 DELFI(I)=DELFI(I)+360.0
   15 S(I) = DELFI(I)*T/360.0
   16 CONTINUE
      DO 18 I=1,NC
      IP1 = I + 1
      IF (IP1.GT.NC)IP1=IP1-NC
      DELS(I)=S(IP1)-S(I)
   18 CONTINUE
      I=0
   20 I=I+1
      IF (B(I)-P1) 25,25,23
   23 IF (B(I)-(P1+P2)) 30,30,35
   25 CRO(I)=CR1*B(I)
      CTO(I)=CT1*B(I)
      IF (I-NC) 20,40,40
   30 CRO(I)=CR1*B(I)-CR2*(B(I)-P1)
      CTO(I)=CT1*B(I)+CT2*(B(I)-P1)
      IF (I-NC) 20,40,40
   35 CRO(I)=CR1*B(I)-CR2*(B(I)-P1)-CR3*(B(I)-(P1+P2))
      CTO(I)=CT1*B(I)+CT2*(B(I)-P1)+CT3*(B(I)-(P1+P2))
      IF (I-NC) 20,40,40
   40 CONTINUE
      DO 70 I=1,NC
      J2=I
      FR(I)=0.0
      FT(I)=0.0
      FF(I)=0.0
      B2=B(I)
   45 J1=J2
      B1=0.0
      SS=0.0
      XN=0.0
      DO 60 J=1,NC
      K=I+J
      IF (K.GT.NC) K=K-NC
      IF (I.EQ.K) GO TO 65
      IF (B(J2)-B(K)) 65,65,50
```

```
 50 SS=SS+S(K)
    XN=1.0
    IF (B(K).LT.B1) GO TO 60
    IF (B(K).GT.B2) GO TO 60
    J1=K
    B1=B(K)
 60 CONTINUE
 65 FR(I)=FR(I)+(CRO(J2)-CRO(J1)*XN)*(S(I)+SS)**0.65
    FT(I)=FT(I)+(CTO(J2)-CTO(J1)*XN)*(S(I)+SS)**0.8
    IF (SS.EQ.0.0) GO TO 70
    B2=B1
    J2=J1
    GO. TO 45
 70 CONTINUE
    DO 107 I=1,NC
    FI(I)=FI(I)*RAD
107 CONTINUE
    I=0
    RX = 0.0
    RY = 0.0
    Y3 = 0.0
108 I=I+1
    RX=RX+FR(I)*COS(FI(I))-FT(I)*SIN(FI(I))
    RY=RY+FR(I)*SIN(FI(I))+FT(I)*COS(FI(I))
    Y3 = Y3+ABS(DELS(I))
    IF(I-NC)108,110,110
110 CONTINUE
    Y1 = ABS(RX-RS)
    Y2 = ABS(RY)
    Y = -(KW1*Y1+KW2*Y2+KW3*Y3)
    RETURN
    END
```

```
      SUBROUTINE STATS (FI,X,P,Q)
      DIMENSION FI(5),X(5),P(5),B(5),CRO(5),CTO(5),CFO(5),FR(5),
     /FT(5),FF(5),TO(5),DELFR(5),DELFT(5),DELFI(5),S(5)
      COMMON NC,D,KSI,N,P1,P2,CR1,CR2,CR3,CT1,CT2,CT3,CF1,CF2,
     /CF3,KW1,KW2,KW3,QS,T,DELTA,Y1,Y2,Y3,S,RX,RY,RZ,FR,FT,FF,TO
     /,RTQ
      PI=3.1415926
      RAD=PI/180.0
      DO 10 I=1,NC
      IC=I+NC
      FI(I)=X(I)
      B(I)=X(IC)
      DELFR(I)=P*FR(I)
      DELFT(I)=Q*FT(I)
10    CONTINUE
      DO 16 I=1,NC
      IP1 = I + 1
      IF (IP1.GT.NC)IP1=IP1-NC
      DELFI(I)=FI(IP1)-FI(I)
      IF (DELFI(I)) 12,15,15
12    DELFI(I)=DELFI(I)+360.0
15    S(I) = DELFI(I)*T/360.0
16    CONTINUE
      I=0
20    I=I+1
      IF (B(I)-P1) 25,25,23
23    IF (B(I)-(P1+P2)) 30,30,35
25    CFO(I)=CF1*B(I)
      CTO(I)=CT1*B(I)
      IF (I-NC) 20,40,40
30    CFO(I)=CF1*B(I)+CF2*(B(I)-P1)
      CTO(I)=CT1*B(I)+CT2*(B(I)-P1)
      IF (I-NC) 20,40,40
35    CFO(I)=CF1*B(I)+CF2*(B(I)-P1)-CF3*(B(I)-(P1+P2))
      CTO(I)=CT1*B(I)+CT2*(B(I)-P1)+CT3*(B(I)-(P1+P2))
      IF (I-NC) 20,40,40
40    CONTINUE
      DO 70 I=1,NC
      J2=I
      FF(I)=0.0
      TQ(I)=0.0
      B2=B(I)
45    J1=J2
      B1=0.0
      SS=0.0
      XN=0.0
      DO 60 J=1,NC
      K=I+J
      IF (K.GT.NC) K=K-NC
      IF (I.EQ.K) GO TO 65
      IF (B(J2)-B(K)) 65,65,50
50    SS=SS+S(K)
      XN=1.0
      IF (B(K).LT.B1) GO TO 60
      IF (B(K).GT.B2) GO TO 60
      J1=K
      B1=B(K)
```

```
60    CONTINUE
65    FF(I)=FF(I)+(CFO(J2)-CFO(J1)*XN)*(S(I)+SS)**0.65
      TQ(I)=TQ(I)+((CTO(J2)-CTO(J1)*XN)*(S(I)+SS)**0.8)
      /*((B(J2)-B(J1)*XN)/2.0+(D/2.0+B(J2)))
      IF (SS.EO.0.0) GO TO 70
      B2=B1
      J2=J1
      GO TO 45
70    CONTINUE
      I=0
      RZ = 0.0
      RTQ=0.0
18    I=I+1
      RZ=RZ+FF(I)
      RTQ=RTQ+TQ(I)
      IF(I-NC) 18,14,14
14    CONTINUE
      DO 11 I=1,NC
      FI(I)=FI(I)*RAO
11    CONTINUE
      I=0
      VARX=0.0
      VARY=0.0
32    I=I+1
      VARX=VARX+((DELFR(I))**2)*((COS(FI(I)))**2)+
      /((DELFT(I))**2)*((SIN(FI(I)))**2)
      VARY=VARY+((DELFR(I))**2)*((SIN(FI(I)))**2)+
      /((DELFT(I))**2)*((COS(FI(I)))**2)
      IF (I-NC) 32,42,42
42    CONTINUE
      DELRX=SQRT(VARX)
      DELRY=SQRT(VARY)
      EPS=0.000001
      K=0
      SUM=0.0
52    SM=SUM
      K=K+1
      SUM=DELRX+(DELPX**2+DELRY**2-SM**2)/(2.0*RX)
      IF (ABS(SUM-SM).GT.EPS) GO TO 52
      DELR=SUM
      DELLA=ATAN(DELRY/(RX-DELRX))/RAO
      WRITE (61,5) K
      WRITE (61,6) DELR
      WRITE (61,7) DELLA
      WRITE (61,8) DELRX,DELRY
5     FORMAT (5X,* K = *,I5)
6     FORMAT (5X,* R VARIATIN IN MAGNITUDE KN = *,F10.6)
7     FORMAT (5X,* R VARIATIN IN DIRECTION DEG =*,F10.6)
8     FORMAT (5X,2F15.6)
      RETURN
      END
```

TABLE A4.2

DATA SHEET FOR OPTIMIZATION OF PRELIMINARY TOOL DESIGNS

	SOLID BORING			TREPANNING	
CASE #	1	2.	3	4	5
NC	3	4	5	3	4
N	5	7	9	3	4
NP			1		
NR			100		
D		56.642			105.283
P1		9.4403			9.333
P2		13.221			9.333
KSI			1.1		
CR1		3.06			2.73
CR2		1.002			2.038
CR3		7.14			2.7495
CT1		1.7355			1.7355
CT2		0.00			0.0
CT3		0.261			0.0
ROW			0.5		
DELTA			0.1		
RS		4.50			3.50
KW1		2.00			3.00
KW2		5.00			4.00
KW3		10.00			10.00
T			0.3		
F			0.001		
X(1)	50.00	45.00	20.00	30.00	45.00
X(2)	180.00	125.00	85.00	150.00	135.00
X(3)	285.00	205.00	145.00	270.00	225.00
X(4)	18.00	305.00	205.00	28.00	315.00
X(5)	15.00	15.00	265.00	28.00	28.00
X(6)	28.321	15.00	15.00	28.00	28.00
X(7)	–	15.00	15.00	–	28.00
X(8)	–	28.321	15.00	–	28.00
X(9)	–	–	15.00	–	–
X(10)	–	–	28.321	–	–

TABLE A4.3

DATA SHEET FOR OPTIMIZATION OF THE THREE TOOL DESIGNS

	SOLID BORING	TREPANNING	
TOOL NO	1	2	3
NP		1	
NR		500	
D [mm]	56.642	105.283	105.283
P1 [mm]	9.440	9.333	9.333
P2 [mm]	13.217	9.333	9.333
KSI	1.1	1.1	1.1
CR1	0.4852	0.4852	0.4852
CR2	0.1587	0.321	0.321
CR3	1.0137	0.4367	0.4367
CT1	2.41	2.41	2.41
CT2	0.0	0.0	0.0
CT3	0.3855	0.0	0.0
CF1	1.4931	1.4931	1.4931
CF2	0.0425	0.0682	0.0682
CF3	− 0.3527	0.01525	0.01525
ROW	0.5	0.5	0.5
DELTA	0.1	0.1	0.1
RS [kN]	8.0	3.5	7.0
KW1	2.0	3.0	3.0
KW2	5.0	4.0	4.0
KW3	10.0	10.0	10.0
T [mm]	0.22	0.22	0.22
F	0.001	0.001	0.001
ZETA	0.5	0.5	0.5
C	0.4	0.6	0.6
BL [mm]	12.5	28.0	28.0
BR [mm]	18.88	28.0	28.0
P	0.215	0.215	0.215
Q	0.08	0.08	0.08
ALFA	40.0	40.0	0.0

CONVERGENCE MONITOR PATTERN

NN	DELTA	Y	X(1)	X(2)	X(3)	X(4)	X(5)	X(6)
1	.10000	-19.05406	40.00000	160.00000	280.00000	12.50000	12.50000	28.32100
2	.10000	-18.69786	40.10000	159.90000	279.90000	12.50000	12.60000	28.32100
3	.10000	-17.98638	40.30000	159.70000	279.70000	12.50000	12.80000	28.32100
4	.10000	-16.92153	40.60000	159.40000	279.40000	12.50000	13.10000	28.32100
5	.10000	-15.50625	41.00000	159.00000	279.00000	12.50000	13.50000	28.32100
6	.10000	-13.74461	41.50000	158.50000	278.50000	12.50000	14.00000	28.32100
7	.10000	-11.64201	42.10000	157.90000	277.90000	12.50000	14.60000	28.32100
8	.10000	-9.20530	42.80000	157.20000	277.20000	12.50000	15.30000	28.32100
9	.10000	-6.44304	43.60000	156.40000	276.40000	12.60000	16.10000	28.32100
10	.10000	-4.58891	44.20000	155.40000	275.70000	12.70000	16.80000	28.32100
11	.10000	-4.22450	44.20000	155.20000	275.90000	12.80000	16.90000	28.32100
12	.10000	-3.94086	44.10000	154.90000	276.00000	12.90000	17.10000	28.32100
13	.10000	-3.60870	44.10000	154.50000	276.10000	13.00000	17.30000	28.32100
14	.10000	-3.28087	44.20000	154.00000	276.20000	13.10000	17.50000	28.32100
15	.10000	-2.95570	44.30000	153.40000	276.30000	13.20000	17.70000	28.32100
16	.10000	-2.60374	44.40000	152.70000	276.40000	13.30000	17.90000	28.32100
17	.10000	-2.25476	44.40000	151.90000	276.50000	13.40000	18.10000	28.32100
18	.10000	-1.86799	44.60000	151.00000	276.60000	13.50000	18.30000	28.32100
19	.10000	-1.44597	44.90000	150.00000	276.70000	13.60000	18.50000	28.32100
20	.10000	-1.02200	45.20000	148.90000	276.70000	13.70000	18.70000	28.32100
21	.10000	-.67598	45.60000	147.70000	276.60000	13.80000	18.80000	28.32100
22	.10000	-.41421	46.10000	147.60000	276.60000	13.80000	18.80000	28.32100
23	.10000	-.40990	46.10900	147.40000	276.60000	13.80000	18.80000	28.32100
24	.10000	-.37155	46.20000	147.40000	276.60000	13.80000	18.80000	28.32100
25	.10000	-.37102	46.30000	147.30008	276.60000	13.80000	18.80000	28.32100
26	.10000	-.36109	46.30000	147.40000	276.60000	13.80000	18.80000	28.32100
27	.05000	-.35651	46.25000	147.37500	276.60000	13.80000	18.80000	28.32100
28	.02500	-.35258	46.27500	147.37500	276.60000	13.80000	18.80000	28.32100
29	.01250	-.34974	46.27500	147.38750	276.60000	13.80000	18.80000	28.32100
30	.00313	-.34944	46.27187	147.38750	276.60000	13.80000	18.80000	28.32100
31	.00156	-.34927	46.27344	147.38750	276.60000	13.80000	18.80000	28.32100
32	.00078	-.34920	46.27266	147.38750	276.60000	13.80000	18.80000	28.32100

```
TOTAL NO OF FUNCTIONAL EVALUATIONS =      478
LARGEST MERIT ORDINATE =               -.349201
NUMBER OF BASE EVALUATIONS =        32
ORIGINAL STEP SIZE =             .100000
FINAL STEP SIZE =          .     .000781
REDUCTION FACTOR FOR STEP SIZE =          .500000
FRACTIONAL REDUCTION OF UNCERTAINTY =        .001000
    46.27266      -.34920
K =.      9
R VARIATIN IN MAGNITUDE KN =   1.242607
R VARIATIN IN DIRECTION DEG =  4.526218
        1.227043         .536165
RX CUTTING FORCE COMPONENT =        8.000039
RY CUTTING FORCE COMPONENT =         .000017
RZ CUTTING FORCE COMPONENT =       21.231418
RESULTANT TORQUE RTQ    =      348.887108
RADIAL CUTTING FORCES       FR(I) =      .982968      1.456268      .628528
TANGENTIAL CUTTING FORCES FT(I) =    3.556280      5.944491     14.374082
FEED CUTTING FORCES FF(I)     =      3.403797      5.466181     12.361439


CUTTING TORQUES TQ(I)       =    76.821706  112.475710  159.589692
EFFECTIVE CUTTING DEPTHS S(I)   =     .061792      .078963      .079244
```

```
10.39.5?.MEA90.
10.39.58.** V.LATINOVIC ***
10.39.58.ACCOUNT,CABSK55,.
10.39.59.FTN,OPT=0.
10.40.30.      7.084 CP SECONDS COMPILATION TIME
10.40.30.LGO.
10.40.52.      STOP
10.40.53.      4.651 CP SECONDS EXECUTION TIME
10.40.52.UEAD,      0.001KUNS.
10.40.52.UEMS,      1.050KUNS.
10.40.52.UECP,     13.044SECS.
10.40.52.AESP,     15.572UNTS.
10.43.56.UCLP, 23,      1.098 KLNS.
```

C O N V E R G E N C E   M O N I T O R   P A T T E R N

NN	DELTA	Y	X(1)	X(2)	X(3)	X(4)	X(5)	X(6)
1	.10000	-10.50000	40.00000	160.00000	280.00000	28.00000	28.00000	28.00000
2	.10000	-10.46045	40.00000	160.10000	279.90000	28.00000	28.00000	28.00000
3	.10000	-10.32394	39.90000	160.30000	279.70000	28.00000	28.00000	28.00000
4	.10000	-10.14792	39.80000	160.60000	279.40000	28.00000	28.00000	28.00000
5	.10000	-9.87439	39.60000	161.00000	279.00000	28.00000	28.00000	28.00000
6	.10000	-9.56131	39.40000	161.50000	277.50000	28.00000	28.00000	28.00000
7	.10000	-9.20929	39.20000	162.10000	277.90000	28.00000	28.00000	28.00000
8	.10000	-8.76283	38.90000	162.80000	277.20000	28.00000	28.00000	28.00000
9	.10000	-8.29404	38.60000	163.60000	276.40000	28.00000	28.00000	28.00000
10	.10000	-7.76945	38.30000	164.50000	275.50000	28.00000	28.00000	28.00000
11	.10000	-7.19585	38.00000	165.50000	274.50000	28.00000	28.00000	28.00000
12	.10000	-6.59076	37.70000	166.60000	273.40000	28.00000	28.00000	28.00000
13	.10000	-5.96753	37.40000	167.80000	272.20000	28.00000	28.00000	28.00000
14	.10000	-5.31810	37.10000	169.10000	270.90000	28.00000	28.00000	28.00000
15	.10000	-4.61826	36.70000	170.50000	269.50000	28.00000	28.00000	28.00000
16	.10000	-3.98259	36.40000	171.80000	268.10000	28.00000	28.00000	28.00000
17	.10000	-3.39769	36.10000	173.10000	266.70000	28.00000	28.00000	28.00000
18	.10000	-2.85040	35.80000	174.40000	265.30000	28.00000	28.00000	28.00000
19	.10000	-2.34934	35.50000	175.60000	263.90000	28.00000	28.00000	28.00000
20	.10000	-1.88562	35.20000	176.80000	262.50000	28.00000	28.00000	28.00000
21	.10000	-1.46757	34.90000	178.00000	261.10000	28.00000	28.00000	28.00000
22	.10000	-1.08405	34.60000	179.10000	259.70000	28.00000	28.00000	28.00000
23	.10000	-.92546	34.30000	180.20000	258.30000	28.00000	28.00000	28.00000
24	.02500	-.91940	34.30000	180.20000	258.32500	28.00000	28.00000	28.00000
25	.02500	-.91049	34.32500	180.20000	258.35000	28.00000	28.00000	28.00000
26	.02500	-.90760	34.35000	180.20000	258.37500	28.00000	28.00000	28.00000
27	.02500	-.89821	34.37500	180.20000	258.42500	28.00000	28.00000	28.00000
28	.02500	-.88683	34.42500	180.17500	258.47500	28.00000	28.00000	28.00000
29	.02500	-.87016	34.45000	180.15000	258.55000	28.00000	28.00000	28.00000
30	.02500	-.84825	34.50000	180.15000	258.62500	28.00000	28.00000	28.00000
31	.02500	-.83169	34.55000	180.15000	258.70000	28.00000	28.00000	28.00000
32	.02500	-.82360	34.60000	180.15000	258.77500	28.00000	28.00000	28.00000
33	.01250	-.82293	34.60000	180.13750	258.77500	28.00000	28.00000	28.00000
34	.00625	-.82167	34.60000	180.14375	258.76875	28.00000	28.00000	24.00000
35	.00625	-.81994	34.60000	180.15625	258.76250	28.00000	28.00000	28.00000

TABLE A4.4

DATA SHEET FOR CORRECTION OF THE THREE TOOL DESIGNS

	SOLID BORING	TREPANNING	
TOOL NO	1	2	3
NC	3	3	2
D [mm]	56.642	105.283	105.283
P1 [mm]	9.440	9.333	9.333
P2 [mm]	13.217	9.333	9.333
CR1	0.4852	0.4852	0.4852
CR2	0.1587	0.321	0.321
CR3	1.0137	0.4367	0.4367
CT1	2.41	2.41	2.41
CT2	0.0	0.0	0.0
CT3	0.3855	0.0	0.0
CF1	1.4931	1.4931	1.4931
CF2	0.0425	0.0682	0.0682
CF3	0.3527	0.01525	0.01525
B(1) [mm]	14.7	28.0	28.0
B(2) [mm]	18.88	28.0	28.0
B(3) [mm]	28.321	28.0	-
FI(1) [DEG]	46.3	44.0	-24.7
FI(2) [DEG]	147.4	188.4	189.1
FI(3) [DEG]	276.6	275.7	-
T [mm]	0.22	0.22	0.22
P	0.215	0.215	0.215
Q	0.08	0.08	0.08

```
ANGULAR LOCATIONS      FI(I)   =     44.832327  145.932327  275.132327
CUTTING WIDTHS         B(I)    =     14.700000   18.880000   28.321000
EFFECTIVE CUTTING DEPTHS S(I)  =       .056167     .071778     .072055
RADIAL CUTTING FORCES     FR(I) =      .969047    1.382814     .564474
TANGENTIAL CUTTING FORCES FT(I) =     3.539299    5.531094   13.148768
FEED CUTTING FORCES FF(I)       =     3.411678    5.159666   11.495000
CUTTING TORQUES TQ(I)           =    74.222647  104.432586  145.534524
RX CUTTING FORCE COMPONENT =          7.094589
RY CUTTING FORCE COMPONENT =          -.000000
RZ CUTTING FORCE COMPONENT =         20.066344
RESULTANT TORQUE RTQ       =        324.189757
K =      0
R VARIATIN IN MAGNITUDE KN =     1.147075
R VARIATIN IN DIRECTION DEG =    4.769078
     1.132049           .497448
```

```
10.38.54.ME890,T20.      **EXPRESS**
10.38.54.*V.LATINOVIC**
10.38.54.ACCOUNT,CARSK55,.
10.38.56.FTN,OPT=0.
10.39.07.    2.406 CP SECONDS COMPILATION TIME
10.39.08.LGO.
10.39.14.    STOP
10.39.14.    .062 CP SECONDS EXECUTION TIME
10.39.14.UEAD,    0.001KUNS.
10.39.14.UEMS,    0.578KUNS.
10.39.14.UECP,    3.652SEGS.
10.39.14.AESR,    5.156UNTS.
10.42.91.UCLP, 23.     0.337 KLNS.
```

```
ANGULAR LOCATIONS      FI(I)   =     22.651564  167.051564  254.351564
CUTTING WIDTHS         B(I)    =     24.000000   28.000000   28.000000
EFFECTIVE CUTTING DEPTHS S(I)  =       .088244     .053350     .078406
RADIAL CUTTING FORCES     FR(I) =      .725956     .523421     .672263
TANGENTIAL CUTTING FORCES FT(I) =     9.676649    6.469677    8.803443
FEED CUTTING FORCES FF(I)       =     8.862046    6.389614    8.206539
CUTTING TORQUES TQ(I)           =   373.920219  249.998032  340.178232
RX CUTTING FORCE COMPONENT =          3.279241
RY CUTTING FORCE COMPONENT =          -.000000
RZ CUTTING FORCE COMPONENT =         23.458248
RESULTANT TORQUE RTQ       =        984.096483
K =     12
R VARIATIN IN MAGNITUDE KN =      .872873
R VARIATIN IN DIRECTION DEG = 19.911366
      .772366         .908039
```

```
11.21.31.ME890.T20.      **EXPRESS**
11.21.31.*V.LATINOVIC**
11.21.32.ACCOUNT,CARSK55,.
11.21.32.FTN,OPT=0.
11.21.42.     2.450 CP SECONDS COMPILATION TIME
11.21.42.LGO.
11.21.47.   .STOP
11.21.47.      .060 CP SECONDS EXECUTION TIME
11.21.47.UEAD,     0.001KUNS.
11.21.47.UEMS,     0.576KUNS.
11.21.47.UECP,  .  3.694SECS.
11.21.47.AESR,     5.206UNTS.
11.24.34.UCLP, 23,     0.337 KLNS.
```

```
ANGULAR LOCATIONS        FI(I)    =   -39.290787.  174.509213
CUTTING WIDTHS           B(I)     =.   28.000000    28.000000
EFFECTIVE CUTTING DEPTHS S(I)     =      .130656     .089344
RADIAL CUTTING FORCES    FR(I) =       .936908      .731826
TANGENTIAL CUTTING FORCES FT(I) =    13.245775     9.773027
FEED CUTTING FORCES FF(I)        =    11.437216     8.933695
CUTTING TORQUES TQ(I)            =   511.836621   377.644438
RX CUTTING FORCE COMPONENT =          7.449477
RY CUTTING FORCE COMPONENT =           .000000
RZ CUTTING FORCE COMPONENT =         20.370912
RESULTANT TORQUE RTQ .    =         889.481059
K =     7
R VARIATIN IN MAGNITUDE KN =      .789394
R VARIATIN IN DIRECTION DEG =  9.583938
        .710439        1.137880
```

```
11.44.10.ME890.T20.      **EXPRESS**
11.44.10.*V.LATINOVIC**
11.44.10.ACCOUNT,CARSK55,.
11.44.11.FTN,L=0.
11.44.19.     2.443 CP SECONDS COMPILATION TIME
11.44.19.LGO.
11.44.24.     STOP
11.44.24.      .046 CP SECONDS EXECUTION TIME
11.44.24.UEAD,     0.001KUNS.
11.44.24.UEMS,     0.494KUNS.
11.44.24.UECP,     3.546SECS.
11.44.24.AESR,     5.025UNTS.
11.44.31.UCLP, 23,     0.081 KLNS.
```

APPENDIX V

LAYOUTS AND DETAIL DRAWINGS OF THE THREE
OPTIMIZED MULTI-EDGE HEADS

Parts List
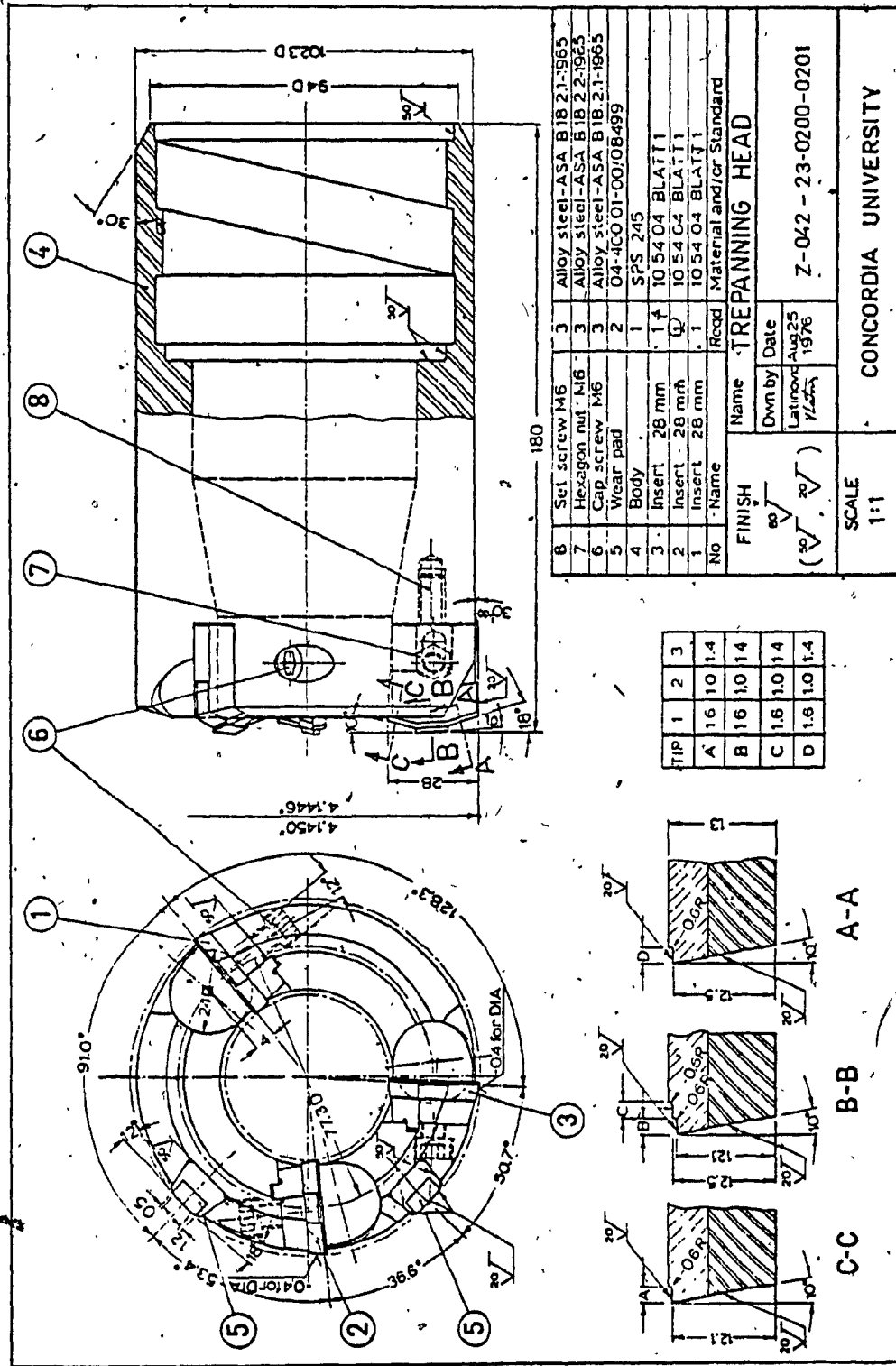
No	Name	Reqd	Material and/or Standard
8	Set screw M6	3	Alloy steel-ASA B 18.2.1-1965
7	Hexagon nut M6	3	Alloy steel-ASA B 18.2.2-1965
6	Cap screw M6	3	Alloy steel-ASA B 18.2.1-1965
5	Wear pad	2	04-4CO 01-00/08499
4	Body	1	SPS 245
3	Insert 28 mm	1.4	10 54 04 BLATT 1
2	Insert - 28 mm	1.2	10 54 C4 BLATT 1
1	Insert 28 mm	1	10 54 04 BLATT 1

	Name	Date
Dwn by	Latinovic	Aug 25 1976

TREPANNING HEAD

Z-042 - 23 - 0200 - 0201

CONCORDIA UNIVERSITY

FINISH

SCALE 1:1

TIP	1	2	3
A	1.6	1.0	1.4
B	1.6	1.0	1.4
C	1.6	1.0	1.4
D	1.6	1.0	1.4

A-A

B-B

C-C

VIEW B

VIEW C

A-A

THE THREE INSERT POCKETS ARE IDENTICAL

THE TWO WEAR PAD POCKETS ARE IDENTICAL

TREPANNING HEAD

Z-042-23-0200-0202

CONCORDIA UNIVERSITY

SCALE 1:1

Trepanning Head — engineering drawing, Concordia University, Z-042-23-0200-0204

Parts list:

No	Name	Reqd	Material and/or Standard
8	Set screw 6-40 UNF	1	Alloy steel - ASA B18 2.1-1955
7	Set screw 1/4-28 UNF	2	Alloy steel - ASA B18 2.1-1955
6	Hexagon nut M6	2	Alloy steel - ASA B18 2.2-1955
5	Cap screw M6x30	2	Alloy steel ASA B18 2.1 1955
4	Wear pad	2	04-400.01-00/08499
3	Body	1	Alloy steel 125 PSI
2	Insert 28 mm	1	1054 04 BLATT 1
1	Insert 28 mm	1	1054 04 BLATT 1

TIP	1	2
A	1.6	1.1
B	15	1.1
C	1.6	1.1
D	1.6	1.1

Name: TREPANNING HEAD

Dwn by: Latunov   Date: Dec. 23 1976

FINISH

Z-042-23-0200-0204

CONCORDIA UNIVERSITY

SCALE 1:1

Sections: A-A, B-B, C-C

6-40 UNF DIA GAUGE

102.3 D   94 D   180

4.1450°   4.1446°

0.4 for DIA

VIEW B

VIEW C

VIEW D

THE TWO INSERT POCKETS ARE IDENTICAL. LOCATIONS OF THE 4 mm SLOTS MUST BE AXIALLY SYMMETRIC WITH RESPECT TO THE HEAD AXIS.

THE TWO WEAR PAD POCKETS ARE IDENTICAL.

ALLOY STEEL

TREPANNING HEAD

Z-042-23-9200-0203

CONCORDIA UNIVERSITY

SCALE
1:1